

AD-A157 109

# Production of Neutral Beams from Negative Ion Beam Systems in the USSR

Nikita Wells

DTIC  
ELECTE  
AUG 1 1985  
S

DTIC FILE COPY

This document has been approved  
for public release and sale; its  
distribution is unlimited.

**Rand**

85 7 17 024

The research described in this report was sponsored by the Defense Advanced Research Projects Agency under ARPA Order No. 3520-17, Contract No. MDA903-82-C-0067, Director's Office.

**Library of Congress Cataloging in Publication Data**

Wells, Nikita, 1937-

Production of neutral beams from negative ion beam systems in the USSR.

"R-2909/1-ARPA."

"December 1982."

"Prepared for the Defense Advanced Research Projects Agency."

1. Neutral beams—Research—Soviet Union. 2. Ion sources—Research—Soviet Union. 3. Ion bombardment—Research—Soviet Union. 4. Anions—Research—Soviet Union. I. United States. Defense Advanced Research Projects Agency. II. Title  
QC793.3.B4W443 1985 623.4'46 85-3651  
ISBN 0-8330-0641-X

The Rand Publications Series: The Report is the principal publication documenting and transmitting Rand's major research findings and final research results. The Rand Note reports other outputs of sponsored research for general distribution. Publications of The Rand Corporation do not necessarily reflect the opinions or policies of the sponsors of Rand research.

UNCLASSIFIED

SECURITY CLASSIFICATION OF THIS PAGE (When Data Entered)

REPORT DOCUMENTATION PAGE		READ INSTRUCTIONS BEFORE COMPLETING FORM	
1. REPORT NUMBER R-2909/1-ARPA	2. GOVT ACCESSION NO. <b>A157 109</b>	3. RECIPIENT'S CATALOG NUMBER	
4. TITLE (and Subtitle) Production Of Neutral Beams from Negative Ion Beam Systems in the USSR		5. TYPE OF REPORT & PERIOD COVERED Interim	
		6. PERFORMING ORG. REPORT NUMBER	
7. AUTHOR(s) Nikita Wells		8. CONTRACT OR GRANT NUMBER(s) MDA903-82-C-0067	
9. PERFORMING ORGANIZATION NAME AND ADDRESS The Rand Corporation 1700 Main Street Santa Monica, CA. 90406		10. PROGRAM ELEMENT, PROJECT, TASK AREA & WORK UNIT NUMBERS	
11. CONTROLLING OFFICE NAME AND ADDRESS Defense Advanced Research Projects Agency Department of Defense Arlington, VA 22209		12. REPORT DATE December 1982	
		13. NUMBER OF PAGES 107	
14. MONITORING AGENCY NAME & ADDRESS (if different from Controlling Office)		15. SECURITY CLASS. (of this report) Unclassified	
		15a. DECLASSIFICATION/DOWNGRADING SCHEDULE	
16. DISTRIBUTION STATEMENT (of this Report) Approved for Public Release; Distribution Unlimited			
17. DISTRIBUTION STATEMENT (of the abstract entered in Block 20, if different from Report) No Restrictions			
18. SUPPLEMENTARY NOTES			
19. KEY WORDS (Continue on reverse side if necessary and identify by block number) Particle beams Ion beams Thermonuclear reactions, Plasma temperatures Charged particles.			
20. ABSTRACT (Continue on reverse side if necessary and identify by block number) See reverse side			

DD FORM 1 JAN 73 1473

EDITION OF 1 NOV 65 IS OBSOLETE

UNCLASSIFIED

SECURITY CLASSIFICATION OF THIS PAGE (When Data Entered)



↓ This report, a sequel to [The Development of High-Intensity Negative Ion Sources and Beams in the USSR], R-2816-ARPA, examines (1) Soviet research on the formation of intense, high-energy neutral particle beams and the associated investigation of charge exchange and beam stripping and (2) the deployment in the USSR of high-intensity negative ion sources of the direct-extraction and double-charge-exchange types, beam neutralizers, and neutral beam injectors, as reported in Soviet open-source technical publications. Based on open-source literature, the study finds no overt evidence of a program to develop exoatmospheric particle-beam weapons in the USSR. The author suggests, however, that such a program may exist as a classified effort paralleling the nuclear fusion research described in the literature. Originator.  
Supplied keywords include:

See DD14731

R-2909/1-ARPA

# Production of Neutral Beams from Negative Ion Beam Systems in the USSR

Nikita Wells

December 1982

Prepared for the  
Defense Advanced Research  
Projects Agency



Accession For	
NTIS GRA&I	<input checked="checked" type="checkbox"/>
DTIC TAB	<input type="checkbox"/>
Unannounced	<input type="checkbox"/>
Justification	
By	
Distribution/	
Availability Codes	
Dist	Avail and/or Special
A-1	

APPROVED FOR PUBLIC RELEASE; DISTRIBUTION UNLIMITED

PREFACE

This report was prepared in the course of a continuing study, sponsored by the Defense Advanced Research Projects Agency, of Soviet research and development of high-current, high-energy, charged particle beams and their scientific and technological applications. The report examines (1) Soviet research on the formation of intense, high-energy neutral particle beams and the associated investigation of charge exchange and beam stripping and (2) the development in the USSR of high-intensity negative ion sources of the direct-extraction and double-charge-exchange types, beam neutralizers, and neutral beam injectors, as reported in Soviet open-source technical publications.

This report is a sequel to The Development of High-Intensity Negative Ion Sources and Beams in the USSR, R-2816-ARPA, November 1981, by the same author. Both reports may be of interest to those dealing with pulsed-power and energy-related research.

### SUMMARY

Soviet research on the formation of intense, high-energy neutral particle beams, the associated investigation of charge exchange and beam stripping, and the development of neutral beam injectors, which appears to have increased in the late 1960s, continues at a lively pace to the present. The injection of neutral particle beams into magnetically confined plasmas is considered the most effective method of heating these plasmas to obtain the conditions for thermonuclear fusion. Theoretically, such beams may also be used as an exoatmospheric particle-beam weapon (PBW).

Before 1960, Soviet investigations were limited largely to basic measurements and calculations of charge-exchange cross sections and neutral beam conversion coefficients at the Ioffe Physico-Technical Institute (IPI) in Leningrad and Nuclear Physics Institute (NPI) in Novosibirsk. Between the mid-1960s and early 1970s, the Physico-Technical Institute (PTI) in Kharkov, Solid State Physics Institute (IFTT) near Moscow, and Kurchatov Institute of Atomic Energy in Moscow, along with NPI and IPI, began to develop vapor targets for double charge exchange and beam neutralization (of both positive and negative ions). In the late 1970s, Kurchatov, IFTT, NPI, and IPI investigated neutral beam injection systems and their components.

The Soviets have made good progress in the development of intense negative ion sources (of both the direct-extraction and double-charge-exchange types), gas and plasma beam strippers, various metal vapor targets for double charge exchange, neutral beam injection systems (based on both positive and negative ions), and diagnostic neutral beam injectors. At the Nuclear Physics Research Institute (NPRI) and Radiotechnical Institute (RTI) in Moscow, the formation of negative ion beams at high energies, as well as their charge exchange and beam-stripping problems, have been considered theoretically since the mid-1970s for use in linear accelerators for a meson factory.

NPI researchers were the first to develop the two key components for the production of intense neutral beams: an intense, high-brightness,

low-emittance negative ion source and a high-efficiency plasma beam neutralizer. The surface-plasma negative ion source, originally developed in 1971 with a planotron and a Penning-type discharge chamber, eventually evolved into the present version, a multiple slit design, which produces 4 A of pulsed  $H^-$  ion beam current. The negative ion beam current output was increased dramatically by introducing cesium vapor into the arc discharge region of the source.

The importance of the high-brightness, low-emittance surface-plasma source lies in its use for high-current accelerators and its possible use for PBWs.

Although the source must still be upgraded to operate satisfactorily at long pulse lengths or even DC at these high beam currents, the gap between the achieved and required current is being narrowed. For fusion application, this type of source must produce beams to rival the intense negative ion beams now being produced by the double-charge-exchange source and the direct-extraction magnetic-cusp source.

The NPI plasma beam neutralizer was able to convert high-intensity negative ion beams into neutral beams with an efficiency as high as 85%. NPI researchers have demonstrated the formation of an 80 cm long stable plasma target with a plasma thickness of  $2.2 \times 10^{15}$  atoms/cm<sup>2</sup>, the optimum for the neutralization of 1 MeV  $D^-$  ions. This NPI work is apparently coming to an end, however, and research personnel are being transferred to the AMBAL magnetic mirror trap project.

Other major Soviet experimental research on intense neutral beam formation using negative ion beams is centered at the Kurchatov Institute. This research also seems to be limited to thermonuclear fusion applications. A large, well-equipped facility is developing a high-power deuterium neutral beam injector. Kurchatov researchers are committed to the double-charge-exchange method of converting positive ion beams to negative beams, using alkali metal vapor charge-exchange targets to obtain the required high-current DC beams. The double-charge-exchange source has disadvantages, however, stemming mostly from its bulk and complexity and from the tendency of the vacuum system to become contaminated. Researchers in the United States have stopped using the



double-charge-exchange ion source for fusion applications and are now primarily using surface-plasma and volume-production-type ion sources.

In 1977, Kurchatov produced 1.4 A of  $H^-$  ion beam currents at 40 keV, using an initial  $H^+$  beam of 8 A at 10 keV. Recent technical problems, however, involving high-voltage breakdown in the accelerator when high-current beams are run and the sodium vapor jet is operating, have slowed this research. The basic problem was attributed to the large volume of electrons entering the high-voltage gap from the vapor target. The fine-mesh grids are being replaced by a long, negatively biased suppression tube in the hope of suppressing the undesirable electrons. In an effort to reduce the pumping requirement of the injector vacuum system, Kurchatov and IFTT recently undertook the joint development of an optimum charge-exchange target based on the vapor jet's pumping and gas-blocking mechanisms and its ability to recirculate gas.

A 400 to 600 keV deuterium beam injector system is being studied conceptually at Kurchatov using double-charge-exchange to create a  $D^-$  beam. The  $D^-$  beam is then converted to  $D^0$  using a Li stripper target. Several modules of this injector are to be used in parallel to obtain a total neutral beam power of 30 to 40 MW.

The Yefremov Institute, working on the hollow-beam surface-plasma source under contract to the Kurchatov Institute, has produced 2.4 A of  $H^-$  ions with an emission diameter of 10 cm. No further information on this research has been published in the open literature.

In the area of high energy, the only consideration of negative ion beam stripping in the USSR is the theoretical work at NPRI and RTI. This research involves negative ion beam neutralization at 100 to 600 MeV accelerated in linear accelerators. Although Soviet authors refer to the acceleration of  $H^-$  beams, to date they have published no experimental data on beam stripping at high energies in the open literature. Their investigations show, however, that the Soviets possess the basic theory of the negative ion stripping process and have carried out calculations of angular and energy distributions of ions emerging from various charge-changing targets. They have also investigated the angular and energy distributions of electrons in these targets for diagnostic information about the primary ion beam.

This study, based on a review of the Soviet open-source literature on the production and transport of negative-ion and neutral beams, found no overt evidence of a program to develop exoatmospheric particle-beam weapons in the USSR. Reason suggests, however, that such a program may exist in conjunction with the nuclear fusion research described in the literature. The commonality to both nuclear fusion and PBW systems of many components and basic physical problems in the generation, acceleration, and transport of intense particle beams gives the USSR the basis for considering the development of an exoatmospheric particle-beam weapon.

ACKNOWLEDGMENTS

The author would like to thank Gordon W. Hamilton and Edwin B. Hooper, Jr., of the Lawrence Livermore National Laboratory, and George H. Gillespie of Physical Dynamics, Inc., for their reviews of this report and for their many useful suggestions. He is also grateful to his colleagues at The Rand Corporation: Robert W. Salter for reviewing the report; Simon Kassel for direction and support of and interest in the project; and Erma Packman for editing the report.

CONTENTS

PREFACE .....	iii
SUMMARY .....	v
ACKNOWLEDGMENTS .....	ix
Section	
I. INTRODUCTION .....	1
II. OVERVIEW OF SOVIET AND WESTERN RESEARCH ON CHARGE-CHANGING PROCESSES AND NEUTRAL BEAM PRODUCTION .....	4
1. Basic Measurements of Charge-Exchange and Electron Detachment Cross Sections and Neutral Beam Conversion Coefficients .....	4
2. Direct-Extraction Negative Ion Sources .....	6
3. Double-Charge-Exchange Negative Ion Sources .....	8
4. Neutralization of Intermediate-Energy Negative Ion Beams .....	10
5. Neutralization of High-Energy Negative Ion Beams .....	11
6. Neutral Beam Injectors .....	13
III. DEVELOPMENT OF HIGH-INTENSITY NEGATIVE ION SOURCES IN THE USSR .....	17
1. Direct-Extraction Surface-Plasma Ion Sources .....	17
2. Double-Charge-Exchange Ion Sources .....	18
i. Alkali Metal Vapor Target Developments .....	20
ii. Comparison of Cesium and Sodium Vapor Targets ....	26
iii. Vacuum Properties and Mechanics of Vapor Targets .	30
IV. ION BEAM NEUTRALIZERS FOR NEUTRAL BEAM PRODUCTION .....	36
1. Gas Neutralizers .....	37
2. Hydrogen Plasma Neutralizers for $H^-$ and $D^-$ Beams .....	38
3. High-Energy Beam Neutralizers .....	46
V. NEUTRAL BEAM INJECTION SYSTEMS .....	49
1. Early Research on Neutral Beam Injectors .....	49
2. The MIN Injector Test Facility .....	53
3. The Deuterium Beam Injector Test Facility .....	56
4. Injection Systems Based on Positive Ion Beams .....	60
i. The OGRA-IV .....	60
ii. The AMBAL .....	60
iii. Diagnostic Neutral Beam Injectors .....	61
VI. CONCLUSIONS .....	68
Appendix	
BASIC CHARGE-CHANGING PROCESSES IN NEUTRAL BEAM FORMATION ..	71
REFERENCES .....	95



## I. INTRODUCTION

This report assesses the state of the art of the Soviet development of intense, high-energy, neutral-particle beams. While these beams are used principally for magnetic-confinement fusion experiments, they may also have application in military research and development. Therefore, the consideration of Soviet progress in the understanding of neutral beam dynamics and the technology of beam production provides insight into Soviet capabilities to use neutral beams for possible military applications.

The injection of intense, high-energy neutral particle beams into magnetically confined plasmas is now considered the most effective method of heating and fueling these plasmas to obtain the conditions for thermonuclear fusion. Neutral atom beams have been found to be especially well suited to this application: They can pass through the magnetic field confining the plasma without being deflected; they can easily be trapped after they enter the plasma; and they can transfer almost all of their energy to the target plasma. The main objective of current tokamak research is to produce plasmas of higher ion density and temperature. Higher-energy neutral beams are needed to penetrate these plasmas.

In addition to their thermonuclear fusion application, neutral beams are also being considered for use as exoatmospheric particle-beam weapons (PBW), because they are not bent by the earth's magnetic field or defocused by the vacuum conditions of outer space. In the space environment, the presence of atoms causes some stripping of electrons from the neutral particle beam and the formation of ions that are eventually bent out of the beam by magnetic fields. This effect completely degrades the beam over long beam-transport distances. The neutral beam, therefore, can be used above the atmosphere only at a height where the background gas pressure is low enough to allow unperturbed propagation of the neutral beam. A well-collimated neutral beam--if it could be produced above the atmosphere with sufficient beam intensity and energy--could serve as both an antisatellite and an antiballistic missile weapon.

A major obstacle to the possible use of intense neutral beams as PBW arises, however, from the need to propagate the beam over long

distances. The primary problem involves beam divergence, which sets the ultimate limit on the range of the beam weapon system. Two key elements in the production of the neutral beam affect the beam divergence. First, the initial negative ion source produces an inherent divergence of the negative ion beam that is transported to the beam neutralizer in the last stage of the PBW system. Second, the beam neutralizer imposes an additional divergence on the exiting neutral beam.

Intense, high-energy neutral-particle beams can be produced by passing either positive or negative ion beams through a charge-changing target (consisting, for example, of a gas volume, alkali metal vapor jet, ionized plasma, solid foil, or photodetachment cell). When negative ion beams are used to produce neutrals, the negative beams are first accelerated to at least 100 keV and then neutralized by stripping the electrons from the negative ions in a beam neutralizer. The main advantage of using negative rather than positive ions lies in the negative ions' high neutralization efficiency, which remains constant as the beam energy increases. Neutral beam production using positive ions, although advantageous from the standpoint of the high beam currents that are presently available from positive ion sources, is limited at the higher energies by the sharp decrease in neutralization efficiency as the beam energy increases. At 100 keV, the conversion coefficient of positive to neutral ions for deuterons, for example, is already considerably lower than that of negative ions; above about 120 keV, the use of positive ion beams becomes impractical.

Two methods are currently used to produce intense negative ion beams. The first involves the direct extraction of ions from such negative ion sources as the surface-plasma and volume-production multicusp types. The surface-plasma ion source is especially well suited to the production of well-collimated negative ion beams. The Soviet and U.S. research on surface-plasma ion sources was described in an earlier Rand report [1]. More recent Soviet developments are discussed in this report.

The second method of producing intense negative ion beams is based on the double-charge-exchange ion source, which uses alkali metal vapor

targets to convert the positive ion beam into a negative beam. Soviet researchers have investigated the use of charge-changing targets for both the conversion of positive to negative ions and beam neutralization, especially the conversion of negative ion beams to neutral beams.

This report reviews Soviet open-source literature published during the past 15 years on neutral beam production for thermonuclear fusion and other applications. Soviet research on the two key elements of neutral beam production--the formation of intense negative ion beams and their conversion into neutral beams--as well as the use of these neutral beams in injector systems is described. Special note is made in the report of the institutions engaged in this research and the relevance of the research to neutral particle-beam weapon development. The study also presents the observations of U.S. experts in this field.

Section II begins with a general overview of Soviet and Western research and development of neutral particle beams between 1965 and 1981. This is followed by a technical discussion of Soviet research in the two key areas of neutral beam production: the formation of intense negative ion beams and their conversion into neutral beams. The formation of intense negative ion beams by direct extraction and double-charge-exchange negative ion sources is considered in Section III. The conversion of the negative ion beams into neutral beams, using gas, alkali metal vapor, and plasma neutralizers (beam strippers), is described in Section IV. Section V reports on recent Soviet neutral beam injector systems and experimental test facilities, including the INES, MIN, 40-MW deuterium atom injector system, and OGRA-IV experiment, all at the Kurchatov Institute of Atomic Energy. Research on diagnostic neutral beam injectors at the Nuclear Physics Institute in Novosibirsk is also considered in this section.

The report ends with conclusions and an appendix presenting details of the basic charge-changing processes involved in converting positive and negative ions into neutral atoms and the results of experimental measurements of the principal beam-quality indicators. Particular emphasis is given in the appendix to the collision cross sections for neutral atoms produced by electron detachment (stripping) of negative ions.

## II. OVERVIEW OF SOVIET AND WESTERN RESEARCH ON CHARGE-CHANGING PROCESSES AND NEUTRAL BEAM PRODUCTION

Soviet researchers have been investigating charge-changing processes for the past 25 years. The following research institutes participated in this work at some time during this period: the Ioffe Physico-Technical Institute (IPI), Leningrad; Nuclear Physics Institute (NPI), Novosibirsk; Kurchatov Institute of Atomic Energy (Kurchatov), Moscow; Solid State Physics Institute (IFTT), Chernigolovka; Physico-Technical Institute (PTI), Kharkov; Nuclear Physics Research Institute (NPRI) at Moscow State University; and Radiotechnical Institute (RTI), Moscow.

Early basic research on atomic and molecular collisions, electron capture and detachment from ions and atoms, formation of excited atoms and negative ions, and conversion of positive to negative ions by double charge exchange led to the development of negative ion beam and neutral beam injectors for tokamaks and open traps. Recent work involves the evaluation and testing of injector system components, including gas and plasma targets, negative ion sources and strippers, and neutral beam diagnostic injectors. Figure 1 shows the chronology of key Soviet research on neutral beam production by institutes and leading researchers.

This section describes the main phases of Soviet and western research leading to neutral beam production, including, where possible, a direct comparison of Soviet and western subject treatment and results. References to Soviet publications, omitted from this section, are provided in connection with detailed technical analysis in subsequent sections.

### 1. BASIC MEASUREMENTS OF CHARGE-EXCHANGE AND ELECTRON DETACHMENT CROSS SECTIONS AND NEUTRAL BEAM CONVERSION COEFFICIENTS

The Ioffe Physico-Technical Institute made the earliest basic measurement of atomic and molecular collisions with gases. A team now headed by V. A. Ankudinov, and including V. M. Dukel'skiy, N. V. Fedorenko, and Ya. M. Fogel', measured collision cross sections and



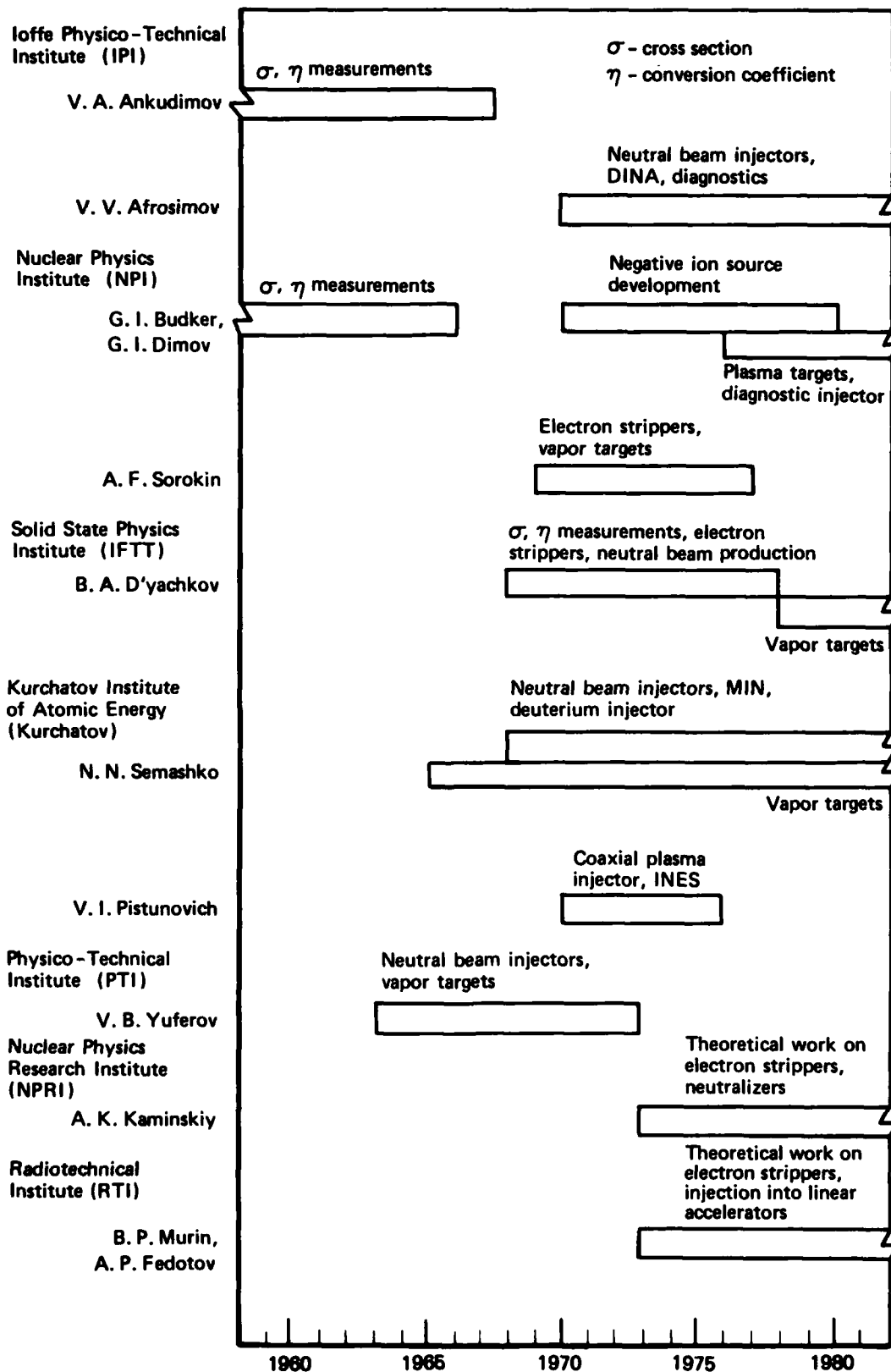


Fig. 1 — Chronology of key Soviet research on neutral beam production

investigated electron capture and electron detachment, formation of excited ions and atoms, and conversion of positive to negative ions by double charge exchange in gases and alkali metal vapors. Most of the basic research done by this team had ended by the mid-1960s. Research on atomic and molecular collisions in gases and plasmas at the Nuclear Physics Institute was begun in 1954 under the leadership of G. I. Budker. In the mid-1960s, this research involved electron detachment cross-section measurements of  $H^-$  beams in various gases, as well as neutral beam formation as a function of gas target thickness. The team headed by B. A. D'yachkov at the Solid State Physics Institute measured electron-detachment and charge-exchange cross sections for the conversion of positive to negative ions using alkali metal vapors.

Extensive basic research on charge-changing cross sections and neutral beam conversion coefficients has also been conducted in the West.

## 2. DIRECT-EXTRACTION NEGATIVE ION SOURCES

NPI has been working on multiampere direct-extraction negative ion sources for use in neutral beam injectors and accelerators. Under the leadership of G. I. Dimov, NPI researchers in 1971 developed two versions of a surface-plasma negative ion source, one with a planotron and one with a Penning-type discharge chamber. The introduction of cesium vapor into the source discharge chamber greatly increased the negative ion output of this high-brightness, low-emittance ion source. The latest, multiple slit version of this source produced 4 A of pulsed  $H^-$  ion beam current. A hollow beam version of the surface-plasma source developed at the Yefremov Institute under contract to the Kurchatov Institute produced 2.4 A of  $H^-$  ions with an emission beam diameter of 10 cm.

The main work on the surface-plasma-type direct-extraction negative ion source in the United States is being done at the Brookhaven National Laboratory (BNL), which is developing a DC source as part of a high-energy neutral beam injector. Following the recent successes of the 1 A  $H^-$  pulsed beam using modified planotron (magnetron) surface-plasma sources, as described in [2,3,4], the neutral beam development group at BNL is experimenting with a 1 to 2 A  $H^-$  DC ion source. Other experiments

are investigating plasma injection from a hollow cathode discharge, a method that should significantly decrease the source operating pressure and improve the source performance [5]. The new version of the magnetron source has focusing grooves on the cathode with an asymmetric anode-cathode geometry that allows the source to operate at a power efficiency of 8 kW/A and a 6% gas efficiency [2].

Researchers at the Lawrence Berkeley Laboratory (LBL) have developed a large-volume, multicusp (magnetic-bucket-type) negative ion source that produces  $H^-$  and  $D^-$  ions by the impact of plasma positive ions on a molybdenum converter [6,7]. An  $H^-$  beam current of 1 A was obtained by introducing cesium vapor into the discharge from a hot oven. The beam will be accelerated to energies of at least 40 keV by a four-electrode electrostatic accelerator. The goal of this research is to produce long-pulse and CW high-energy neutral beams.

The Oak Ridge National Laboratory (ORNL) has been concentrating on the direct extraction of negative ions, using a modified colutron source with surface ionization and transverse magnetic field extraction. The first version of the planned source, called SITEX, is to operate with a 1 A, CW, ion-beam current at 40 kV extraction potential [8].

The U.S. negative ion neutral beam development program and its future goals and requirements are discussed in [9,10,11] and compared with positive-ion-based systems. The completion of the 1 A development work and the conceptual design of a 10 A, 200 keV system is planned [12]. A final system will be chosen once proof of principle has been demonstrated.

NPI in the USSR and BNL in the United States are engaged in equivalent research and are making similar progress. American researchers are presently concentrating on obtaining 1 A of DC beam and are planning higher outputs in the future. The Soviets announced that they have obtained 4 A of pulsed beam, but have said nothing about their DC beam outputs. There appears to be no Soviet effort directly comparable to the LBL development of the multicusp, bucket-type negative ion source.

### 3. DOUBLE-CHARGE-EXCHANGE NEGATIVE ION SOURCES

The Kurchatov Institute has been involved since the late 1960s in the development of injection systems for large tokamaks and open traps. The team headed by N. N. Semashko developed intense negative ion beams by double charge exchange and studied various gas targets for negative ion and neutral beam injectors. A special test facility, the MIN, was constructed to study charge-exchange systems. In 1977, a negative hydrogen ion beam current of 1.4 A and pulse length of 10 ms at 40 keV was produced with an 8 A  $H^+$  beam at 10 keV, using both sodium and cesium vapor targets.

Researchers at IFTT have been developing alkali metal vapor targets for double-charge-exchange conversion, concentrating on the targets, vacuum, pumping, and gas recirculation characteristics. The IFTT targets were incorporated into the injectors at Kurchatov, and researchers of both institutes are working together to further develop the targets, despite the difficulties caused by the formation of large amounts of electrons that aggravate the high-voltage breakdown in the accelerator.

The U.S. production of negative hydrogen and deuterium ions by double charge exchange of positive hydrogen ion beams in alkali metals, a joint development of LBL and LLNL, was described in [13,14,15]. Using a sodium vapor target, LLNL produced a 2.2 A  $D^-$  ion beam at an energy of 10 keV, comparable to Kurchatov's achievement of 1.4 A at long pulse lengths. It was determined that the plasma produced by the beam in the sodium target cell is confined to the charge-exchange region and does not propagate along the beam line. The 2.2 A beam was found to have an angular distribution of  $0.7^\circ \times 2.8^\circ$ , energy of 7 to 13 keV, and peak current density of 15 mA/cm<sup>2</sup>. These experiments determined that in the charge-exchange target the space-charge neutralization of the beam is complete and the charge-exchange losses of  $D^-$  on  $Na^+$  are negligible; no beam plasma instabilities were observed [13].

Although LBL and LLNL had originally planned to operate their negative-ion-based neutral-beam system with the negative ions produced by double charge exchange in Na vapor, in early 1980 they shifted to a negative ion beam extracted directly from a multicusp, bucket-type negative ion source (see subsection 2, above). Their immediate goal is



to accelerate a 1 A  $H^-$  beam to at least 40 keV. LLNL is considering a high-current negative ion beam program in the several hundred keV range in connection with the next generation of mirror devices [11].

ORNL is using a cesium converter to produce negative ions from low-energy positive ions from a duopigatron ion source. A 100 A positive ion source (PDS/ISX-B) and a 28 cm diameter Cs converter will be used to form large negative ion beams. Researchers hope to achieve 10 A of  $H^-$  at energies above 50 keV, if the conversion efficiency can be made to approach 10% [16]. They are investigating double charge exchange using a 1 keV positive ion beam and an alkali vapor charge-exchange cell [17]. An insulated grid technique provides minimum beam divergence of the low-energy positive-ion beam before the charge exchange.

In France, a double-charge-exchange  $D^-$  ion source using a supersonic Cs target has been developed jointly by the Nuclear Research Center in Grenoble and the Ecole Polytechnique in Palaiseau [18,19]. The French researchers have obtained  $D^-$  beam currents of 160 mA at 1 keV, using 750 mA  $D^+$  beams. Average current densities of 12 mA/cm<sup>2</sup> of  $D^-$  with pulse durations of 1 s have been measured.

Investigating basic double charge exchange at low beam currents for 0.3 to 3 keV  $D^+$  to  $D^-$  ions in alkaline earth vapor targets, LBL researchers observed an anomalously large increase in the  $D^-$  thick target yield ( $F^\infty$ ) when  $D^+$  ions of energies less than 5 keV passed through strontium vapor [20]. A 50% negative deuterium ion yield was obtained with strontium; the yields with calcium and barium equaled or surpassed that of cesium. Experiments at Wesleyan University using magnesium, strontium, and calcium vapor targets confirmed the LBL results [21]. LBL also measured  $D^-$  formation, conversion coefficients, and equilibrium thick target yields in cesium, sodium, and rubidium metal vapor targets [22,23].

Double charge exchange has been shown to produce high DC negative ion beam currents that can be transformed into intense neutral beams, but owing to the complexity of the system as compared with direct extraction, its use in the United States in the near future appears doubtful. The Soviets, however, continue to devote a large effort to this line of research at Kurchatov and IFTT.

#### 4. NEUTRALIZATION OF INTERMEDIATE-ENERGY NEGATIVE ION BEAMS

Soviet researchers have been studying the neutralization of negative ion beams by electron stripping in gases and plasmas for the past 20 years. A research team under V. B. Yuferov at the Physico-Technical Institute, working from 1963 to 1973, designed ultrasonic gas jets and nozzles for the neutralization of negative ion beams and investigated the vacuum properties of gas targets. Since then, this team has been involved in the design and start-up of the superconducting Crystal-2 torsatron.

An NPI team headed by G. I. Dimov recently developed a highly efficient plasma target to neutralize negative ion beams for the formation of intense neutral particle beams. The stable, 80 cm long plasma target has a plasma thickness of  $2.2 \times 10^{15}$  atoms/cm<sup>2</sup>, optimum for the neutralization of 1 MeV D<sup>-</sup> ions. A second NPI team, headed by A. F. Sorokin, studied electron stripping of negative ions and charge exchange in oil vapor targets.

American research on a variety of gas and vapor targets included that at the University of Wisconsin on the stripping of 30 to 200 keV H<sup>-</sup> ions [24]. The neutral fractional yields and the total charge-exchange cross sections were measured. In the range of 100 to 200 keV incident H<sup>-</sup> ion beam energy, lithium, sodium, cesium, and hydrogen were shown to be good neutralizers, yielding neutral fractions of 0.63, 0.60, 0.58, and 0.58, respectively, at 100 keV. Calculations at BNL demonstrated that a simple deuterium gas cell can provide values above 60% neutralization for an H<sup>-</sup> ion beam of energies above 40 keV [25]. A double gas cell scheme can increase the neutralization to above 75%. BNL had previously investigated the use of various gas and vapor jets for neutralizing 150 keV H<sup>-</sup> beams and measured optimum target thicknesses and neutralization efficiencies as a function of beam energy [26].

Neutralization of negative ions other than hydrogen were recently investigated by BNL in conjunction with Princeton University. Researchers there investigated the stripping of negative lithium, carbon, oxygen, and silicon beams at energies up to 7 MeV, using nitrogen, argon, and carbon

dioxide neutralizers [27]. Tests with negative lithium beams showed neutral fractions of 45% to 48%; smaller values (28% or less) were achieved with the heavier ions.

Plasma targets for neutralizing negative ion beams have been investigated at LBL [28] and BNL [29]. LBL used a pulsed hydrogen plasma discharge and a low-density Cs plasma as neutralizers for a  $D^-$  beam produced by a 300 keV research accelerator [28]. The hydrogen plasma neutralizer used a 100 A discharge with a 1 ms pulse duration, creating a highly ionized hydrogen plasma 2 cm by 10 cm in cross section with a maximum electron line density of  $10^{15}$  atoms/cm<sup>2</sup>. The Cs plasma neutralizer, confined by an axial magnetic field, has a diameter of 5 cm and reaches densities of about  $10^{10}$  atoms/cm<sup>2</sup>. Conversion coefficients have not yet been reported from these experiments. BNL calculated the optimum target thickness and maximum neutralization efficiency as a function of  $H^-$  beam energy, target thickness, and percentage of target gas ionized. It is considering a plasma target having a series of small jets that should be able to neutralize an  $H^-$  beam of up to several amperes at 150 keV with a neutralization efficiency of 80% to 87% [29].

The use of laser photodetachment for the neutralization of  $H^-$  and  $D^-$  ion beams has been considered at the Avco Everett Research Laboratory [30]. Calculations made to determine the efficiency of the laser neutralization of negative ions as a function of beam energy, power, and ion source emittance indicated that the neutral beam production efficiency can approach 100%, considering only neutralizer losses. In the interaction geometries considered, the laser was assumed to be either collinear or perpendicular to the ion beam. LLNL has also considered laser photodetachment [31].

There is no indication that the Soviets are developing photodetachment targets equivalent to those being considered in the United States.

## 5. NEUTRALIZATION OF HIGH-ENERGY NEGATIVE ION BEAMS

Negative ion beam stripping at high energies has been studied theoretically for at least ten years at the Institute of Nuclear Physics

Research and the Radiotechnical Institute. This research has been conducted in conjunction with the development of a linear accelerator to be used in a meson factory at the Intermediate Energy Physics Complex of NPRI. An NPRI team headed by A. K. Kaminskiy is working on  $H^-$  ion beam neutralization in linear accelerators of 100 to 600 MeV and calculating angular and energy distributions of ions emerging from various charge-exchange targets. An RTI research team under B. P. Murin and A. P. Fedotov is involved in theoretical calculations of electron stripping of high-energy  $H^-$  beams in background gases. RTI is also studying the formation of  $H^-$  ion bunches and their injection into linear accelerators. No experimental data on  $H^-$  beam stripping at high energies have yet been reported.

Several U.S. research laboratories have been investigating negative hydrogen ion beam stripping at very high energies. LASL incorporated a new type of charge-changing injection technique into the design of the high-current proton storage ring. The 800 MeV negative hydrogen ion beam formed by the LAMPF linear accelerator is neutralized by the dissociation of  $H^-$  ions when they are passed through a specially configured magnetic field. The 100% neutral hydrogen beam is then converted to protons by a stripping foil and becomes part of the stored circulating beam [32].

LASL also measured the  $H^-$  electron detachment rate as a function of rest-frame electric field. These values can now be used to calculate with good accuracy the loss of ions along the transport line and the quality of the neutral beam that can be obtained by field stripping of the ion beam [33]. The stripping of the weakly bound second electron from the  $H^-$  ions can be accomplished with the help of very high electric fields (of the order of  $10^8$  V/m). However, for high energy beams of 800 MeV  $H^-$  ions, the electric fields can readily be obtained in the center of the mass frame by applying a transverse magnetic field of over 0.4 Tesla in the laboratory frame [32]. The  $H^-$  electron stripping rates were measured in [33] and calculated in [32] using  $H^-$  decay rates obtained as part of the Triumf  $H^-$  ion cyclotron design effort [34].

Electron-loss cross-section measurements were made at the Fermi National Accelerator Laboratory (Fermilab) in 1979 by injecting a 200 MeV



$H^-$  ion beam from the linac into the booster accelerator for up to  $140\ \mu s$  and stripping the beam with carbon stripping foils [35,36]. Beam currents of up to 43 mA were used. Various stripping methods were investigated, including charge exchange in gases, dissociation in magnetic fields, photodetachment, and the use of organic and inorganic foils. Only carbon foils and metallic films were finally chosen as potential candidates for strippers at these energies [36].

BNL is using its 200 MeV linac for injecting  $H^-$  into the alternating gradient synchrotron [37]. A new magnetron surface-plasma source (of the Fermilab design) has been adapted to provide 40 mA of  $H^-$  ion beam for the linac. The source operates at a repetition rate of 5 Hz, with pulse lengths of up to  $250\ \mu s$  duration. Beam current emittance and stability of the source have been measured as a function of source parameters.

The Argonne National Laboratory (ANL) measured emittance on the 50 MeV  $H^-$  linear accelerator, which was used as an injector into the IPNS-1 rapid-cycling synchrotron. The measurements involved a novel technique using the single charge stripping of negative ions passing through thin and narrow foils to measure the divergence and momentum spectra of the ion beam [38]. ANL had previously shifted from a double-charge-exchange to a Dimov-type Penning surface-plasma source as the intense  $H^-$  source for the IPNS-1 [39]. The surface-plasma source, designed by P. Allison [40], can operate continuously for more than a week at 45 mA of  $H^-$  at 15 Hz with an  $80\ \mu s$  pulse length [41].

Soviet research on the neutralization of high-energy negative ion beams is apparently limited to the theoretical work at NPRI and RTI, and no experimental data on high-energy stripping have yet been published.

## 6. NEUTRAL BEAM INJECTORS

Soviet research on neutral atom injectors for fusion purposes is centered mainly at the Kurchatov Institute. Here, a team headed by N. N. Semashko recently developed a deuterium atom injector with a proposed total neutral-beam power of 40 MW to inject deuterons into tokamak

plasmas for thermonuclear fusion applications. This injector uses a low-energy positive ion beam which is transformed into a negative ion beam in a vapor target and then into a neutral beam by an electron stripper.

The OGRA-IV is currently being built at Kurchatov for an experiment in which four neutral beams will be injected into a superconducting "baseball" plasma trap. Using positive rather than negative ions, simple magnesium jets will form the neutral beams and block the gas flows.

From 1970 to 1976, a Kurchatov team led by V. I. Pistunovich studied charge-exchange processes for plasmas flowing through gases and for plasma heating in tokamaks. This team developed the INES coaxial plasma injector. The tokamak T-11 is now operating with neutral beam injections. The tokamak T-15 facility, incorporating 80 keV neutral beam injection and niobium-tin superconducting toroidal field coils, now under construction, is expected to begin operation in December 1985 [42].

The AMBAL ambipolar trap facility, now being assembled at NPI for start-up in 1983, will use 25 keV neutral hydrogen atom beams to heat and sustain the plasma. NPI has also been working since 1976 on the development of diagnostic injectors for analyzing the density and other characteristics of magnetically confined thermonuclear plasmas. These injectors demand relatively intense monoenergetic beams of high enough energy to penetrate the dense plasma.

At IPI, a research team led by V. V. Afrosimov and M. P. Petrov has been experimenting on T-4, T-6, T-10, and Tuman-2 tokamaks, concentrating on the formation of neutral atomic beams, the scattering of these beams by plasmas, and the development of systems to analyze the beams.

In the United States, LBL and LLNL are jointly developing a megawatt, DC injection system for heating and fueling fusion devices, using negative ion beams. Optimization of the transmittance of DC negative ion beams using either double charge exchange or direct extraction (planotron surface-plasma sources and the LBL bucket source) have been investigated theoretically at LBL for energies up to 200 keV [43]. A proposed system utilizes a multiple-aperture source that creates an array of separate, well-defined beamlets extracted at 200 kV and neutralized by a magnetic bucket plasma target [28,43,44]. The beamlets pass between rows of

permanent magnets into and out of the plasma neutralizer. Beam divergences have been calculated to be small enough to allow the product beams to emerge on the far side of the neutralizer 50 to 100 cm downstream.

The Princeton Plasma Physics Laboratory is reassessing the engineering test facility (ETF) tokamak in the form of the fusion engineering device (FED), which uses  $D^-$  instead of  $D^+$  beams so as to avoid some of the problems inherent in the ETF [10]. The reassessment showed the considerable advantages of using  $D^-$  beams. An optimal heating energy of about 250 keV is being considered on the assumption that a 65 A negative ion source will become available [45].

A neutral beam injection system has been considered by TRW for the current drive of the Starfire tokamak at the Argonne National Laboratory, which is to use 2 MeV  $D^-$  beams from an ESQ accelerator. The beams are focused and bent toward the tokamak by a single magnet and then neutralized by laser beams [46].

The Institute of Nuclear Engineering in Karlsruhe, West Germany, is working on a 1 A negative ion source using neutral clusters [47,48]. The neutral clusters, formed by the partial condensation of the expanding gas flow, are ionized by an electron beam to form positive ion clusters, which are then accelerated and passed through a Cs gas jet. The clusters are transformed into a negative ion cluster beam in the jet by the following sequence: destruction of the clusters; dissociation of the  $D_2$  molecules; and charge-exchange to convert the  $D^0$  to  $D^-$  with a conversion efficiency of about 20% to 30%. The negative beam can then be accelerated to the required energies (about 500 keV) and neutralized by a gas target. Tests have shown that the accelerated cluster ions interacting with a gas target disintegrate into neutral fragments with high efficiency. A compact tandem design, incorporating the source, a Cs vapor jet, and gas beam neutralizer, is being considered so as to keep the complex system for producing positive cluster ions at ground potential [48]. No total beam output measurements have yet been reported. The Soviets also experimented with the formation of neutral clusters, using the old INES injector at Kurchatov. This research appears to have ended in 1976, since which time no further mention has been made in the open literature of this work or the researchers involved.

The joint development of an injector system by LLNL and LBL in the United States parallels the Soviet work at Kurchatov. The Kurchatov injector, which is to operate at 400 to 600 keV, will eventually provide a total neutral beam power of 30 to 40 MW from several accelerator modules operating in parallel. In the U.S. version, the multiple beam array will be extracted at 200 kV.

### III. DEVELOPMENT OF HIGH-INTENSITY NEGATIVE ION SOURCES IN THE USSR

#### 1. DIRECT-EXTRACTION SURFACE-PLASMA ION SOURCES

The Soviets can now produce negative ion beams for both pulsed and continuous beam operation. Recent revisions and upgrading of the Soviet surface-plasma ion source are described below.

The surface-plasma ion source was developed at NPI with both a planotron (magnetron) and a Penning-type discharge chamber. The major breakthrough came in 1971, when NPI researchers introduced cesium vapor into the source discharge chamber and observed a marked increase in the source's negative ion yield. This increase in negative ions is attributed to the cesium's coating the cathode surface, thereby lowering the surface electron work function and increasing the probability of electron capture from the cathode.

Since then, the surface-plasma source has been redesigned several times. In 1980, NPI developed a multiple-slit version that increased plasma uniformity by feeding hydrogen gas and cesium vapor into each cathode groove through a thin slit. This new source design improved both the beam current and beam optics and reduced the cathode heat load [49]. A maximum negative hydrogen ion beam current of 4.0 A was obtained from a source with five emission slits (each  $0.8 \times 50 \text{ mm}^2$  in area), with a discharge current of 400 A, energy consumption of 10 keV/ion, and gas efficiency of 10%. The current density in the extraction gap reached  $440 \text{ mA/cm}^2$ . More efficient operation was obtained by running the source at a reduced  $\text{H}^-$  output of 1 to 2.8 A with pulses of 1 ms duration, energy consumption of 4 keV/ion, and reduced heat load of 0.1 to 1 kW/cm<sup>2</sup>. The  $\text{H}^-$  beam is now extracted at 30 kV. A test stand is being constructed for postacceleration of the beam to 150 kV, using a single aperture.

In 1981, NPI researchers developed a honeycomb multiple-aperture source with a beam current and current density equivalent to those of the multislit version [50]. The honeycomb version provided 4 A of  $\text{H}^-$  with a  $445 \text{ mA/cm}^2$  beam current density at a discharge current of

600 A, and a gas efficiency of about 20%. The focusing of the individual  $H^-$  ion beams was accomplished with spherical depressions on the cathode surface for each circular emission aperture in the anode. NPI researchers seem satisfied with their latest source developments.

Research at NPI is now being diverted from negative ion beam systems to the AMBAL ambipolar magnetic trap, however, and negative ion research at that institute is expected to slow down or even to end [42,51]. The AMBAL facility uses the injection of neutral beams for heating and maintaining the plasma. The neutral beams are formed by direct charge exchange of a 25 keV positive hydrogen ion beam in a magnesium vapor jet target. Initial tests of this experiment with a 10 keV  $H^+$  beam showed an  $H^0$  beam conversion of 85% [52].

Researchers at the Yefremov Institute, working under contract for N. N. Semashko of the Kurchatov Institute, measured 2.4 A of  $H^-$  ion output from their hollow, negative-ion surface-plasma source with an emission diameter of 10 cm [53]. No further information on this source is presently available.

## 2. DOUBLE-CHARGE-EXCHANGE ION SOURCES

Double charge exchange is the alternative to direct extraction for obtaining intense negative ion beams for neutral beam production. In double charge exchange, an intense beam of positive ions is passed through a vapor target (usually an alkali metal jet of sodium or cesium, which converts the positive ions into negative ions by double electron capture). The negative ion beam is then accelerated to the required energy and neutralized by stripping the electrons from the negative ions in a beam neutralizer. With this method, the positive ion beam is accelerated to energies of only several keV so as to make best use of the high cross-section values existing at low energies for this charge-exchange process. The success of this method of neutral beam production stems primarily from its high neutralization efficiency, the high currents that are now available from positive ion sources [54,55], and the recent development of efficient vapor jet targets that minimize gas loads to the high-vacuum system of the

injector. The disadvantage of this method lies in the higher beam emittance, the inherent possibility of contaminating the injector vacuum system, and the difficulties of extracting and transporting large beam currents at low voltages.

The development of more efficient vapor-jet charge-exchange targets is minimizing some disadvantages of double charge exchange. Such targets are now being used as pumps, providing both vacuum pumping and source gas recirculation, as well as establishing the required gas target thickness for maximum conversion of positive to negative ions. The recirculation of the ion source gas, which is pumped through the target vapor jet and returned to the source to be reused, decreases the total gas load to the injector vacuum system. Soviet researchers are studying and designing vapor-jet charge-exchange targets for both the production of negative ion beams by transforming positive ion beams into negative ion beams (double charge exchange) and the transformation of negative ion beams into neutral beams (electron stripping of the negative ion beams).

The intensity and angular spread of the initial positive ion beam, the effectiveness of transforming positive into negative ions, and the scattering of the particles in the charge-exchange target affect the intensity and angular spread of the formed negative ions. The effectiveness of the negative ion formation, the energy of the charge-exchanged particles, and the thickness of the vapor target depend on the choice of the target material.

This section discusses the development and refinement of vapor targets at the Kurchatov, IFTT, and NPI, with particular attention given to the mechanics of the vapor jet, the choice of material for the jet, its vacuum properties, its optimum target thickness, and its ability to act as a pump, a vacuum lock, and a gas recirculator. A typical neutral beam injector system based on the use of double charge exchange to form negative ion beams is described in Section V, 3. In this type of system, the  $D^0$  beam output may range from 60% to 90%  $D^0$ , with an output from the charge-exchange target of about 15%  $D^-$  going into the accelerator module [56].

### 1. Alkali Metal Vapor Target Developments

Researchers at the Kurchatov Institute initially used small target apertures (10 cm in diameter) [57,58] and 5 keV negative ion beams with currents of up to 150 mA and a pulse length of 10 ms to test alkali-metal-vapor charge-exchange targets. The positive ions for the charge exchange were generated by an IBM-3 positive ion source without external magnetic fields [55]. This source, which operates with a three-element ion optical system, was designed for use at low energies. Another positive ion source, the IBM-5, developed at Kurchatov in 1979 for use in the tokamak T-11 injector, can provide up to 35 A of  $H^+$  at 25 keV with a pulse length of 20 ms [54]. This source uses no external magnetic field, has an emission aperture consisting of 42 slits (each  $8 \times 0.2 \text{ cm}^2$ ), and produces an initial beam cross section of  $8 \times 18 \text{ cm}^2$ . The dispersion angle of the beam is  $\leq .06^\circ$  along the slits and  $2.5^\circ$  perpendicular to the slits.

The latest sodium charge-exchange target developed at the Kurchatov Institute [59,60] has beam apertures of  $22 \times 48 \text{ cm}^2$  (see Fig. 2). Intended for use with the IBM-6 positive ion source [61], this target design will eventually be able to handle 5 to 10 A of negative ion beam current. In this version, two electromagnetic pumps pump molten sodium along heated pipes from the condenser (7) to the vapor generator (1), where sodium vapor is formed. The vapor is transmitted from the generator to the separator (2) through a flat Laval nozzle with the critical dimension of  $1 \times 500 \text{ mm}^2$ . In the separator, the large-angle peripheral part of the jet is cut off. The collimated central part of the jet is then passed through the hydrogen beam charge-exchange region and collected by the horizontal and vertical surfaces of the condensers (5) and (7). The temperature of all surfaces exposed to the vapor jet are maintained above the melting point of sodium with help of controlled silicon oil (type PES-3) flow through the cooling coils. The sodium condenses on these surfaces, flows down to the inputs of the electromagnetic pump, and then is pumped back to the vapor generator. The silicon oil, with a boiling point of  $300^\circ\text{C}$ , is also used to melt the sodium at the start-up



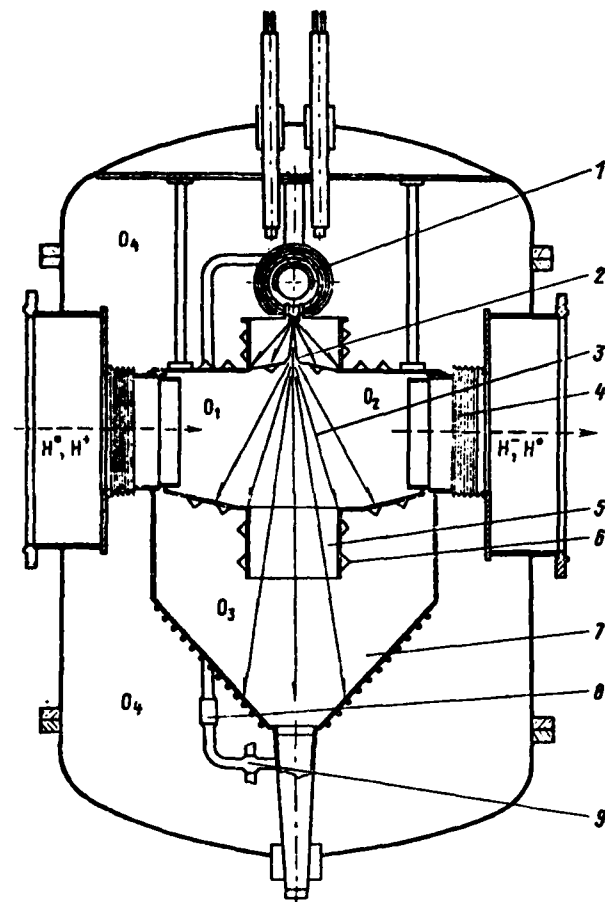


Fig. 2--Sodium charge-exchange target [59,60]

- 1--vapor generator
- 2--separator
- 3--area of ion beam charge exchange
- 4--bellows
- 5--intermediate condenser
- 6--cooling coils
- 7--condenser
- 8--one-way valve
- 9--electromagnetic pump

Solid arrows indicate Na vapor flow  
Dashed arrows show ion and atom beams

- O<sub>1</sub>--ion drift space between the positive ion source and vapor target
- O<sub>2</sub>--ion drift space between vapor target and negative ion preacceleration system
- O<sub>3</sub>--condenser (7)
- O<sub>4</sub>--target envelope

of the target operation. The  $O_3$  and  $O_4$  areas are pumped by diffusion pumps H5T and H2T, respectively, both equipped with absorption traps.

Details of the vapor generator are shown in Fig. 3. The liquid sodium is stored in the pocket formed by the inner cylinder (2) and

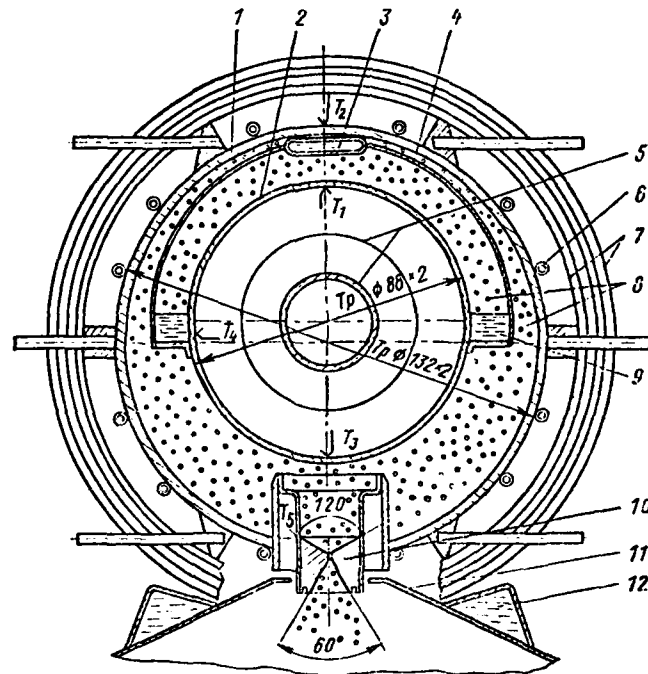


Fig. 3--Vapor generator [59,60]

- 1--external cylinder
- 2--internal cylinder
- 3--distribution pipe
- 4--semicylinder
- 5--internal heater
- 6--external heater
- 7--shields
- 8--Na vapor
- 9--liquid Na pocket
- 10--nozzle
- 11--separator body
- 12--separator cooling duct
- $T_1$  to 5--thermocouples

the semicylinder (4). The internal coaxial tantalum heater (5) provides up to 10 kw of power for the evaporation process. An auxiliary molybdenum heater (6) on the external cylinder (1) has a power of up to 5 kW. All elements of the vapor generator, except the heaters and the three external stainless steel shields (7), are made of niobium. Sodium is fed into the vapor generator once every 60 to 90 seconds with a 5- to 10-second flow duration. The sodium evaporates immediately on entering the pocket. The vapor is channeled to the nozzle through an area opening of approximately  $5 \text{ cm}^2$  in the top part of the semicylinder. The temperature at various points of the vapor generator is controlled by chromel-alumel thermocouples  $T_1$  to  $T_5$ . The separator, condenser, and other parts of the target are made of stainless steel and the electrical connections of copper.

The sodium target was able to operate continuously and to provide a constant vapor thickness of up to  $5 \times 10^{15} \text{ atoms/cm}^2$ . The only limit was the power input to the inner heater of the vapor generator. The sodium vapor density distribution in the proximity of the charge-exchange area was measured by placing 40 metal cups along the beam line, 10 cm below the beam axis. The sodium jet was turned on for 20 to 40 minutes. Each cup was then weighed to measure the amount of collected sodium. Figure 4 shows the results of the measurements.

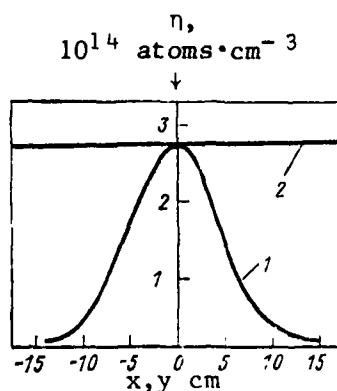


Fig. 4--Distribution of sodium vapor density in jet [59]

x--in direction of charge-exchange beam  
y--along vapor generator nozzle

Zero on abscissa corresponds to point on vapor jet 10 cm below the ion beam axis

In 1980, Kurchatov Institute researchers experimented with the injection of hydrogen, deuterium, helium, nitrogen, and argon gases into the sodium vapor jet [59]. Measurements were taken of the pressure ratio  $p_1/p_2$  as a function of  $p_1$  at various gas flows from the ion source for vapor target thicknesses  $\delta$  from  $2$  to  $5 \times 10^{15}$  atoms/cm<sup>2</sup>. The pressure drops across the vapor jet for the various gases with a constant  $\delta = 3.5 \times 10^{15}$  atoms/cm<sup>2</sup> are shown in Fig. 5.

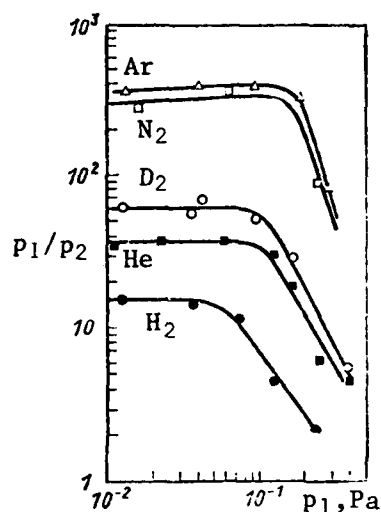


Fig. 5--Pressure drop across Na vapor target as a function of ion source volume pressure for various gases [59]

The relationship of the  $p_1/p_2$  values taken at the plateaus of the different gas curves demonstrates the dependence of these values on the mass and size of the gas molecules, which is tied to the mechanics of gas penetration through the vapor jet. For the same operating conditions, the pumping speed of the jet was measured for each gas at a constant gas load of  $0.8 \text{ m}^3 \text{ Pa/s}$ , with the following results [59].

Gas	Pumping Speed
H <sub>2</sub> .....	6.7 m <sup>3</sup> /s
He .....	6.2 m <sup>3</sup> /s
D <sub>2</sub> .....	6.0 m <sup>3</sup> /s
N <sub>2</sub> .....	4.0 m <sup>3</sup> /s
Ar .....	3.6 m <sup>3</sup> /s

The maximum pressure drop  $p_1/p_2$  of 100 was obtained for  $H_2$  with  $\delta = 3$  to  $5 \times 10^{15}$  atoms/cm<sup>2</sup> and  $p_1 \approx 10^{-1}$  Pa. For the same target thickness, the ratio of  $p_3/p_2$  was a factor of 10 higher than for  $p_1/p_2$ , with the pressure  $p_3$  under the beam axis greater than 1 Pa. The pressure  $p_1$  in the  $O_1$  area is determined by the gas flow out of the positive ion source and can reach  $5 \times 10^{-1}$  Pa. The pressure  $p_2$  in the  $O_2$  area should not exceed the pressure at which noticeable negative ion stripping would occur before the negative ions have had a chance to be preaccelerated to the required energy. In the MIN injector at Kurchatov, this value of  $p_2$  should be less than  $1 \times 10^{-3}$  Pa.

With the use of the Na vapor target the maximum conversion of the  $H^+$  (or  $D^+$ ) ions into  $H^-$  ions was found to be 0.12 (see Fig. 7, below) [62]. This means that about 88% of the beam passing through the vapor target consists of atoms that have to be pumped out of the  $O_2$  area.

The angular distribution of the  $H^-$  beam current density was measured using an electrostatic deflection system and a slit current detector, with a vapor target thickness of 1 to  $5 \times 10^{15}$  atom/cm<sup>2</sup>, positive ion beam energy of 3 to 8 keV, and beam current density of 5 mA/cm<sup>2</sup>. The measurements showed a widening of the distribution function by  $0.15^\circ$  when the target thickness was increased by  $\Delta\delta = 1 \times 10^{15}$  atoms/cm<sup>2</sup> at a 5 keV beam energy.

These experiments also detected the presence of components of the  $H^-$  beam, which had energies of one-half and one-third that of the initial energy  $E_0$ . The presence of these components results from the dissociation of the molecular components of the positive ion beam ( $H_2^+$ ,  $H_3^+$ ) and their charge exchange in the vapor target. At a target thickness of  $\delta = 2.5 \times 10^{15}$  atoms/cm<sup>2</sup> and energy  $E_0 = 6.5$  keV, the composition of the analyzed  $H^-$  beam was found to be in the ratio of 0.45:0.28:0.27, corresponding to an  $H^-$  beam having energies of  $E_0$ ,  $1/2 E_0$ , and  $1/3 E_0$ , respectively. The presence of large low-energy components indicates considerable molecular ion dissociation in the Na jet even before it approaches equilibrium thickness. The beam-current-density angular-distribution measurements showed that the  $1/2 E_0$  and  $1/3 E_0$  components of the negative ion beam had increased in angular distribution by  $0.1^\circ$  and  $0.3^\circ$ , respectively, over the  $E_0$  value [59].

### 11. Comparison of Cesium and Sodium Vapor Targets

The choice of target material was not obvious because of the scarcity of data on the angular dispersion of negative ions formed by the charge exchange of protons in Cs and Na vapors. Although considerable data had been collected on the conversion coefficient of positive to negative ions  $\eta^-$ , the results obtained by various authors for Cs differed, largely because of the low transmittance of the optical system for beams having energies of 1 keV or less--the type of system that must be used with Cs. A recent high-transmittance system [62], however, allows 100% transmission of both positive and negative ion beams through the system, even at the lowest energies. This apparatus was used to measure the charge-exchange coefficient of positive to negative hydrogen and deuterium ions and the dispersion of the negative ions formed in Cs and Na vapors. Cs and Na vapor targets were compared for optimum charge exchange of ion beams.

A schematic of the experimental apparatus used to compare charge exchange in Cs and Na vapor targets is shown in Fig. 6. The proton or deuteron ion beam is formed in the radio-frequency source (1), separated by the magnetic analyzer (2), decelerated to the required energy and focused by the ion optical system (4), and then collimated before it enters the target (9). The beam current at the target entrance is measured by a movable faraday cup (8) and the energy spectrum by a retractable grid analyzer (7). To determine the background signal caused by neutrals entering the target, an electrostatic deflection system (6) deflects the charged component of the beam out of the beam line. The system analyzing the beam leaving the target consists of an electrostatic lens (10), aperture (11), and faraday cup (12). The lens potential is chosen so as to focus the component of the ion beam being measured and to reject the opposite charge component of the beam. The experiment differed from earlier ones (as in [63]) only in that it did not use permanent magnets, which were found to deflect the beam at energies below 0.5 keV and thus to produce erroneous results. The alkali metal vapor target used in the present experiments is described in [58,64].

To measure the beam dispersion angle, the lens, aperture, and faraday cup (10, 11, and 12 of Fig. 6) are replaced by a scanning

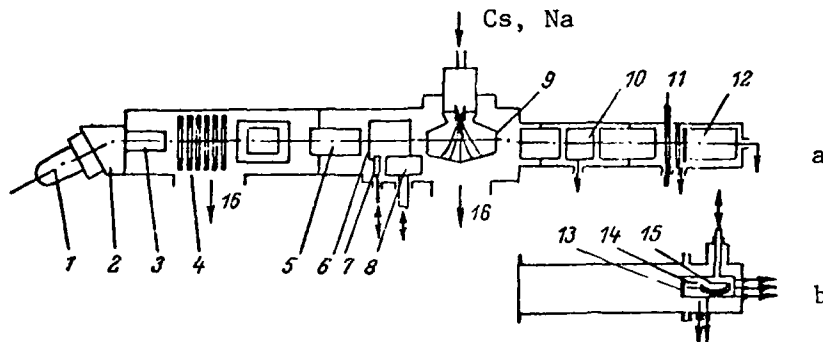


Fig. 6--Experimental apparatus used to compare charge exchange in Cs and Na vapors [62]

a--Apparatus for measuring conversion coefficient  
b--Apparatus for measuring beam dispersion angle

- 1--positive ion source
- 2--magnetic analyzer
- 3, 5, 13--collimators
- 4--ion optical system
- 6--electrostatic deflection system
- 7--grid analyzer
- 8--movable faraday cup
- 9--target
- 10--electrostatic lens
- 11--iris diaphragm
- 12--faraday cup
- 14--electrostatic deflection system
- 15--electron multiplier
- 16--pumps

detector composed of a 0.3 mm diameter collimator (13) and channel electron multiplier (15). The conversion coefficient  $\eta^-$  was determined by the ratio of the negative ion beam current measured beyond the vapor target to the positive ion beam current measured at the entrance to the target. For each specific beam energy,  $\eta^-$  was recorded as a function of target thickness. The maximum value of  $\eta^-$ , corresponding to a homogenous target thickness, is shown in Fig. 7. Measurement errors are about 15% in Cs and about 10% in Na. The results agree well with the data of A. S. Schlachter [22] in the proton energy range above 1 keV. Earlier measurements of  $\eta^-$  for protons in Cs are given in [65].

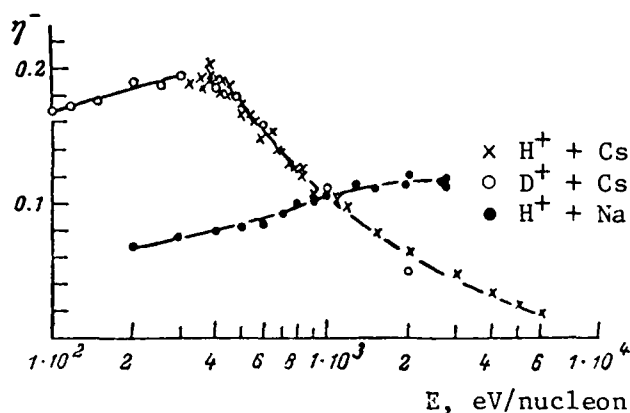


Fig. 7--Dependence of conversion coefficient  $\eta^-$  on ion beam energy  $E$  in Cs and Na vapors [62]

Data on the dispersion of the formed negative ions are shown in Fig. 8, in which each data point represents an average of several measurements. Although the scatter of data in the individual measurements was not great, an analysis of systematic errors indicated that the measured values of the half-angle divergence  $\theta/2$  and target thickness  $\delta$  deviated as much as 50% from the real values [62].

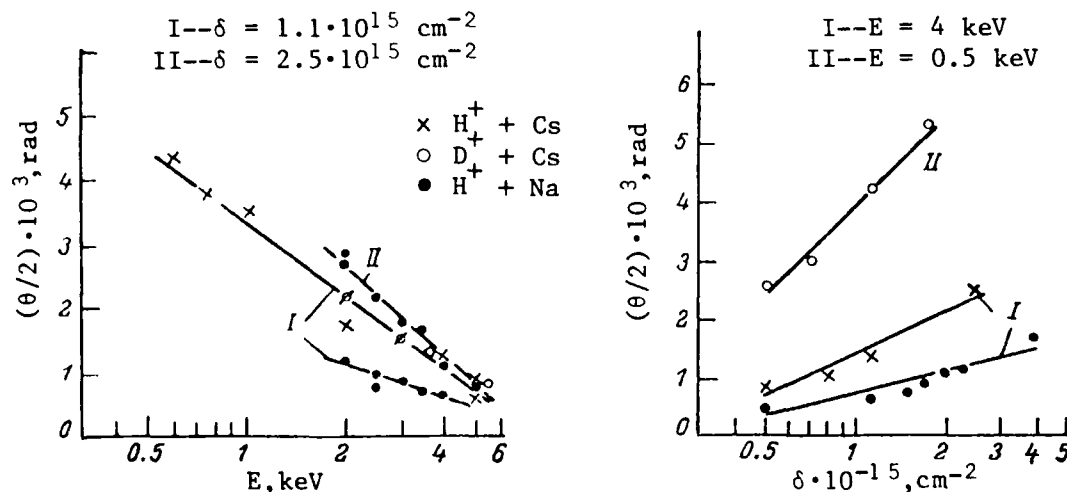


Fig. 8--Dependence of half-angle divergence of negative ions on energy (left) and target thickness (right) [62]



The experimental results and other pertinent information comparing Cs and Na charge-exchange vapor targets are presented in Table 1. One notes the low  $H^+$  and  $D^+$  energy required for the maximum production of negative ions in Cs. For this optimum energy ( $E_{opt}$ ), the positive ion beam current density that can be produced is an

Table 1 [62]

## COMPARISON OF Na AND Cs CHARGE-EXCHANGE TARGETS

	Sodium	Cesium
Conversion coefficient $\eta_{max}^-$	0.116	0.195
Ion energy $E_{opt}$ , corresponding to $\eta_{max}^-$	2.5 to 5.0 keV ( $H^-$ ) 5.0 to 10.0 keV ( $D^-$ )	300 to 400 eV ( $H^-$ ) 600 to 800 eV ( $D^-$ )
Positive ion current density at $E_{opt}$	$\sim 50$ to $100$ mA/cm <sup>2</sup>	$\sim 5$ mA/cm <sup>2</sup>
Optimum charge-exchange target thickness $\delta_{opt}$	$\sim 2$ to $10^{15}$ atoms/cm <sup>2</sup>	$\sim 1 \times 10^{15}$ atoms/cm <sup>2</sup>
Half-angle dispersion of negative ions at $E_{opt}$ , $\delta_{opt}$	$2.2 \times 10^{-3}$ rad ( $H^-$ )	$\sim 5 \times 10^{-3}$ rad ( $H^-$ ) $4 \times 10^{-3}$ rad ( $D^-$ )
Target thickness $\delta_{block}$ required to cut gas flow by factor of 1000 (calculated values)	$\sim 4 \times 10^{15}$ atoms/cm <sup>2</sup>	$\sim 2 \times 10^{15}$ atoms/cm <sup>2</sup>
Half-angle dispersion of negative ions at $E_{opt}$ , $\delta_{block}$	$3.5 \times 10^{-3}$ rad ( $H^-$ )	$\sim 7 \times 10^{-3}$ rad ( $D^-$ )
Saturated metal vapor pressure at operating temperature of condenser	$\sim 10^{-6}$ Torr	$\sim 10^{-5}$ Torr
Corresponding atom concentration	$2.4 \times 10^{10}$ atoms/cm <sup>3</sup>	$3.0 \times 10^{11}$ atoms/cm <sup>3</sup>
Nuclear charge	11	55
Atomic weight	23	133

order of magnitude lower in Cs than that for the optimum energy in the case of Na. Because the positive ion beam has a considerably larger dispersion at the lower energies, the dispersion in Cs at the optimum negative ion production energy is also considerably larger. Even when the lower  $\eta_{\max}^-$  in Na is considered, these factors lead to the conclusion that the ion source using a Na vapor target provides a denser negative ion beam with much lower dispersion.

Sodium was also found to be more suitable than other materials for the target vapor when the target jet was used as a vacuum lock or gas recirculator. In this mode of operation, the target thickness must be maintained at a higher value, thus producing a larger dispersion of the negative ion beam. There remains, however, no alternative to using the gas recirculating feature of the vapor jet, since this is the only way, at present, of decreasing the gas load to the high-vacuum system of the injector.

Other advantages of using Na in the system include its lower vapor pressure at the operating temperature of the condenser, leading to a smaller emission of the Na into the high-vacuum system, and its lower chemical activity, making it safer to use [57,62]. Thanks to sodium's lower nuclear charge, the plasma radiation loss with Na is a factor of 600 lower than the loss when Cs is used [45].

### iii. Vacuum Properties and Mechanics of Vapor Targets

According to investigations conducted at IFTT in 1979 [66], the alkali metal vapor jet can be used as a vacuum lock, a pump for gas flowing out of the positive ion source, and a compressor for recirculating the gas from the beam back into the discharge chamber of the positive ion source.

Large-aperture  $H^+$  ion sources used in high-intensity charge-exchange negative ion sources operate at a gas efficiency of 20 to 30% [64]. To prevent the destruction of negative ions extracted from the source, the pressure beyond the charge-exchange target, in the area where the negative ions are formed, should be less than  $10^{-5}$  Torr. At such pressure,  $H^-$  ion injectors need pumping speeds of hundreds of thousands of liters per second for each ampere of  $H^-$

ion beam. When the target operates as a vacuum lock and pump, practically all of the gas flowing from the positive ion source is displaced by the vapor jet to the area under the jet, where the gas can be pumped at a pressure of about  $10^{-2}$  Torr. All of the unused gas can therefore be recirculated from the area under the jet to the discharge chamber with the help of an electrically insulated gas flow path. This gas recirculation scheme increases the gas efficiency of the charge-exchange negative ion source, decreases the vacuum pumping requirements in the high-vacuum system, and makes the injector more compact.

The experimental apparatus for investigating alkali metal vapor targets with large (45 and 75 mm in diameter) beam apertures is shown in Fig. 9. The vacuum lock, pumping, and recirculating capabilities of the vapor flow were studied in detail. The supersonic sodium vapor jet is formed by a flat Laval nozzle (1), with  $S_{\text{exit}}/S_{\text{crit}} = 10$  and a 1 mm critical cross-section slit width. The densest part of the jet is collimated by the separator (4), passes through the charge-exchange area, and then condenses on the walls of the condensers (7) and (8). An electromagnetic pump (9) pumps the liquid Na back to the vapor generator (2) [64,66].

To simulate conditions in the actual vacuum system of the  $H^-$  ion injector, a radio-frequency ion source (10), of the type described in [67], was mounted on the experimental apparatus with vacuum plumbing connections. The gas flow out of this ion source runs along the beam pipe (5), is deflected downward by the Na vapor jet, and either passes through the pump manifold (11) to the booster pump (22), if valve (12) is open, or is pushed back towards the source through the manifold (14), if valve (13) is open and (12) is closed.

The pumping speed  $S$  of the Na vapor jet was determined by measuring the hydrogen gas flow through the jet and the input pressure  $p_1$ . Measurements were taken with  $p_1 = 10^{-3}$  to  $10^{-5}$  Torr and vapor target thickness = 2 to  $5 \times 10^{15}$  atoms/cm<sup>2</sup>. The results are shown in Fig. 10 for beam aperture 45 mm in diameter and a pressure  $p_3$  below the beam line of less than or equal to  $10^{-2}$  Torr [64].

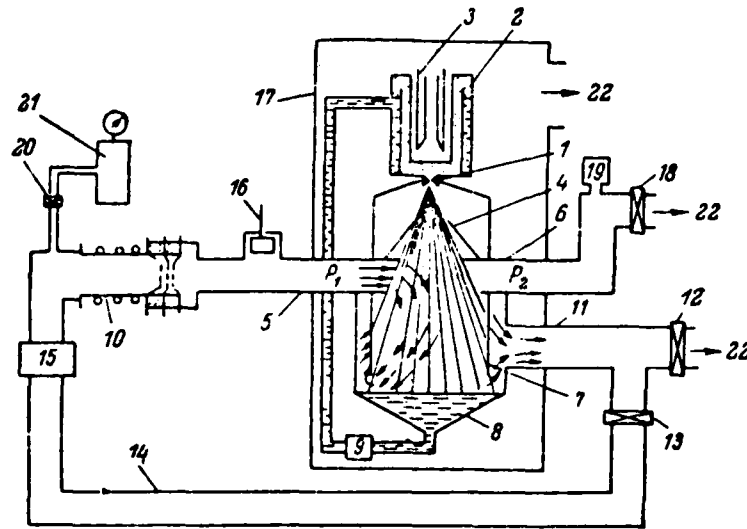


Fig. 9--Experimental apparatus for testing alkali metal vapor targets with 45-mm and 75-mm beam apertures [64]

- 1--Laval nozzle
- 2--vapor generator
- 3--heater
- 4--separator
- 5, 6--beam pipes
- 7, 8--condensors
- 9--electromagnetic pump
- 10--ion source
- 11--pump manifold
- 12, 13, 18--vacuum valves
- 14--gas manifold
- 15--electrically insulated gas pipe
- 16--Na vapor detector
- 17--target chamber
- 19--partial pressure analyzer (APDM-1)
- 20--gas leak
- 21--hydrogen bottle
- 22--manifold leading to pump

As can be seen from Fig. 10, the pumping speed is almost independent of  $p_1$  for this pressure range and of  $\delta$  for thicknesses greater than  $3 \times 10^{15}$  atoms/cm<sup>2</sup>. With a vapor target thickness of 2 to  $5 \times 10^{15}$  atoms/cm<sup>2</sup> and  $p_3$  from  $10^{-3}$  to  $10^{-5}$  Torr, the specific hydrogen pumping speed was found to be 5 l/s-cm<sup>2</sup> for the Na jet and 3.9 l/s-cm<sup>2</sup> for the He jet. These values are close to those

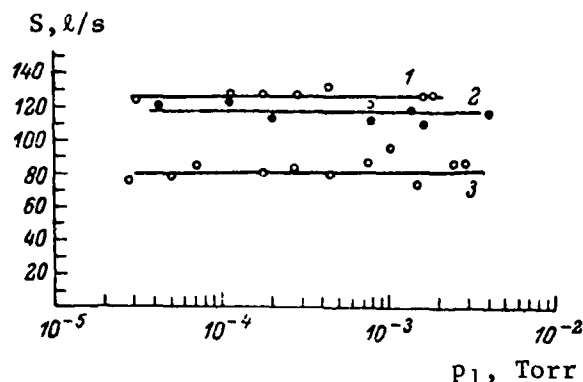


Fig. 10--Dependence of pumping speed of Na vapor jet on pressure [64]

- 1-- $\delta = 5 \times 10^{15}$  atoms/cm<sup>2</sup>  
 2-- $\delta = 3 \times 10^{15}$  atoms/cm<sup>2</sup>  
 3-- $\delta = 2 \times 10^{15}$  atoms/cm<sup>2</sup>

obtained by diffusion pumps. Pumping speeds were also measured using the inert gases Ne, Ar, and Xe.

Another test was made with hydrogen flowing from pipes (5) and (6) simultaneously (see Fig. 9, above). The results demonstrated equal gas loading on both sides of the vapor jet and a doubling of the pumping speed of the system. This shows that both sides of the vapor jet operate with equal efficiency [64]. Inasmuch as both sides of the vapor jet possess the same pumping speed, the gas-blocking capabilities of the jet can be determined by the value of the pressure ratio  $p_1/p_2$  as long as the jet is the sole means of pumping its surrounding areas. In this case, the gas is fed into the pipe (5) and valves (13) and (18) are closed. Table 2 gives the experimental values of the pressure ratios  $p_1/p_2$  for various jet thicknesses  $\delta$  and gases [66]. For these measurements, the pressure before the vapor jet  $p_1$  was kept at  $3$  to  $4 \times 10^{-3}$  Torr, corresponding to the actual values of the pressure to be found in negative ion injectors.

These investigations showed that the Na vapor jet, in addition to serving as a charge-exchange medium for a hydrogen ion beam, can also provide a substantial barrier to the gas flowing out of the

Table 2 [66]

GAS PRESSURE RATIO AS A FUNCTION OF TARGET THICKNESS

$p_1/p_2$	$\delta$ , atoms/cm <sup>2</sup>		
	$2 \times 10^{15}$	$3 \times 10^{15}$	$5 \times 10^{15}$
H <sub>2</sub>	$1 \times 10^2$	$1.2 \times 10^2$	$4.6 \times 10^2$
He	$1.3 \times 10^2$	$1.4 \times 10^2$	$1 \times 10^3$
Ne	$1.1 \times 10^3$	--	--
Ar	$6 \times 10^2$	--	--
Xe	$1 \times 10^3$	--	--

positive ion source. Thanks to the gas-blocking capability of the jet, the gas can be pumped away by the forepump in the  $10^{-2}$  to  $10^{-3}$  Torr range, decreasing the high vacuum-pumping requirement beyond the vapor jet by a factor of 100 or more.

In 1980, the Kurchatov Institute made a theoretical analysis of gas penetration through an ultrasonic vapor jet, on the assumption that the gas dynamics in the vapor jet acquire diffusion characteristics [68]. Expressions were derived to calculate the pressure drop across the vapor jet, various gas flows, and pressures for a series of geometries and materials used in the vapor jets.

The IFTT experiment also investigated the recirculation properties of the Na vapor jet to determine the possibility of pumping the positive ion source gas load back into the source discharge chamber, using the apparatus shown in Fig. 9, above [64]. To maintain the required ion source pressure of approximately  $10^{-2}$  Torr, the hydrogen flowed out of the bottle (21) through the gas leak (20) at a rate of  $1.4 \text{ atm-cm}^3/\text{s}$  and was pumped through valve (12). When the system was set up to test the gas recirculation capability, valves (18) and (12) were closed and (13) was open. Then the gas from the area below the beam was forced to flow through the manifold (14) and insulated pipe (15), back to the ion source discharge chamber. To maintain the  $10^{-2}$  Torr source pressure, the hydrogen gas flow from the bottle had to be lowered to  $8 \times 10^{-2} \text{ atm-cm}^3/\text{s}$ .

Typical pressures for this experiment were  $p_1 = 5 \times 10^{-3}$  Torr,  $p_2 = 4.5 \times 10^{-5}$  Torr,  $p_3 = 3 \times 10^{-2}$  Torr (under the beam line), and source pressure  $\sim 10^{-2}$  Torr. The measurements showed that about 95% of the hydrogen gas flowing out of the source was recirculated to the source, with only a 5% loss to the high-vacuum side. The recirculating hydrogen flow rate was  $1.32 \text{ atm-cm}^3/\text{s}$ . To pump this gas load at a pressure of  $4.5 \times 10^{-5}$  Torr would require a pumping speed of about  $2 \times 10^4 \text{ l/s}$ , but with the Na jet recirculating the hydrogen, this pumping requirement could be dispensed with.

Finally, the IFTT experiment was used to study the formation of sodium hydride as a result of the reaction of the hot Na jet and the hydrogen gas pumped by the jet. The chemical reaction is  $2\text{Na} + \text{H}_2 \rightleftharpoons 2\text{NaH}$ . The conditions in the condenser, where the liquid Na is  $100^\circ$  to  $120^\circ\text{C}$  and the hydrogen gas pressure  $p_3$  is  $10^{-2}$  to  $10^{-3}$  Torr, are right for the formation of sodium hydride; the reverse reaction (the dissociation of the hydride) takes place in the vapor generator at a temperature of approximately  $700^\circ\text{C}$ . Measurements with the partial pressure analyzer (item 19 of Fig. 9), however, showed no presence of NaH peaks. This can be explained, first, by the very small hydride formation at the liquid Na temperature of  $120^\circ\text{C}$  and, if it is formed, by its complete dissociation in the vapor generator at the  $600^\circ$  to  $700^\circ\text{C}$  temperatures needed to obtain the vapor thickness of  $1$  to  $5 \times 10^{15} \text{ atoms/cm}^2$  in the Na jet [64].

#### IV. ION BEAM NEUTRALIZERS FOR NEUTRAL BEAM PRODUCTION

High-energy neutral beams can be formed most efficiently by injecting negative ions into gas or plasma targets (i.e., by removing an electron from the negative ion). As shown in the appendix, the effectiveness of this method stems from the large cross section for the detachment of one electron from the negative ion as compared with the cross section for electron detachment from the resulting neutral atom. At ion energies greater than 100 keV, up to 65% of the  $H^-$  ions can be converted to hydrogen atoms in gas targets and up to 85% in plasma targets. The  $H^- \rightarrow H^0$  transformation can be achieved with almost 100% conversion efficiency by a photodetachment cell. The optimization of the qualitative and quantitative elements in the neutralization of high-energy negative ion beams can best be achieved by maximizing the neutral beam conversion coefficient and minimizing the angular distribution of the resulting atomic beam. A survey of various negative ion neutralization schemes [69] showed the maximum neutralization efficiency of  $H^-$  ions to be independent of negative ion beam energy at 100 keV to 1000 MeV.

Soviet experimental and theoretical work on the three types of ion beam neutralizers are discussed in this section. Early Soviet research (1965 to 1973) concentrated on the development of gas neutralizers, involving for the most part the creation of various gas jets for neutralizing both positive and negative ion beams; gas neutralizers are treated in subsection 1. Since the late 1970s, the Soviets have also been developing plasma neutralizers for converting negative ion beams into neutral beams; these are described in subsection 2. In addition, the Soviets have been engaged for at least ten years in the theoretical investigation of negative ion beam neutralization at high energies; high-energy beam neutralizers are discussed in subsection 3. Further Soviet data on electron detachment cross sections, neutral conversion coefficients, and neutral beam angular dispersion measurements are given in the Appendix.



## 1. GAS NEUTRALIZERS

The investigation of gas neutralizers at the Kurchatov Institute between 1965 and 1967 focused on the development of an atomic hydrogen injector for the OGRA-II magnetic trap.  $\text{CO}_2$  and Mg ultrasonic gas jets were used as the neutralizing targets, with target thicknesses of  $5 \times 10^{15}$  atoms/cm<sup>2</sup> and beam apertures of 250 cm<sup>2</sup> at the entrance and exit of the neutralizer [70,71]. The design and construction of the neutralizer allowed an operating pressure of  $2 \times 10^{-5}$  Torr at the ion source and  $1 \times 10^{-9}$  Torr at the magnetic trap, ensuring a pressure drop of a factor of  $10^6$  between the gas neutralizer and the magnetic trap. The experiments obtained high production of highly excited hydrogen atoms in a 20 keV hydrogen beam and demonstrated the superiority of Mg over  $\text{CO}_2$  as a charge-exchange material.

At about the time of the Kurchatov research, IFTT was investigating Li as a vapor neutralizer, with 6.5 mm diameter apertures and target thicknesses of up to  $4 \times 10^{15}$  atoms/cm<sup>2</sup> [72,73]. Absolute measurements were made of the concentration of Li atoms and the Li gas in the vapor jet. The Li neutralizer was further developed in 1973, using a 45 mm aperture diameter and a target thickness of  $5 \times 10^{15}$  atoms/cm<sup>2</sup> [74]. In these experiments, Li was recirculated by the condenser (11) and Laval nozzle (6), as shown in Fig. 11. The vacuum measured 5 to  $7 \times 10^{-7}$  Torr in the neutralizer with the Li jet operating. This neutralizer can in principle operate with any alkali metal; thus, it can also be used to convert positive to negative ion beams by double charge exchange (as described in Section III) and to form highly excited neutral particles (as described in [75,76]).

The Physico-Technical Institute researched gas neutralizers from the early 1960s through 1973, trying various designs of gas jets and nozzles using Ar,  $\text{CO}_2$ , and Mg vapors [77,78,79,80]. Jets operating under several atmospheres of pressure proved more advantageous than jets operating at lower pressures. At 5 atmospheres, the jet demonstrated a factor of  $10^6$  difference between the pressure inside the jet ( $3 \times 10^{-2}$  Torr) and the pressure 15 cm orthogonal to the jet axis ( $3 \times 10^{-8}$  Torr) [78]. The gas flow from the source into the high-voltage end was determined in 1969 to decrease by a factor of 100 with the operation of the gas jets [81].

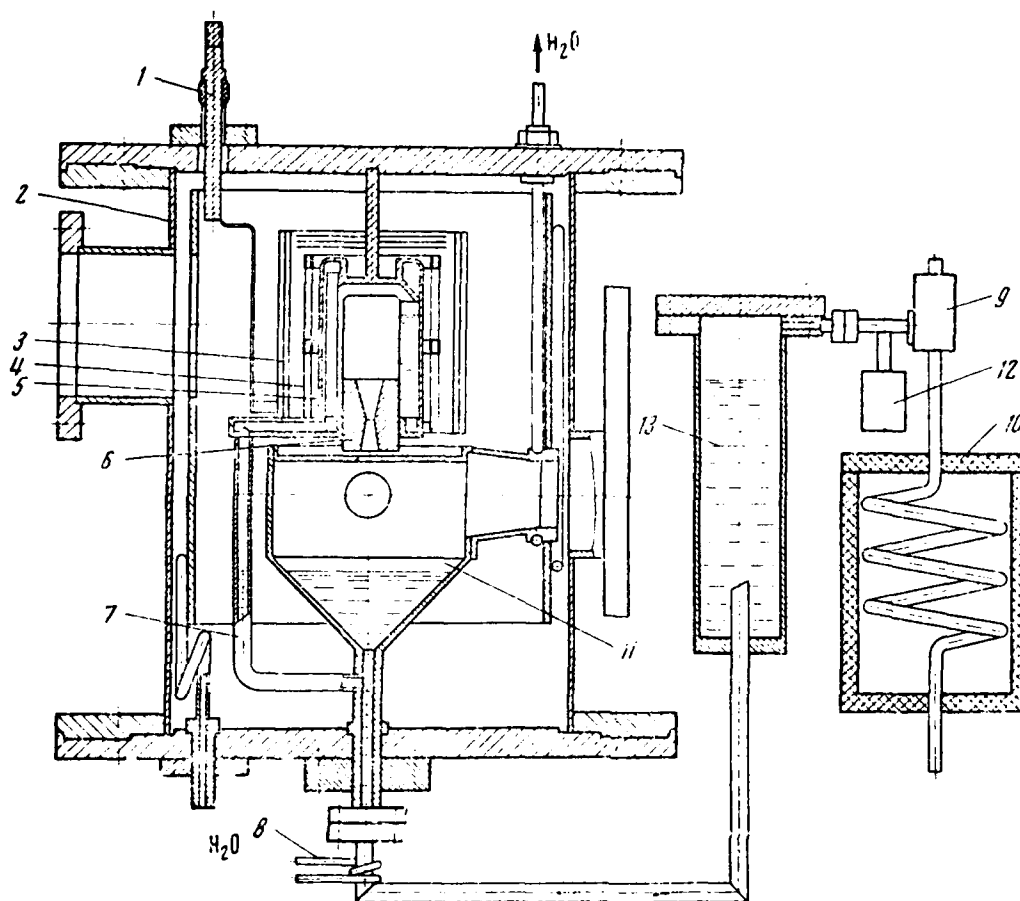


Fig. 11--Cross section of a Li vapor neutralizer [74]

- 1--current feed for the vapor generator
- 2--neutralizer housing
- 3--heat shields
- 4--vapor generator heater
- 5--vapor generator
- 6--Laval nozzle
- 7--electromagnetic pump return line
- 8--water lock
- 9--vacuum valve
- 10--nitrogen trap
- 11--condenser
- 12--manometer
- 13--Li charge cylinder

## 2. HYDROGEN PLASMA NEUTRALIZERS FOR $H^-$ AND $D^-$ BEAMS

Soviet researchers are concentrating on the development of an economically feasible plasma target to be used as a neutralizer for  $H^-$  and  $D^-$  beams in the production of high-energy neutral beams. Plasma

targets, although more complex and more expensive than gas targets, in theory can have a conversion coefficient of as much as 80 to 90%.

The diagram of a hydrogen plasma target developed at NPI in 1980 is shown in Fig. 12 [82,83]. The hydrogen (or deuterium) plasma is generated in the plasma source (1), which has an  $\text{LaB}_6$  thermionic cathode. The plasma flows along the lines of force of the magnetic field formed by solenoid coils (3). In the straight section of solenoids next to the source, the plasma flow pumps out the un-ionized hydrogen. The second straight section of solenoids is the actual plasma target; at the end of the target, coils (5) create a reverse magnetic field that deflects the plasma into pumping manifolds (4). The  $90^\circ$  turn of the plasma path allows the neutralized beam to exit unimpeded from the plasma target. The hydrogen (or deuterium) plasma flow has a diameter of about 4 cm and a total path length of 1.5 meters, of which 0.8 m is the plasma target.

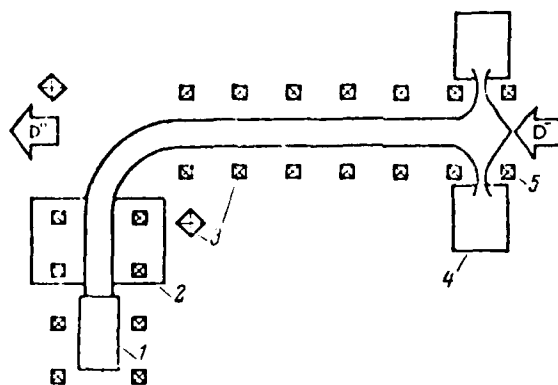


Fig. 12--Diagram of the NPI hydrogen plasma target [82]

- 1--plasma source
- 2--differential pumping area
- 3--solenoid coils
- 4--pumping manifolds
- 5--coil providing reverse magnetic field

The stripping efficiency of the hydrogen plasma target was measured in the experimental setup shown in Fig. 13. A pulsed  $\text{H}^+$  beam with a pulse length of 0.3 ms and energy of 500 keV at the exit of a Van de Graaff accelerator was analyzed with a magnet (1) and collimated by a diaphragm (2), 0.5 to 1.0 cm in diameter, located

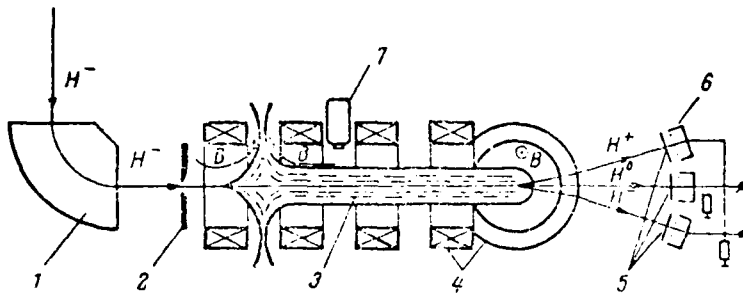


Fig. 13--Experimental apparatus used to convert  $H^-$  beam into neutral atoms [82]

- 1--analyzing magnet
- 2--collimating aperture
- 3--plasma beam
- 4--solenoid coils
- 5--stripping foils
- 6--faraday cups
- 7--pulsed gas leak

coaxially with the solenoid (4) of the plasma target. After passing through the target, the ion beam was separated into its three components ( $H^-$ ,  $H^0$ , and  $H^+$ ) by the magnetic field of the bent solenoid. Each of the separated beams was then passed through a Lausen stripping plate 3500 Å thick, and the proton beams thus formed were collected by faraday cups.

The experimental results of this work are shown in Fig. 14, which gives the dependence of the neutral hydrogen beam produced from 500 keV  $H^-$  ions as a function of the plasma target thickness. The maximum value of the neutral beam production conversion coefficient  $\eta^0 = I^0/(I^0 + I^- + I^+)$  is observed to be  $84.5 \pm 0.5\%$ , at a target thickness of  $2 \times 10^{15} \text{ cm}^{-2}$  [82]. The maximum calculated value of this coefficient for a 500 keV  $H^-$  beam and the same target thickness is 84.3%, showing excellent agreement between Soviet theory and experiment. The plasma target thickness was determined by the attenuation of the negative ion beam, using cross sections provided in [84,85]. These values also agree well with the calculations made by Grossman at BNL [29]. Assuming a 500 keV  $H^-$  beam passing through a hydrogen

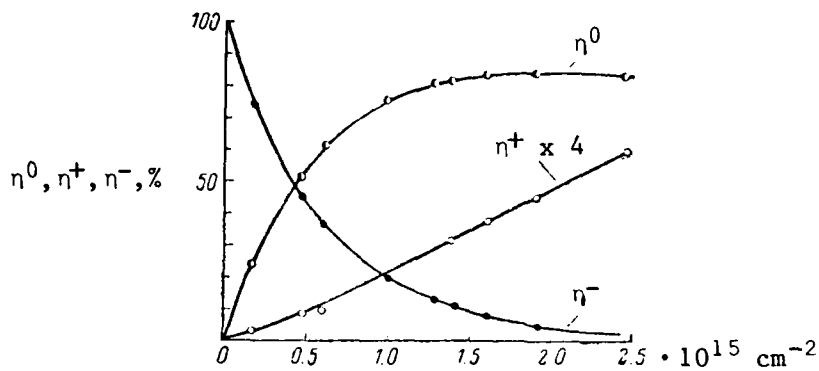


Fig. 14--Beam component outputs as a function of plasma target thickness [82]

plasma that is 80% ionized (as determined in [83]), one obtains a maximum conversion coefficient (neutralization efficiency) of 86.7 to 87.0% from Grossman's data (Fig. 5 of [29]).

The NPI investigations of the plasma target neutralizer shown in Figs. 12 and 13, above, used a 500 keV  $\text{H}^-$  beam (equivalent to a deuteron beam energy of 1 MeV) [82]. Experiments at other energies were considered unwarranted, because NPI researchers had in 1975 showed neutral hydrogen beam production to be relatively independent of energy in the range of 0.5 to 1 MeV [86].

NPI researchers used the apparatus shown in Fig. 15 to analyze the plasma density, degree of ionization, plasma stability, atomic and molecular ion composition, plasma dispersion, beam profile, and pumping properties of the plasma target neutralizer and to find the optimum plasma parameters for stable operation [82,83,87]. The plasma was formed in these experiments with a square-wave, 1000 A, 1.5 ms pulsed discharge in the plasma source, powered by a 1 ohm forming line. Probes measured the plasma electron temperature at 5 eV. According to mass-spectroscopic measurements at typical operating conditions, the plasma at the plasma source exit was composed of 85%  $\text{H}^+$  and 15%  $\text{H}_2^+$  and had a density of about  $10^{13} \text{ cm}^{-3}$  [83].

The plasma was made to follow a  $90^\circ$  bend with a radius of 25 cm by a 1 to 1.5 kgauss magnetic field without substantial loss of plasma

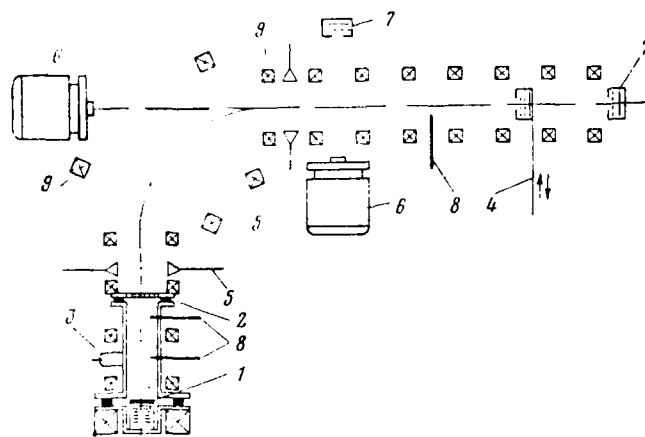


Fig. 15--Schematic of experimental apparatus for investigating plasma characteristics [83]

- 1--LaB<sub>6</sub> cathode
- 2--anode grid
- 3--gas valve
- 4--three-element probe
- 5--microwave antenna
- 6--diagnostic hydrogen atom injector
- 7--faraday cup
- 8--langmuir probe
- 9--solenoid coils

to the chamber walls. Plasma density, which decreased about 20% after the plasma made the turn, reached a maximum of over  $2 \times 10^{13} \text{ cm}^{-3}$  in the target. The loss in density was attributed to the recombination of molecular ions in the plasma flow. The  $90^\circ$  turn creates conditions for the formation of a flute instability, which causes the loss of plasma to the chamber walls; however, the experimenters were able to control the flute instability by having the plasma flow make contact with the face of the emitting cathode.

The maximum density of the plasma flow in these experiments was controlled by nullifying a microwave signal having a 7 to 11 mm wavelength. The transmitting and receiving antennas (5) were located before and after the  $90^\circ$  turn. The plasma density and degree of ionization were determined by observing the attenuation of the  $\text{H}^0$ ,  $\text{H}^+$ , and  $\text{H}^-$  beams produced by the diagnostic injector (6), described

in [88] and Section V, 4, iii, below. The attenuation of the  $H^0$  beam from a similar injector operating with energy of 5keV was used to determine the plasma target thickness along the straight portion of the plasma beyond the  $90^\circ$  turn (the actual plasma target).

NPI experiments in 1979 [83] to investigate the quality of the plasma flow replaced the plasma source anode grid with a plate incorporating an array of apertures. The plasma beam was turned on and the image of this aperture array was imprinted on a metal plate 100 cm from the anode along the beam axis. The orientation of the image on the plate coincided with the orientation of the apertures in the anode and the size of the aperture image was only 1 mm larger than the actual apertures of the anode. These findings confirmed the insignificance of the dispersion and rotation of the plasma flow.

The current density distribution of the hydrogen plasma beam was measured 100 cm from the anode of the plasma source, using a langmuir probe (item 8 of Fig. 15). The results of these measurements are shown in curve 1 of Fig. 16. To investigate the plasma diffusion in the source discharge and its effect on the beam profile, a 1 cm diameter insulated tantalum disc was placed 0.5 cm from the cathode along the axis of the source so as to block the discharge near the axis. The beam profile, as measured by the probe and shown by curve 2 of Fig. 16, demonstrates a well-defined hollow with sharp edges; at 100 cm from the anode, the hollow did not fill in during the time of the beam flow.

The total flow of the plasma was measured with two three-element probes (item 4 of Fig. 15), located immediately after and 50 cm from the source anode. The probe measurements showed a discrepancy of 10% to 15% with the data obtained using the microwave measurements; the discrepancy is probably due to the molecular ion recombination in the beam, since the recombination path length of the  $H_2^+$  ion in a plasma with a density of  $10^{13}$  atoms/cm<sup>3</sup> is only about 5 cm [83].

The relative atomic and molecular ion composition of the plasma flow was measured 10 cm from the anode (curve 1 of Fig. 17) and at the pumping manifold, 130 cm from the anode (curve 2 of Fig. 17) [83]. The

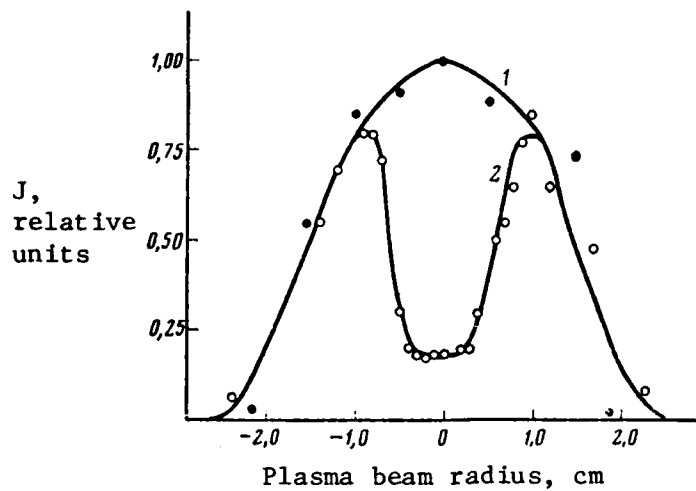


Fig. 16--Current density distribution in hydrogen plasma beam, measured 100 cm from anode grid [83]

- 1--beam normally generated by plasma source
- 2--beam with 1 cm diameter disc placed on beam line, 0.5 cm from cathode surface

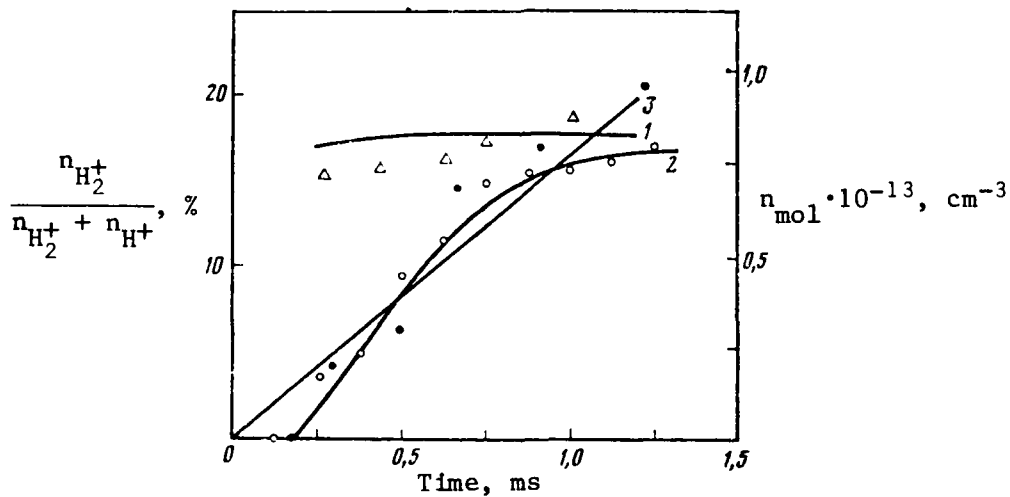


Fig. 17--Molecular hydrogen ion concentration and gas density in plasma as a function of time [83]

- 1-- $H_2^+$  concentration at plasma source exit
- 2-- $H_2^+$  concentration at end of plasma flow (pumping manifold)
- 3--un-ionized gas density in plasma flow



molecular component of the hydrogen ion in the beam at the plasma source exit measured about 15% and remained unchanged during the pulse length. The absence of the  $H_2^+$  ion component in the plasma at the beginning of the pulse, as measured at the end of the plasma flow (curve 2, Fig. 17), was due to the removal of the molecular component from the beam by dissociative electron attachment. The subsequent increase of the  $H_2^+$  ions in the latter part of the pulse can be explained by the pressure increase of the hydrogen gas at the pump manifold and the associated formation of the  $H_2^+$  by gas ionization.

Curve 3 of Fig. 17 represents un-ionized gas density in the plasma as a function of time. The gas buildup in the plasma during the discharge results from the accumulation of gases liberated from the vacuum chamber walls. These un-ionized gases surround the plasma flow, which isolates itself from the un-ionized gas, ionizes the gas, and pumps it to the pumping manifolds [82]. This phenomenon was measured by introducing pulses of un-ionized gas through the gas leak (item 7 of Fig. 13) near the end of the target.

The dependence of plasma density and un-ionized gas density in the plasma, measured as a function of the discharge power input, is shown in Fig. 18. The degree of ionization of the plasma flow beyond the

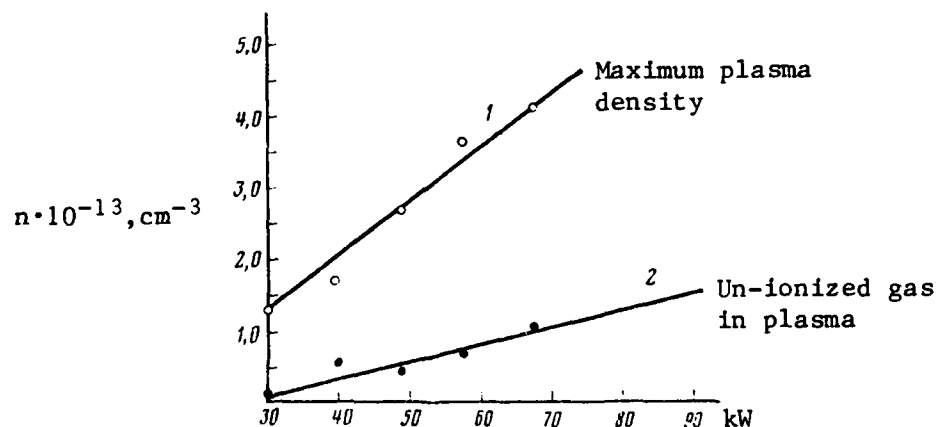


Fig. 18--Maximum plasma density and un-ionized gas in plasma as a function of discharge power input [83]

90° turn was approximately 80% for hydrogen. The maximum plasma density was determined by the attenuation of a 10 keV  $H^-$  ion beam passing orthogonally through the plasma flow. The measurement of the amount of un-ionized gas in the plasma target was made by cutting off the source discharge current after 5  $\mu s$  and turning on the diagnostic  $H^-$  beam 50  $\mu s$  after the current was turned off.

These measurements demonstrated that a stable plasma flow can be maintained with a density of up to  $3 \times 10^{13} \text{ cm}^{-3}$ , plasma target length of 80 cm, and integral plasma thickness of  $2.2 \times 10^{15} \text{ atoms/cm}^2$ , the optimum for the neutralization of 1 MeV  $D^-$  ions. The high values obtained for the conversion of negative ions into neutral atoms and the added advantages of the pumping action of the plasma flow make this type of plasma target promising for high-energy neutral beam injectors. Researchers at NPI indicate that the target will be used for further experiments on the conversion of negative ions to neutrals.

### 3. HIGH-ENERGY BEAM NEUTRALIZERS

Researchers at the Nuclear Physics Research Institute (NPRI) of Moscow State University and at the Radiotechnical Institute (RTI) in Moscow made theoretical calculations on the neutralization of negative ion beams at high energies. The NPRI research, which has been going on for at least ten years, is concentrated on determining the angular and energy distributions of ions emerging from various charge-exchange targets. From 1974 to 1979, RTI investigated the electron stripping of  $H^-$  ion beams by the background gas in linear accelerators [89,90].

The NPRI and RTI theoretical research was conducted in conjunction with the development of a linear accelerator that will go into operation at the Intermediate Energy Physics Complex of NPRI. The linac is to accelerate  $H^-$  beams along with proton beams for application in a meson factory [91,92]. In one mode of proposed operation, the linac will accelerate  $H^-$  beams with a full average current of 1 mA. Consideration has also been given to the acceleration of  $H^-$  beams up to average currents of 100 mA, while keeping the radiation cleanliness of the accelerator at an optimum [90].

The acceleration of  $H^-$  beams in a linear accelerator, using charge-exchange injection at energies of 600 to 1000 MeV, allows the development of high-intensity proton storage. The  $H^-$  beam is accelerated in a linac and then passed through a charge-exchange target located in the chamber of the storage ring. The target, in this case a solid film made of a light element (Be or C), allows the  $H^-$  ions to be converted into protons with close to 100% effectiveness. Preliminary studies showed the increase in emittance of the stored beam to be an insignificant part of the emittance of the injected beam [93].

At NPRI, calculations were made for the neutralization of linac-accelerated  $H^-$  ion beams to energies of 100 to 600 MeV [94,95,96]. NPI determined various target thicknesses for optimum stripping of  $H^-$  beams [97]. More recently, the angular and energy distributions of electrons emerging from the charge-exchange targets were investigated theoretically [98]. Electron spectra were studied for use as a diagnostic of the primary ion beam. In this case, when the charge exchange occurs on very thin targets, the electron parameters can be measured without disturbing the primary ion beam. The angular and energy spreads of electrons emanating from a high-quality  $H^-$  ion beam do not exceed the corresponding spreads of the primary ion beam and may therefore be used to measure the angular and energy distributions of the incident ion beam [98]. NPRI researchers also calculated the electron detachment cross sections of hydrogen beams at high energies (10 to 1000 MeV) in light target materials (see Appendix, Figs. 37 and 38) [99,100].

In addition to electron stripping of  $H^-$  beams in background gases, RTI researchers theoretically investigated the formation of  $H^-$  ion bunches at the input to the linear accelerator. They developed an ion buncher with a pulse length of 15 to 20 ns and repetition rate of 10 MHz. Bunching led to a 50% to 60% decrease in the loss of particles at the exit of the injector, instead of the normal 80%, and reduced the drift space from about 25 meters to 2.5 meters [101]. The formation of  $H^-$  bunches with pulse lengths of 200 ns and repetition rates of 4.129 MHz at the entrance to the linear accelerator was also calculated [102]. In this case, the  $H^-$  injection energy was 750 keV, with a maximum beam current of 150 mA, to provide the 75 mA pulsed input

beam current for the linear accelerator, which had a working coefficient of  $k = 0.5$  [102]. The references to high-energy acceleration of  $H^-$  ion beams in linear accelerators cited in this section were the only ones found in a search of the Soviet literature, and all point to future experiments. Experimental data have not yet been published in this high-energy range.

## V. NEUTRAL BEAM INJECTION SYSTEMS

Soviet research on neutral beam injectors has been concentrated mainly at the Kurchatov Institute, while various components are being developed at NPI, IFTT, IPI, and the Yefremov Institute of Electrophysical Equipment in Leningrad. This section discusses injector systems and their general operating parameters and describes the INES and MIN injector test facilities at Kurchatov, the Kurchatov deuterium atom injector system, and research on various diagnostic neutral beam injectors. The efficiency of an injector based on the neutralization of negative ions is determined not only by the energy used to form the negative ions but by the loss of ions in the transport, acceleration, and/or neutralization of the beam.

### 1. EARLY RESEARCH ON NEUTRAL BEAM INJECTORS

An intense hydrogen atom injector developed at Kurchatov and reported in 1970 [103,104] produced a 0.5 A equivalent  $H^0$  beam current at energies of 15 to 30 keV. This injector did not use negative ion beams but transformed an  $H^+$  ion beam directly into a neutral beam in an Mg vapor target. Early tests demonstrated proton beams of 1 A and a maximum  $H^0$  atomic beam of 0.6 A at an energy of 20 kV.

The Kurchatov tests measured the  $H^0$  atomic output formed by the neutralization of the  $H^+$  beam as it passed through the Mg vapor jet; the tests also measured the  $H^+$  atoms that were not neutralized and the neutral equilibrium fraction  $\phi_0^\infty$  as a function of both  $H^+$  beam energy and beam current [104]. In the energy range of 15 to 30 keV, the  $\phi_0^\infty$  did not change with the increase of  $H^+$  beam current up to 1 A; at 1 A, however, the current density rose to about 25 mA/cm<sup>2</sup> and began to affect the  $\phi_0^\infty$ . Figure 19 shows the sharp decrease of  $\phi_0^\infty$  as  $H^+$  beam energy increases. The  $\phi_0^\infty$  was also measured at IPI in 1966-1967, using Mg and Cd [105] and Na and Ne [106]. In the energy range of 10 to 20 keV, the Kurchatov and IPI data for Mg agreed well; at higher energies, however, the Kurchatov data showed a sharper decrease, as shown in Fig. 19. This discrepancy was traced to Kurchatov's

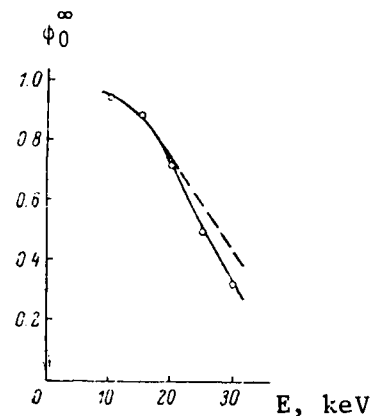


Fig. 19--Neutral equilibrium fraction  $\phi_0^\infty$  as a function of  $H^+$  beam energy in Mg (solid line represents Kurchatov data, dashed line IPI data) [104]

insufficient magnetic shielding in the neutralizer section when the magnetic field of the source was increased as required for higher energy operation.

The Kurchatov experiments also measured vertical neutral beam size as a function of  $H^+$  current, beam energy, and  $H^+$  beam size. Figure 20, showing neutral beam size as a function of  $H^+$  beam current, demonstrates the possibility of obtaining a minimum with the choice of appropriate parameters. The experiments demonstrated further that the formation of a plasma with a density of up to  $10^{13} \text{ cm}^{-3}$  in the target had no effect on the value of  $\phi_0^\infty$  (neglecting any excitation of the hydrogen atoms).

From the mid-1960s to 1973, researchers at the Physico-Technical Institute in Kharkov worked on the development of neutral atomic beam injectors. Their research involved the neutralization of negative ion beams by ultrasonic gas jets, the design of gas jet components and nozzles, and the investigation of the vacuum properties of gas targets (see Section IV, 1).

At the Kurchatov Institute, a team led by V. I. Pistunovich was involved from 1970 to 1976 in the charge exchange of plasma flow through gas, using the INES (injector of neutral clusters), a coaxial plasma injector, to produce intense  $H^0$  atomic beams for heating plasma

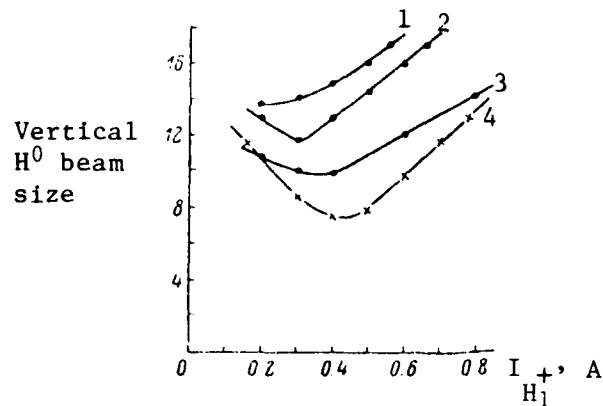


Fig. 20--Vertical neutral hydrogen beam size as a function of  $H_1^+$  beam current, with beam collector placed 2.2 m from ion source [104]

- 1--15 keV beam energy
- 2--20 keV
- 3--25 keV
- 4--25 keV, with reduced angular spread approaching Pierce geometry

in tokamaks [107,108,109]. Like the Kurchatov intense hydrogen atom injector described at the beginning of this section, the INES did not use negative ion beams.

Early research on the INES facility involved the formation of neutral plasma clusters by passing a 2 to 4 keV proton beam through an ultrasonic Mg vapor jet [110]. This work demonstrated that the charge exchange of the plasma clusters, which had an ion density  $n_i \approx 10^{11} \text{ cm}^{-3}$  and current density  $J \approx 1 \text{ A/cm}^2$  when interacting with various gas targets, took place in accordance with the classical model of pair production and showed no appreciable beam scattering up to a target thickness of  $3 \times 10^{16} \text{ cm}^{-2}$ . Further experimentation in 1973 demonstrated the appearance of anomalously high energy scattering of the plasma clusters when the beam current density  $J$  exceeded  $10 \text{ A/cm}^2$  and ion density  $n_i \approx 10^{13} \text{ cm}^{-3}$ . The energy loss of the plasma beam was explained by the scattering of charged beam particles in the target gas and the formation of unstable beam oscillations with turbulent electric fields.

A diagram of the INES injector, interaction chamber, and dosimetry used in the Kurchatov experiments is shown in Fig. 21. The plasma flow created by the coaxial plasma gun (1) was transported along the metallic 12 cm diameter channel (2) into the charge-exchange chamber (4). Target gases of  $H_2$ ,  $CO_2$ , A, and He were introduced into the chamber through the pulsed gas leak (3). High-frequency probes determined the dependence of the plasma oscillations on gas density in the target. The experimental results showed that when the initial plasma flow interacted with the gas target, the beam ions were converted by charge exchange into fast neutral atoms with an effectiveness of about 0.5 [109].

Cold hydrogen ions were formed as a result of the interaction in the gas target, and the density of these ions built up with time. After 0.1 to 0.2  $\mu s$ , unstable oscillations with average electric fields of 10 to 15 kV/cm were induced in the target plasma. The subsequent flow of ions experienced a high rate of scatter. These turbulent electric fields, which were produced by the interaction of the plasma cluster with the gas, were measured using the intensity of the forbidden neutral

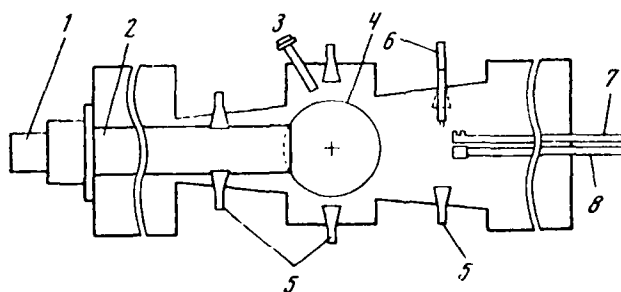


Fig. 21--Schematic of the INES injector [109]

- 1--plasma gun
- 2--plasma channel
- 3--pulsed gas leak
- 4--charge-exchange chamber
- 5--horn-type VHF antenna
- 6--double langmuir probe
- 7--high-frequency probe
- 8--thermoprobe



He lines and the stark broadening of the atomic hydrogen lines [111]. These experiments showed that intense ion-acoustical oscillations formed in the beam interaction region caused the plasma cluster scatter. The electron-langmuir oscillations that were also formed probably heated the plasma electrons.

## 2. THE MIN INJECTOR TEST FACILITY

The MIN test facility, built specifically for research on charge-exchange systems and negative ion beam and neutral beam injectors, went into operation at the Kurchatov Institute in 1976. As reported in 1977, the MIN facility produced  $H^-$  ion beam currents of 1.4 A at 40 keV with an 8 A  $H^+$  beam at 10 keV and a pulse length of 10 ms focused into a Cs or Na vapor target [112]. The negative ion beam formed represented about 18% of the total current of positive ions and neutrals channeled through the charge-exchange cell.

Although the MIN facility has produced beams of over 20 A of  $H^+$  and  $D^+$ , higher negative ion yields have not yet been reported. The electron beam current produced in these experiments has been reported to be one-half of the negative ion beam current [51]. However, problems stemming from the large volume of electrons leaving the vapor target and entering the high-voltage gap, where they create sparking, has slowed the pace of this research. Kurchatov researchers believe that they can decrease this current by modifying the acceleration system and by preventing the electrons' leaving the target area. To suppress the unwanted electrons, the fine-mesh grids were replaced with a long, negatively biased suppression tube [42]. The negative ion beam is presently extracted at 20 kV. The experiments showed the need to maintain a low pressure in the region located immediately after the vapor target. Two mechanisms were noted: the loss of the negative ions due to stripping of the electrons by the background gas and the effect of space-charge neutralization of the negative ion beam by the background gas.

To achieve higher negative ion beam yields and thus to maximize the total neutral beam output, the Kurchatov team is using the molecular components of the positive ion beam ( $D_2^+$  and  $D_3^+$ ) as well as  $D^+$ . The

neutral beams produced from these molecular components are one-half and one-third the original energy and not as clean in energy and divergence. However, Kurchatov researchers consider neutral beams with divergences of  $\pm 1^\circ$  usable and hope to be able to transport the neutral beam distances of about 10 meters.

The MIN power supply allows positive ion currents of up to 100 A at 10 keV and negative ion currents of up to 10 A at 100 keV with pulse lengths of up to 115 s and intervals between pulses of 40 to 60 s.

Figure 22 shows a diagram and Fig. 23 two photographic views of the MIN test injector; Fig. 24 presents two photographs of the Na vapor charge-exchange target (item 6 of Fig. 22). According to Soviet

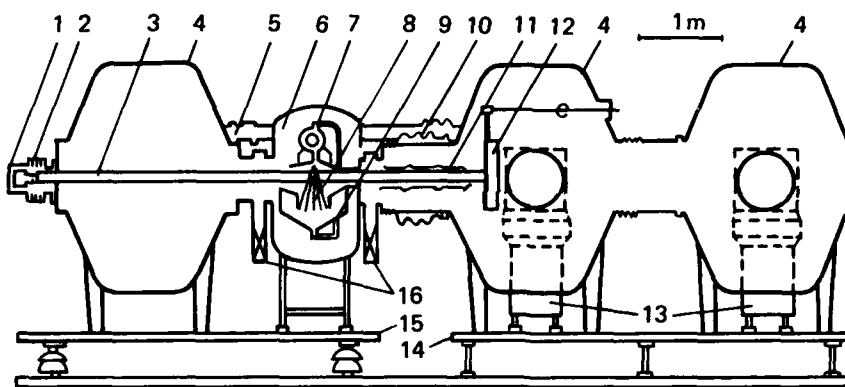


Fig. 22--Schematic of the MIN injector test facility  
[112]

- 1--positive ion source
- 2--source insulator
- 3--ion beam
- 4--vacuum tank
- 5--pumping manifold
- 6--Na charge-exchange target assembly
- 7--vapor generator
- 8--Na vapor jet
- 9--condenser
- 10--high-voltage insulator
- 11--acceleration system
- 12--beam collector
- 13--vacuum pumps
- 14--ground potential floor
- 15--100-kV potential floor
- 16--vacuum valves

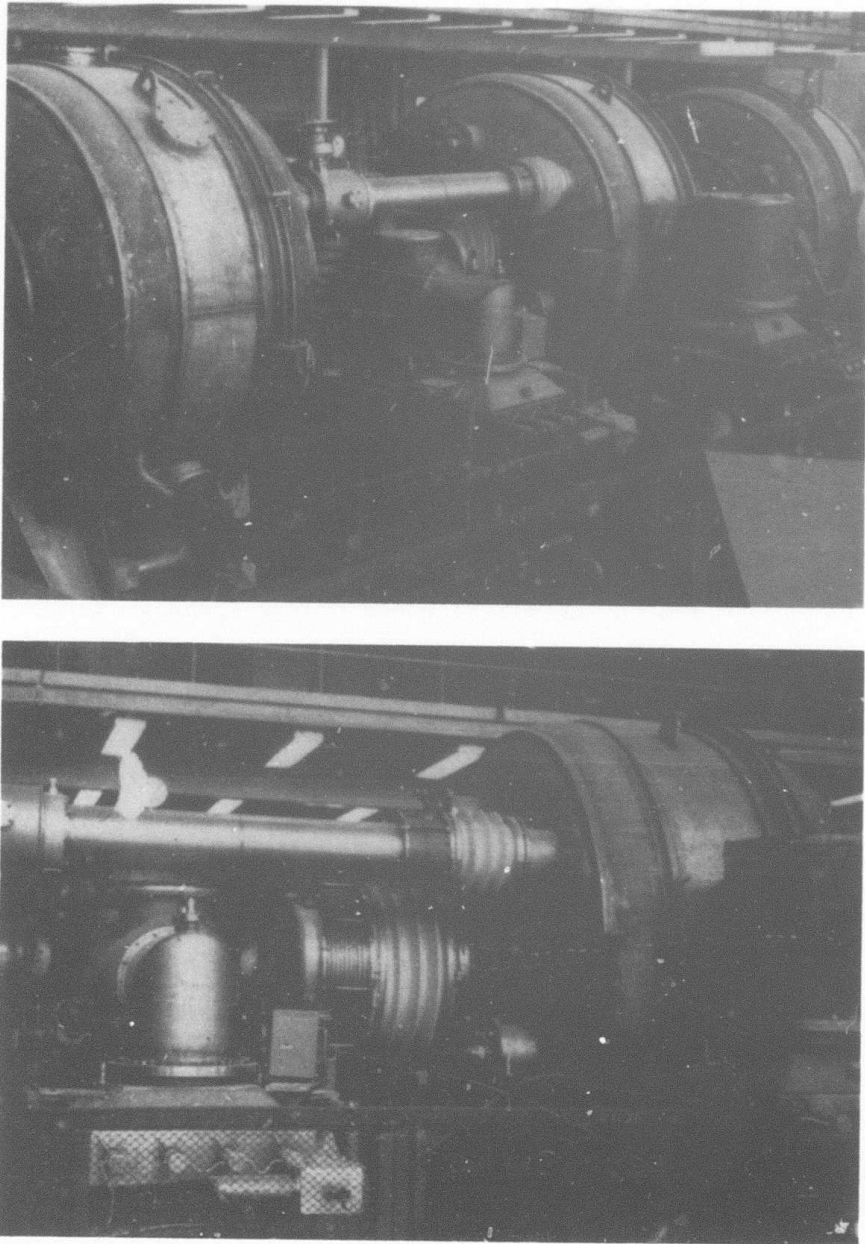


Fig. 23--Two views of the MIN injector test facility [51]

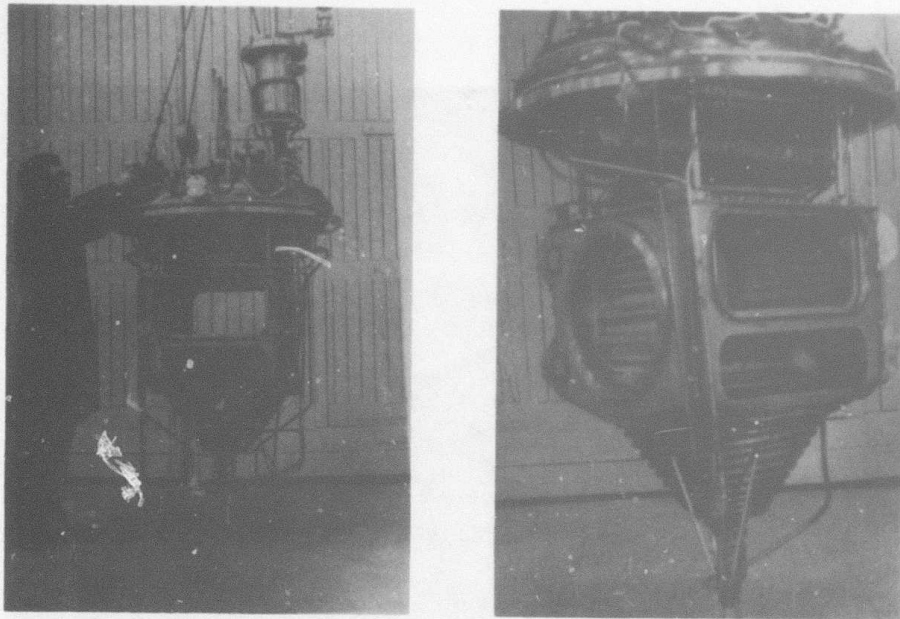


Fig. 24—Two views of the MIN Na vapor charge-exchange target [51]

researchers, the capability of the MIN negative ion injector is still several orders of magnitude lower than that needed for fusion requirements. The facility can, however, simulate one component of a larger-scale injector and the results can be extrapolated to determine the final design parameters for the fusion operation. The facility was found to be useful for the development and testing of the various components of the system (such as the positive ion source, charge-exchange target, acceleration system, and strippers) under conditions approximating the actual operating regime. The vapor jet charge-exchange targets for this facility were recently investigated in detail (see Section III, 2).

### 3. THE DEUTERIUM BEAM INJECTOR TEST FACILITY

A deuterium injector system with an energy of 400 to 600 keV is being conceptually developed at the Kurchatov Institute. This system

extracts  $D^+$  ions at 5 to 10 keV from a deuterium ion source and passes them through a charge-exchange vapor target to convert them into negative ions. These are preaccelerated to the required energy and passed through the electron-stripping target. The low energy of the positive ions is required for maximum conversion of positive to negative ions.

A diagram of one module of the injector system is shown in Fig. 25; several such modules will be used in parallel to obtain a total neutral beam power of 30 to 40 MW [113]. The ion source (1) produces positive ion beam currents of about 100 A with a current density of  $0.25 \text{ A/cm}^2$ . An ultrasonic Na vapor jet (2), used as the charge-exchange target, converts positive into negative ions. The preacceleration system (3), consisting of electrodes mounted inside a high-voltage insulator, is followed by a magnet (4), which bends the negative ion beam through a small angle into the entrance aperture of the thermonuclear reaction chamber. The neutral particles formed in the vapor target (2) are collected on a special collector (5). The negative ion beam then passes through the stripper (7), several types of which are now being developed [74,82].

Injector efficiency should be greatly increased with the incorporation of the newly designed plasma target described in [82]. Beyond the stripper, the beam consists of approximately equal amounts of positively and negatively charged particles, which are deflected with appropriate magnetic fields onto the ion collectors (8).

To limit the loss of  $D^-$  ions, the pressure of the background gas in the drift area near the neutral beam collector (5) is not permitted to exceed  $1.33 \times 10^{-3} \text{ Pa}$  and the area is screened from stray magnetic fields. In the injector modules, the drift areas are equipped with cryogenic pumping elements (6), in addition to the usual pumping systems (9).

The negative ion output from the charge-exchange vapor target at a positive ion energy of about 7 keV reached 0.12 of the  $D_1^+$  beam component. However, the total negative ion output reached 0.18 of the positive beam when the  $D_2^+$  and  $D_3^+$  beam components were taken into

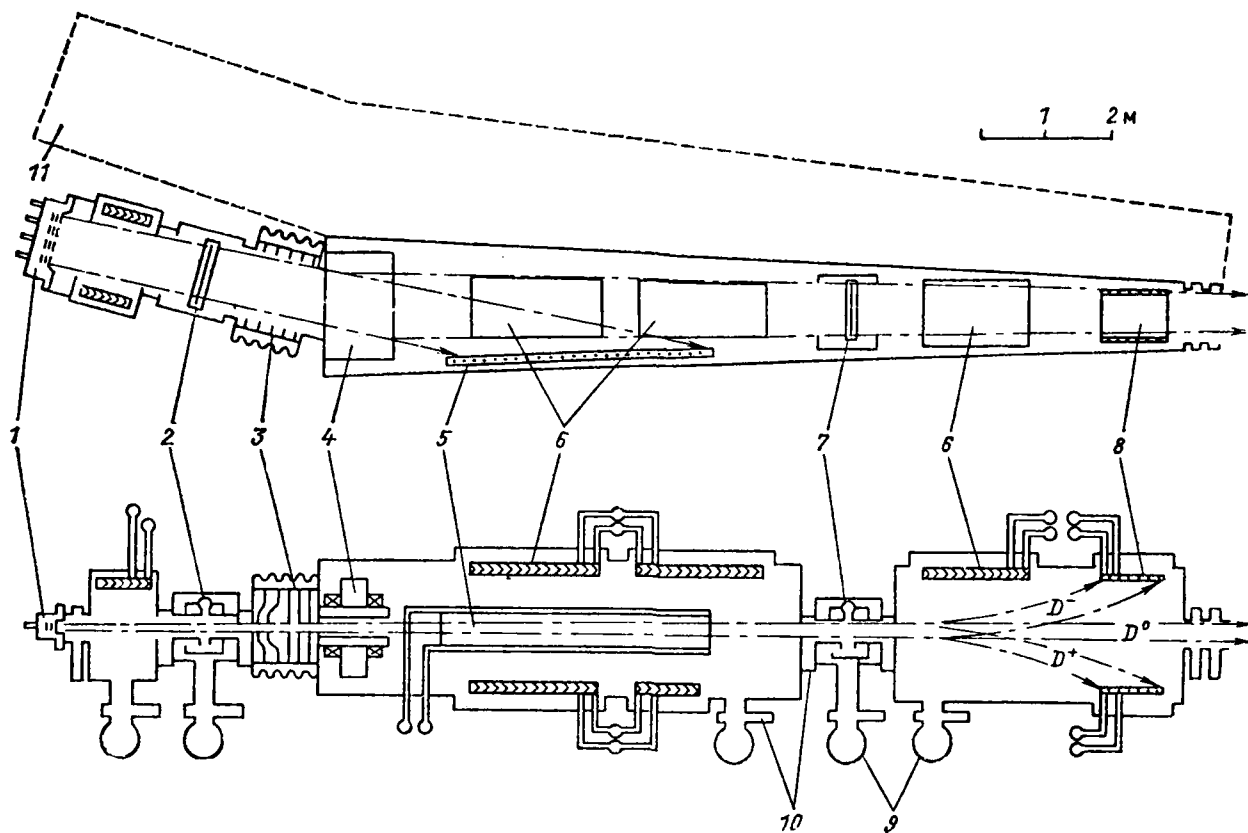


Fig. 25--400 to 600 keV deuterium atom injector module [113]

- 1--positive ion source
- 2--Na charge-exchange target
- 3--preacceleration system
- 4--bending magnet
- 5--10 keV atom collector
- 6--cryogenic pumping elements
- 7--Li stripper target
- 8--400 to 600 keV ion collectors
- 9--vacuum pumps
- 10--vacuum valves
- 11--adjacent injector module

account (see Fig. 26). In the target, these molecular components were dissociated into lower energy ions and then charge exchanged.

The efficiency of the neutral beam injector is shown in Fig. 27 as a function of beam energy for both positive and negative ion beam use. Negative ions (in this case obtained by charge exchange in Cs and Na) provide optimum operation at higher energies.

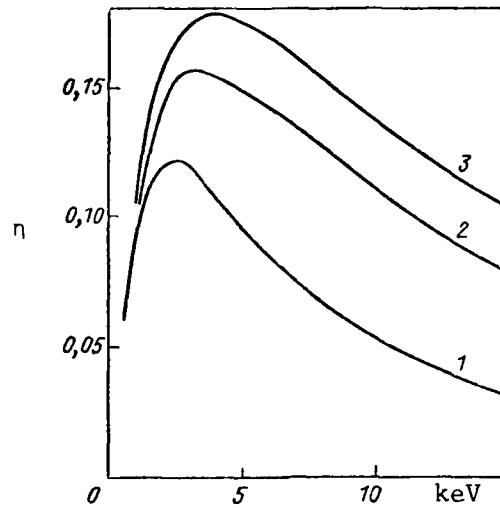


Fig. 26--Negative ion output as a function of  $H^+$  ion beam energy [113]

1-- $H_1^+ = 100\%$

2-- $H_1^+ = 70\%$ ;  $H_2^+ = 20\%$ ;  $H_3^+ = 10\%$

3-- $H_1^+ = 60\%$ ;  $H_2^+ = 20\%$ ;  $H_3^+ = 20\%$

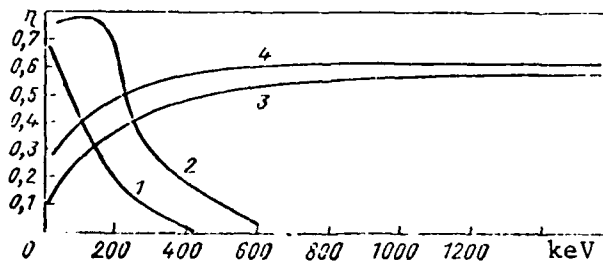


Fig. 27--Deuterium beam injector efficiency as a function of energy [113]

1--positive ion injector

2--positive ion injector plus energy recovery (90% efficiency)

3--negative ion injector (charge exchange in Cs)

4--negative ion injector (charge exchange in Na)

#### 4. INJECTION SYSTEMS BASED ON POSITIVE ION BEAMS

Soviet researchers are developing several neutral beam injectors that operate on the direct neutralization of positive ion beams, the total beam energy of which is well below 100 keV. Foremost among these injection systems are the OGRA-IV, AMBAL, and NPI diagnostic injectors.

##### i. The OGRA-IV

The OGRA-IV neutral beam injector experiment at Kurchatov, which is scheduled to begin in late 1982, will investigate plasma properties for mirror trap research. Based on a technique developed by the Semashko group at Kurchatov, four approximately 30 keV,  $7 \times 18 \text{ cm}^2$  cross-section neutral beams will be injected (two from either side) into the plasma of the superconducting, "baseball"-configured OGRA-IV. The neutral beams will be formed by passing  $\text{H}^+$  ions through Mg gas jets equipped with water-cooled chevron chambers. In addition to neutralizing the beam, the gas jets will block the gas flow [51].

Recent experiments on the OGRA-IIIB provided data on the behavior of the potential and electron component of the plasma at low ion densities. In this experiment, an  $\text{H}^0$  beam was formed and injected into the "baseball" at 20 keV; the beam had a cross section of  $8 \times 8 \text{ cm}^2$ , an equivalent current of 0.2 A, and pulse lengths of 1 to 2 s [114].

##### ii. The AMBAL

The AMBAL ambipolar trap facility now being assembled at NPI will use  $\text{H}^0$  beams of 25 keV to heat and sustain the plasma. The neutral beams will be formed by charge exchanging proton beams in a Mg vapor jet target, which NPI recently tested [115]. A detailed description and diagrams of the AMBAL facility are provided in [116]. Figure 28 shows the location of the neutral beams and the plasma [117].

The output from the 10 keV charge-exchanged  $\text{H}^+$  ion beam consisted of 85%  $\text{H}^0$ . With a target thickness of  $3 \times 10^{15} \text{ atoms/cm}^2$  and a hydrogen pulse of 0.2 s, the relative pressure drop across the target jet measured 400 in the pressure range in front of the jet of  $5 \times 10^{-5}$  to  $10^{-3}$  Torr [115]. The output of  $\text{H}^-$  ions from the vapor jet at a pressure of about  $4 \times 10^{15} \text{ atoms/cm}^2$  was only 5% to 6% of the initial  $\text{H}^+$  beam.



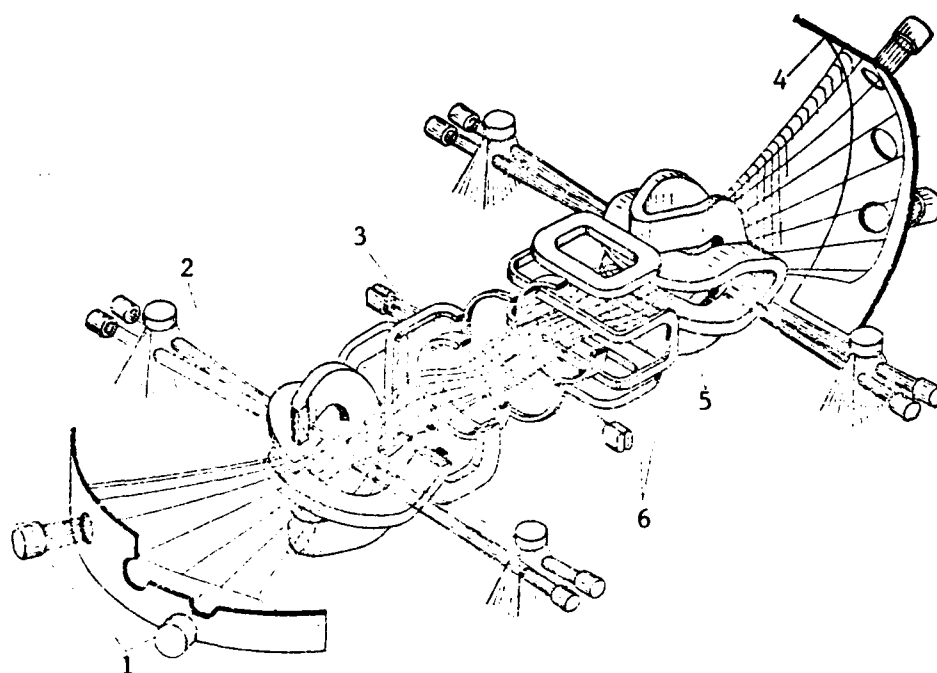


Fig. 28--Diagram of the AMBAL ambipolar trap facility [117]

- 1--plasma beams
- 2--high-energy atomic beams
- 3--low-energy atomic beams
- 4--plasma collector plate
- 5--"yin-yang" coils
- 6--transition coils

According to U.S. researchers familiar with the NPI work, the AMBAL plasma experiments will not begin until 1983. No serious problems are foreseen with this facility. However, a long learning period on the AMBAL as well as delays in associated NPI research (especially negative ion beam experiments) due to the diversion of NPI researchers to the AMBAL experiment, may be expected [42,51].

### iii. Diagnostic Neutral Beam Injectors

The Soviets have developed a number of neutral atom injectors for the diagnostic measurement of the magnetic confinement of thermonuclear plasmas. Such injectors demand a relatively intense monoenergetic atomic beam with a small angular dispersion and low regulating particle energy. The NPI atomic hydrogen beam diagnostic injector used

to determine plasma density and degree of ionization in plasma neutralizers, described in Section IV, 2, above, generally meets these requirements [88,118]. This injector (Fig. 29), developed in 1976, is a

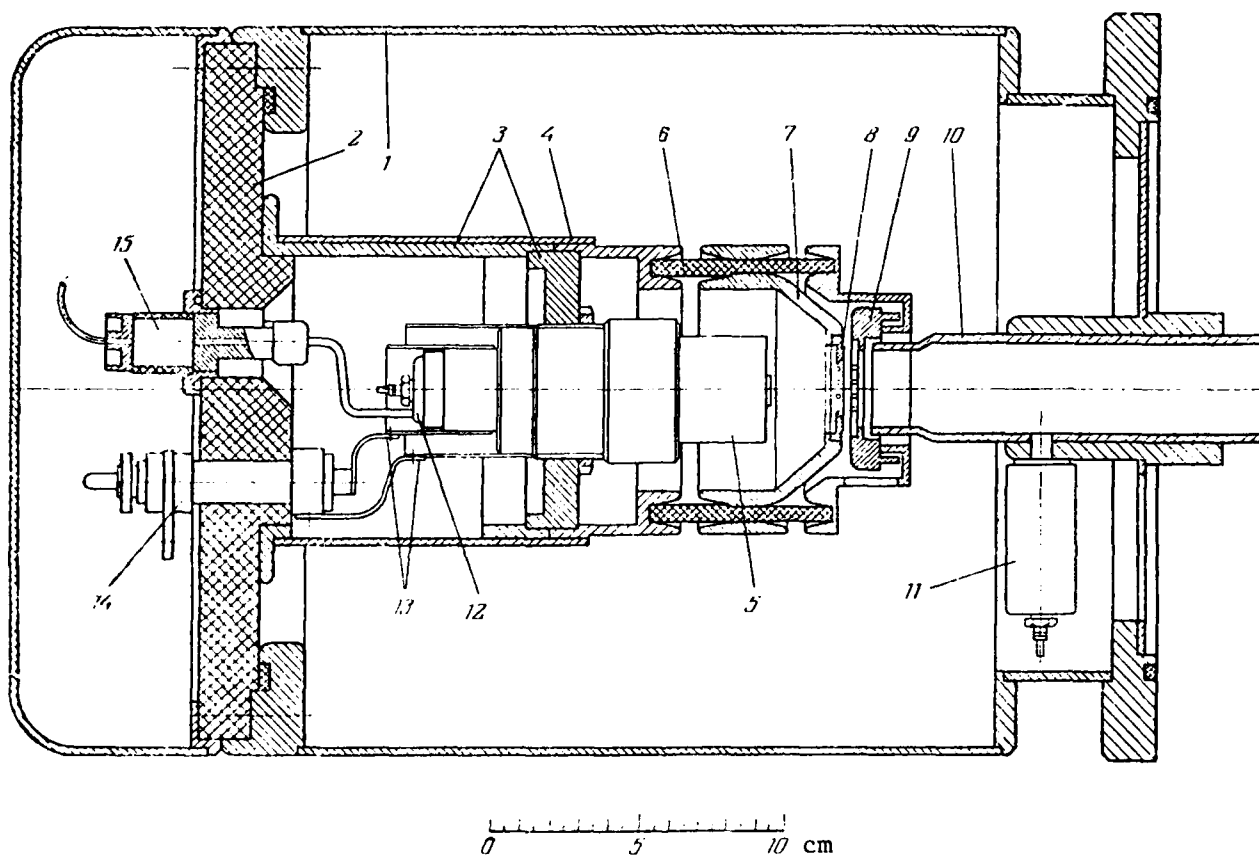


Fig. 29--NPI 1976 diagnostic hydrogen atom injector [88]

- 1--housing
- 2--insulator flange
- 3--plasma source mounting elements
- 4--magnetic shield
- 5--plasma source
- 6--extractor assembly insulator
- 7--expansion electrode
- 8--plasma grid with Pierce-shaped electrode
- 9--extraction electrode
- 10--charge-exchange canal
- 11, 12--gas valve
- 13--coaxial current leads
- 14--coaxial current feedthrough
- 15--insulated hydrogen gas feedthrough

compact charge-exchange pulsed atomic hydrogen source with an equivalent beam current of up to 3 A, a pulse length of 100  $\mu$ s, and an energy of up to 14 keV. The small dispersion angle of the injector (on the order of  $1.5 \times 10^{-2}$  by  $6 \times 10^{-2}$  rad) ensures an  $H^0$  current density of up to 95 mA/cm<sup>2</sup> at a distance of 1 meter from the injector. The measured atomic energy scatter in the beam was  $\pm 16$  eV. Because the range of the atoms and their ability to penetrate the hot, dense plasma proved insufficient at a beam energy of 10 keV, NPI researchers developed a higher energy injector.

The new NPI neutral beam injector (Fig. 30), tested in 1980, has a plasma penetration of 5 meters at a beam energy of 25 keV [119]. The maximum atomic hydrogen beam density in this injector reached 250 mA/cm<sup>2</sup>.

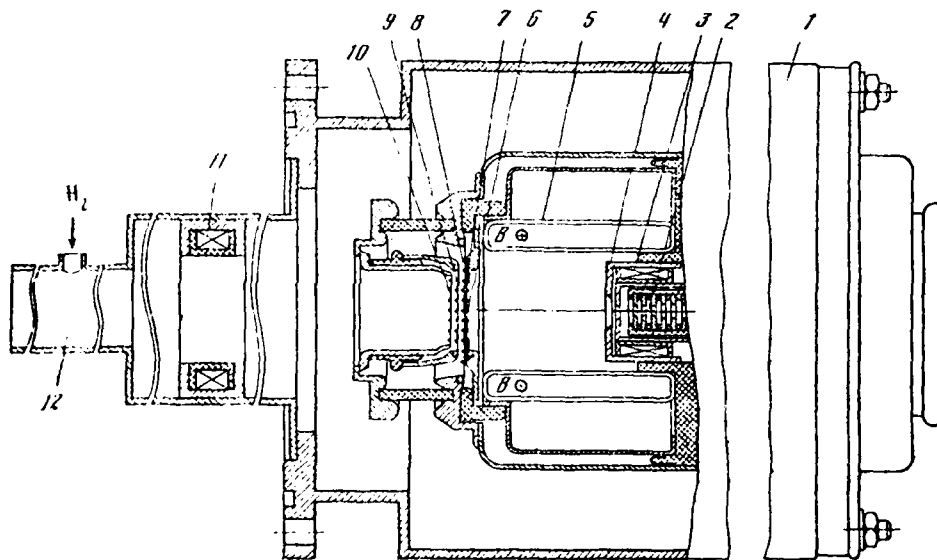


Fig. 30--NPI 1980 hydrogen atom injector [119]

- 1--housing
- 2--plasma source
- 3--solenoid
- 4--solenoid shield
- 5--"magnetic wall" coil
- 6--plasma grid
- 7--diaphragm
- 8--control grid
- 9--extraction grid
- 10--drift electrode
- 11--magnetic lens
- 12--charge-exchange target

The hydrogen plasma beam is generated in the arc discharge source (2), enters the vacuum from the source anode aperture, and interacts with the magnetic field produced by the current through the transparent toroidal winding (5). The reflection of the plasma flow from the "magnetic wall" set up in the plane of the plasma grid (6) forms an ion plasma emitter having a constant proton current density emission in a 5 cm diameter circle. A 3 cm diameter proton beam defined by the diaphragm (7) is chosen from part of the emitter with the help of the four-electrode multislit ion extraction system. The beam is then passed through a pulsed cylindrical magnetic lens (11) and focused on the charge-exchange target (12), where a large portion of the ions are converted into hydrogen atoms. The plasma source is described in [88,120]. The formation of the ion emitter by the interaction of the plasma with the magnetic field localized on the edge of the expansion space is discussed in [121]. The four-element extraction system that extracts the proton beam from the plasma is described in [122].

The increase in the atomic energy spread of the beam as a result of inelastic collisions in a charge-exchange target of the required target thickness is only about 30 eV; the instability of the pulsed extraction voltage,  $\pm 100$  eV at 25 keV energy, actually determines the energy spread of the atoms in the beam [88].

The total hydrogen atomic yield of the injector at 25 keV reached an equivalent current of 3.5 A. The current density distribution of the hydrogen atom beam at 25 keV, measured 1.5 m from the end flange of the injector, is shown in Fig. 31 for optimum emission parameter settings. Curves 1 and 2 represent the current densities parallel and perpendicular to the grid wires of the extractor system, respectively, as measured without any focusing of the proton beam by the lens (11). Curves 3 and 4 correspond to the current density distribution with the best focus of the proton beam by the magnetic lens. The maximum current density, measured calorimetrically, reached  $250 \text{ mA/cm}^2$  [119].

The beam dispersion produced by one electrode of the four-element extraction system was calculated to be  $1.1 \times 10^{-2}$  rad per proton

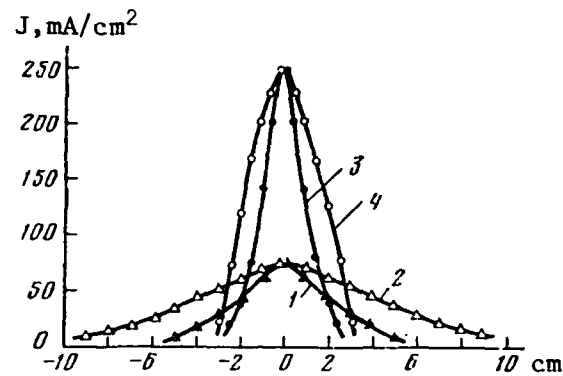


Fig. 31--Hydrogen atomic beam current density distribution at 25 keV, measured 1.5 m from injector [119]

- 1, 2--without focusing of proton beam  
3, 4--with optimum focusing of proton beam

emission from the plasma with an optimum current density and zero radial ion temperature [122]. The considerably larger dispersion observed experimentally was explained by the nature of the four-element extraction system, in which the accelerated beam, on exiting from one element, has a transverse size about one-half the width of the plasma emitting strip. The effective radial ion temperature in the plasma emitter with the magnetic wall operating was determined to be 3 to 4 eV [121].

The initial positive hydrogen ion beam was composed of 93%  $H_1^+$ , 2.5%  $H_2^+$ , 0.5%  $H_3^+$ , and 4% other ions-- $C^+$ ,  $O^+$ ,  $OH^+$ ,  $H_2O^+$ , and  $CO^+$ --with masses between 12 and 40. The collimated and focused ion beam, however, was estimated to contain only about 1% of these impurities.

Atoms of D, He, Ne, and Ar were also generated using the NPI neutral beam injector. The plasma emitting the required ions was formed by the arc discharge in the plasma source into which the gas had been introduced. Hydrogen pulses were fed into the charge-exchange target. The magnetic-wall plasma emitter worked well only for hydrogen, deuterium, and helium ion beams. The neon and argon experiments

operated under a condition of insufficient emission and about a 20% inhomogeneity of the plasma emitter. This condition led to an increased beam dispersion and a limit on the maximum operating energy of the injector. Table 3 shows the output of the neutral atom injector, measured 1.5 m from the injector flange, for the positive ion beams generated. The doubly and triply charged ions and the atoms produced by them have energies of 2 E and 3 E, respectively. Their production was found to depend weakly on the source arc discharge current and gas input. The operational characteristics of deuterium and hydrogen coincide, except for the total current and current density, which are a factor of  $\sqrt{2}F(E)/F(E/2)$  lower for deuterium, where  $F(E)$  is the conversion coefficient of a proton to an atom [119].

Table 3

NEUTRAL ATOM OUTPUT, 1.5 M FROM INJECTOR FLANGE [119]

Neutral Atom	Gas	Equivalent			Ion Beam Composition (%)
		Maximum Energy (keV)	Beam Current (A)	Current Density (mA/cm <sup>2</sup> )	
H	H <sub>2</sub>	25	3.5	250	H <sub>1</sub> <sup>+</sup> , 93; H <sub>2</sub> <sup>+</sup> , 2.5; H <sub>3</sub> <sup>+</sup> , 0.5 other, 4
D	D <sub>2</sub>	25	2.9	205	
He	He	23	2.0	90	He <sup>+</sup> , 95.5; He <sup>2+</sup> , 0.7; other, 3.8
Ne	Ne	20	1.1	15	Ne <sup>+</sup> , 62.5; Ne <sup>2+</sup> , 35; other, 2.5
Ar	Ar	22	0.6	12	Ar <sup>+</sup> , 27; Ar <sup>2+</sup> , 58; Ar <sup>3+</sup> , 14; other, 1

In an ongoing program to determine the optimum conditions for neutral beam output from injectors, IPI researchers are studying the basic characteristics of neutral atom flow, energy spread, angular dispersion, mass composition, absolute intensity, and transient processes of the neutral beam [123]. In 1980, IPI developed the DINA neutral beam diagnostic injector for determining ion temperatures of

hot plasmas inside tokamaks by means of the scattering of fast atoms [124,125,126]. The DINA can form 15 keV atomic beams of H, D, and He with a total beam current equivalent to 2 A, pulse lengths of 200  $\mu$ s, and current densities of up to 30 mA/cm<sup>2</sup> in the target region of the T-4 tokamaks.

## VI. CONCLUSIONS

Soviet open-source literature on the production and transport of negative-ion and neutral beams reveals no evidence of a program to develop an exoatmospheric particle-beam weapon in the USSR. Nor are there other clear indications of such a program. The innovative negative-ion and neutral beam research at the Nuclear Physics Institute appears to have given way to magnetic confinement fusion experiments. The Kurchatov Institute's considerable work on neutral beam production based on negative ion beams, aided by lesser efforts at IFTT and the Yefremov Institute, are explicitly dedicated to fusion research. The absence of reported experimental data on negative ion beam stripping at the Nuclear Physics Research Institute and Radiotechnical Institute, involving energies high enough to be pertinent to weapon development, may be interpreted as indicating that this work remains theoretical. The remainder of reported Soviet charge-exchange research has dealt with basic physical measurements at low beam currents of charge-exchange cross sections and beam neutralization coefficients. The published reports on this work acknowledge no applications other than nuclear fusion research.

The NPI research is important in the context of PBW development. NPI was the first to develop the two key components required for the production of intense neutral beams: the intense, high-brightness, low-emittance negative ion source, and the high-efficiency plasma beam neutralizer. The surface-plasma negative ion source, first developed in 1971, underwent a series of modifications and finally evolved into the present multislit design producing 4 A of pulsed  $H^-$  ion beam current. The source must be further upgraded to operate satisfactorily with DC or long pulses at high beam currents, but the gap between the required and achieved currents is being narrowed. For fusion application, the surface-plasma source must compete with the double-charge-exchange source and the direct-extraction magnetic-cusp-type source, both of which readily produce intense negative ion beams.



The plasma beam neutralizer, the second key component in the production of intense neutral beams, can convert high intensity negative ion beams into neutral beams with an efficiency as high as 85%. Researchers at NPI have demonstrated the formation of an 80 cm long stable plasma target with a plasma thickness of  $2.2 \times 10^{15}$  atoms/cm<sup>2</sup>, the optimum for the neutralization of 1 MeV D<sup>-</sup> ions.

In the area of high energies the only Soviet published contribution to negative ion stripping is the theoretical research at NPRI and RTI. The work of these two groups shows that the Soviets have considered in detail and now possess the basic theory of the negative ion stripping process and the calculated angular and energy distributions of ions emerging from various charge-exchange targets. The absence of experimental Soviet data in this area may indicate either that this work was limited to theory or that the sensitivity of the subject precluded publications of applied research results.

Indications of a Soviet exoatmospheric PBW program are circumstantial. For example, both NPI researchers and U.S. visitors [42,51,127] reported a sudden shift of NPI's work from negative-ion and neutral beam research to the AMBAL magnetic mirror trap project. The apparent deemphasis of NPI's impressive neutral beam research raises the question of why such a large effort was made to develop a plasma ion source and beam neutralizer--both of which are needed for PBW development, as well as thermonuclear fusion--only to abandon the project at a time of successful performance. Although this change at NPI is untypical of Soviet R&D practice, which rarely discontinues a project, and might be interpreted as an indication that the project has been classified, there is no real evidence of NPI involvement in PBW development.

Nuclear fusion research at the Kurchatov Institute seems to have higher priority and greater political and financial support than that at NPI, and exchanges with foreign scientists are more rigidly controlled at Kurchatov than at NPI. Nevertheless, there is again nothing to suggest that Kurchatov is involved in PBW research, and the more stringent controls may indicate only the proximity of other, classified experiments. The absence of evidence of a Soviet

PBW program does not mean, however, that such a program is not being pursued covertly. In fact, it would be unreasonable to assume that the Soviets were not carrying on a classified effort paralleling the reported nuclear fusion research. Thermonuclear fusion and PBW systems have similar high beam current and other parameter requirements. Many components and basic physical problems in the generation, acceleration, and transport of intense particle beams are common to both applications.

## Appendix

BASIC CHARGE-CHANGING PROCESSES IN NEUTRAL BEAM FORMATION

This appendix is presented to show the extent of Soviet research during the past 15 years on basic charge-changing processes involved in beam collisions with charge-changing targets for the conversion of positive or negative ion beams into neutrals. Concepts are defined and experimental data presented on charge-exchange and electron detachment cross sections, conversion coefficients, and angular dispersion of neutral beams formed by electron stripping.

1. CHARGE-EXCHANGE AND ELECTRON DETACHMENT CROSS SECTIONS

The efficiency of charge-changing processes depends on which of six basic processes is involved. Three are based on electron loss, or electron detachment, from ions and atoms:

- o Loss of one electron by the negative ion as a result of a collision with a target particle ( $H^- \rightarrow H^0$ ); this process is expressed by the cross section  $\sigma_{-10}$ .
- o Simultaneous loss of two electrons by the negative ion in a single collision ( $H^- \rightarrow H^+$ ), expressed by the cross section  $\sigma_{-11}$ .
- o Ionization of a neutral atom, which can be found in either the ground or one of the excited states ( $H^0 \rightarrow H^+$ ), expressed by the cross section  $\sigma_{01}$  or  $\sigma_{0*1}$ .

The remaining three processes involve the reverse charge exchange of electron capture by ions or atoms:

- o Electron capture by a positive ion ( $H^+ \rightarrow H^0$ ), expressed by the cross section  $\sigma_{10}$ .
- o Double electron capture by a positive ion ( $H^+ \rightarrow H^-$ ), expressed by the cross section  $\sigma_{1-1}$ .

- o Electron capture by a neutral atom ( $H^0 \rightarrow H^-$ ), expressed by the cross section  $\sigma_{0-1}$ .

Western and Soviet experimental data on the cross sections of electron detachment from atoms and negative ions ( $\sigma_{-10}$ ,  $\sigma_{01}$ ,  $\sigma_{-11}$ ) and the electron capture by positive ions and atoms ( $\sigma_{10}$ ,  $\sigma_{0-1}$ ,  $\sigma_{1-1}$ ) in gas collisions were compiled and published by N. V. Fedorenko in 1970 [128]; other reviews include [129,130] and, more recently [131, 132,133,22,24]. The data are displayed as sets of curves of cross sections as a function of colliding particle energy for each of the six processes, for energy ranging from less than 1 keV to greater than 1 MeV.

The effect of the six basic charge-changing processes of hydrogen ions and atoms is shown in terms of cross section as a function of beam energy in  $H_2$  (Fig. 32) [134] and Ar, which exhibits the typical behavior of a gas having medium mass (Fig. 33) [128]. As

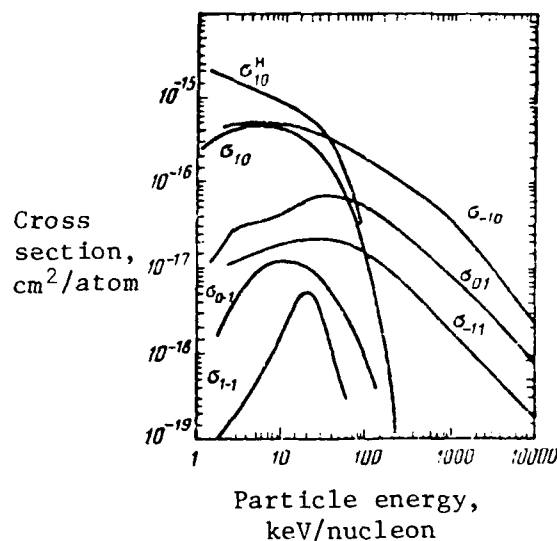


Fig. 32--Energy dependence of electron capture cross sections ( $\sigma_{10}$ ,  $\sigma_{0-1}$ ,  $\sigma_{1-1}$ ) and electron loss cross sections ( $\sigma_{-10}$ ,  $\sigma_{01}$ ,  $\sigma_{-11}$ ) of hydrogen ions and atoms in  $H_2$ ;  $\sigma_{10}^H$  is electron capture cross section by hydrogen ions in atomic hydrogen [134]

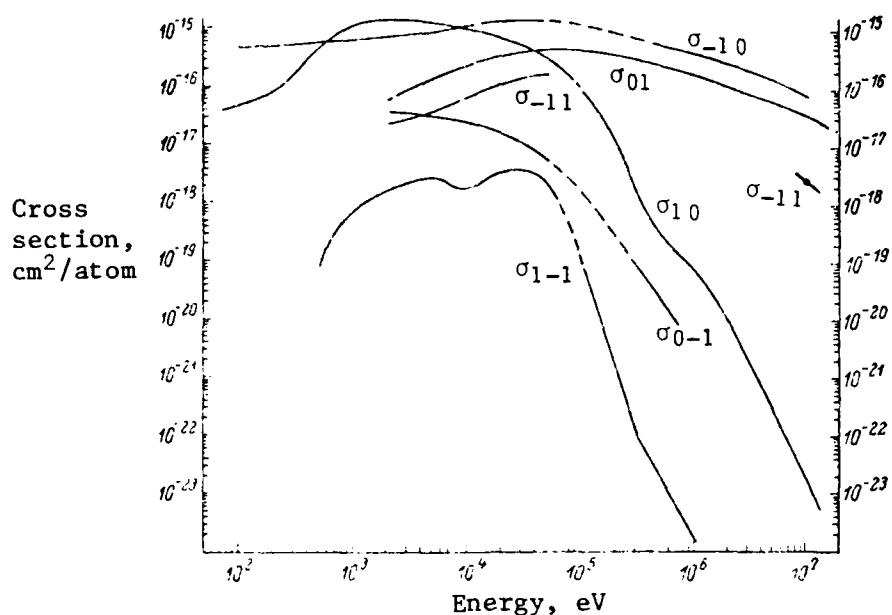


Fig. 33--Cross sections of six charge-changing processes in Ar as a function of beam energy [128]

can be seen from the figures, the electron detachment processes do not cross, and at a given energy their cross sections decrease in the order of  $\sigma_{-10}$ ,  $\sigma_{01}$ , and  $\sigma_{-11}$ . Electron detachment from a negative ion  $\sigma_{-10}$  in Ar, which exhibits the flattest curve and maximum value of the cross section at an energy of about 100 keV, is the most energy independent process.

The curves representing the capture of one or two electrons also do not cross; at a given energy, their cross sections decrease in the order of  $\sigma_{10}$ ,  $\sigma_{0-1}$ ,  $\sigma_{1-1}$ . The cross sections of these processes fall off markedly at energies greater than 50 keV. At the higher energies, the electron capture processes can be neglected because the cross sections have low values compared with electron loss cross sections [129]:

$$\sigma_{1-1} \ll \sigma_{0-1} \ll \sigma_{10} < 10^{-3} \sigma_{01}$$

Figure 34 shows the cross section for neutral hydrogen production by electron detachment from  $H^-$  ions for various target gases, as

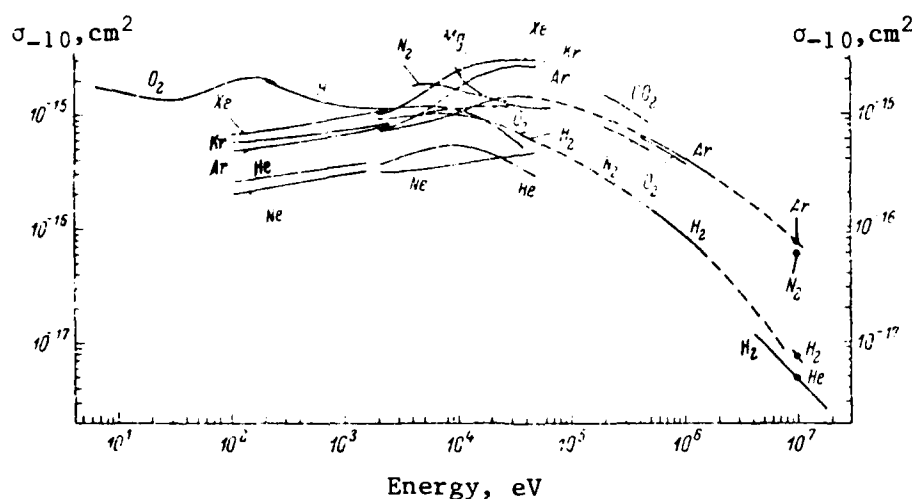


Fig. 34--Cross sections for  $H^0$  production by electron detachment from  $H^-$  ions ( $\sigma_{-10}$ ) [128]

measured by various researchers (identified in [128]). The data in Fig. 34 exhibit relatively small changes in cross section for large changes in energy and relative independence of the target gas. In the high energy range, however, the cross section for  $\sigma_{-10}$  (similarly to those for  $\sigma_{01}$  and  $\sigma_{-11}$ ) quickly falls off, approximating the law  $\sigma_{-10} \sim E^{-1}$  [128].

Soviet cross-section measurements of specific interest to neutral beam production include those by IFTT of the cross sections  $\sigma_{10}$  and  $\sigma_{01}$  for protons and neutral hydrogen atoms in Li in the energy range of 40 to 400 keV, shown in Fig. 35 [135]. In the 10 to 40 keV energy range, the cross-section values were calculated from data in [136]. The values for  $\sigma_{10}$  as measured by IPI researchers are also included in Fig. 35 for comparison. The IPI data for  $\sigma_{10}$  in various alkali metal vapors are shown in Fig. 36.

Electron detachment cross sections for  $H^-$  ions ( $\sigma_{-10}$ ) and  $H^0$  atoms ( $\sigma_{01}$ ) at high energies (10 to 1000 MeV), calculated at NPRI in 1973 [99,100] using light target materials ( $H_2$ , Li, Be, C, and  $N_2$ ) are shown in Figs. 37 and 38 [97]. The curves in these two figures continue the  $\sigma_{-10}$  and  $\sigma_{01}$  data for hydrogen beams in  $H_2$  shown in Figs. 32 and 34, above, and in Li in Fig. 35, above. In the figures,

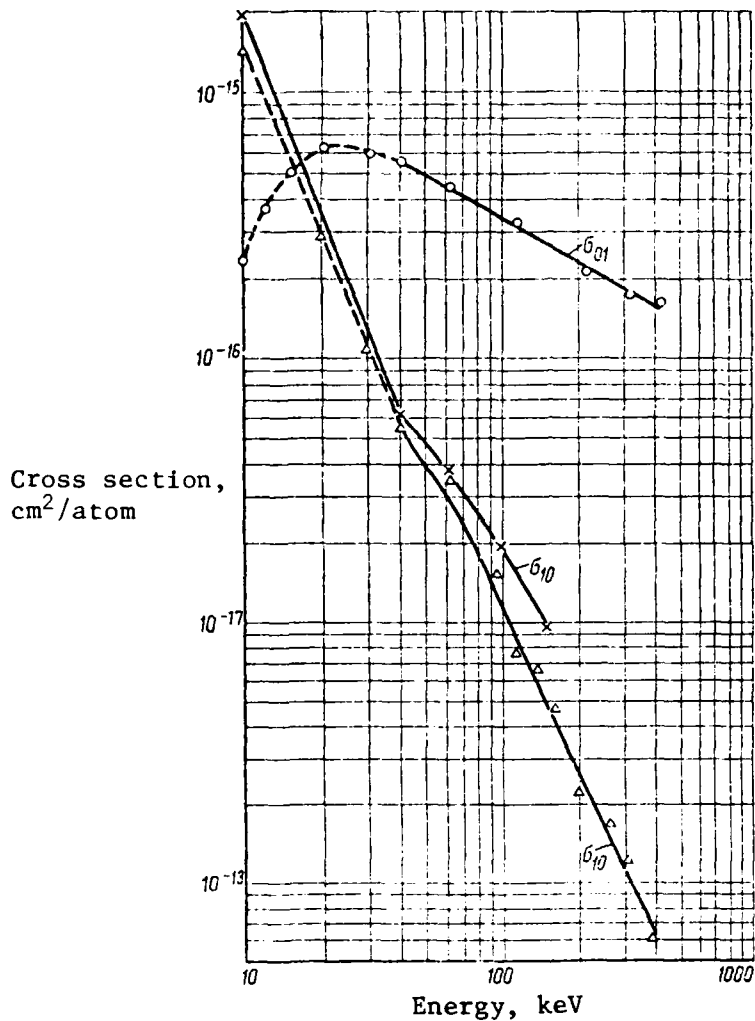


Fig. 35--Cross section measurements of  $\sigma_{10}$  and  $\sigma_{01}$  in lithium as a function of energy [135]

— data of [135]  
 ---- calculated from data of [136]  
 -x-x-x- data of [106]

the cross-section values level off with increasing energy. Charge exchange and electron stripping of the beams at these high energies are of interest for high-energy physics and meson factory applications, as well as for the future development of particle-beam weapons.

In 1965, an NPI team had measured the  $\sigma_{-10}$  and  $\sigma_{-11}$  cross sections for electron detachment from  $H^-$  in various gases--including

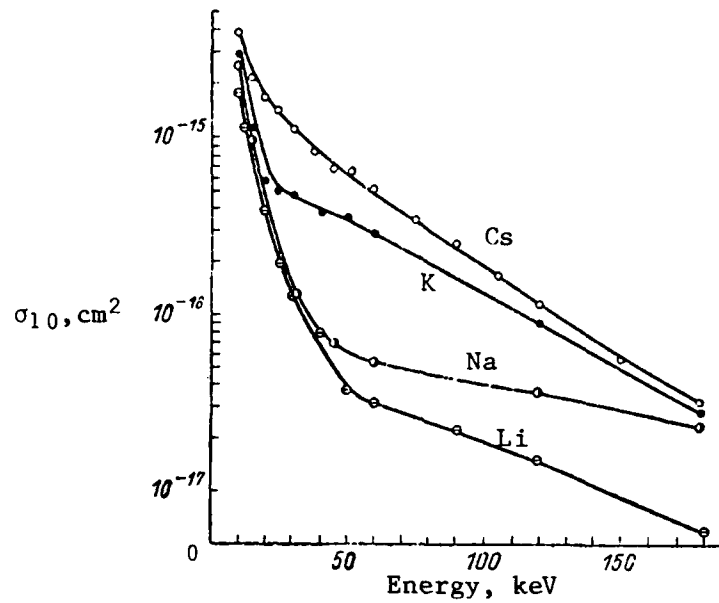


Fig. 36--Total cross section measurements of  $\sigma_{10}$  in alkali metal vapors as a function of proton energy [106]

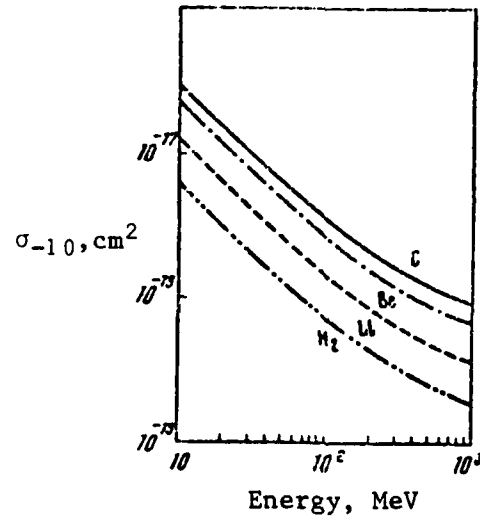


Fig. 37--Calculated electron loss cross sections ( $\sigma_{-10}$ ) from  $\text{H}^-$  ions in  $\text{H}_2$  and in Li, Be, and C atoms [97]



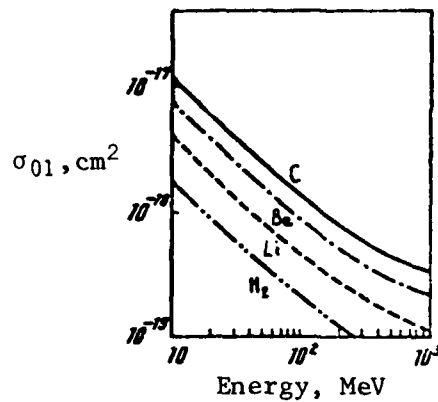


Fig. 38--Calculated electron loss cross sections ( $\sigma_{01}$ ) from hydrogen atoms in  $H_2$  and in Li, Be, and C atoms; the cross section in N atoms (not shown) lies less than 10% that in C atoms [97]

$H_2$ , He,  $N_2$ ,  $CO_2$ ,  $C_3H_8$ ,  $CCl_2F_2$ , and  $SF_4$ --for an ion beam energy range of 0.9 to 1.3 MeV [137]. The total neutral beam output and corresponding optimum target thickness were also measured. The cross sections  $\sigma_{-10}$  and  $\sigma_{-11}$  were found to be inversely proportional to the beam energy and to exhibit a slightly weaker than linear dependence on the atomic number of the gas target.

In 1975-1976, NPI researchers investigated electron detachment from  $H^-$  and  $D^-$  ions and  $H^0$  and  $D^0$  atoms in the 400 to 900 keV energy range by passing these beams through Li and Mg plasma targets [86,138]. They also measured the relative cross sections involved in the interaction of these beams with the plasma targets. The maximum neutral beam production obtained in these experiments reached 80% to 82%.

The apparatus used to measure conversion coefficients is shown in Fig. 39. A Van de Graaff accelerator produced a pulsed beam of  $H^-$  ions [139]. The  $H^-$  beam was passed through the magnetic analyzer (1), focused by a pair of magnetic lenses (2) onto a  $0.5 \times 8 \text{ mm}^2$  collimating aperture (3) located just before the plasma target (4). After interacting with the plasma target, the beam was divided by the magnetic separator (5) into its three components ( $H^-$ ,  $H^0$ , and  $H^+$ ).

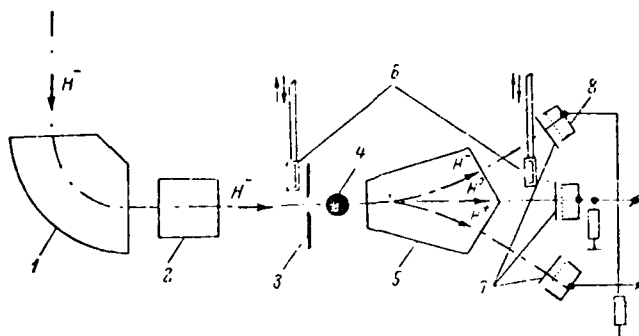


Fig. 39--Diagram of apparatus used to measure conversion coefficients [86,138]

- 1--magnetic analyzer
- 2--lens
- 3--collimator
- 4--plasma target
- 5--magnetic separator
- 6--movable detectors
- 7--stripping film
- 8--faraday cups

Each beam component was measured by passing it through a 2  $\mu\text{m}$  thick dacron stripping film, and the resulting proton beams were measured with the faraday cups (8). The plasma target (4) is a cylindrical plasma column 0.8 cm in diameter and 3 cm high.

The components of the plasma target are shown in Fig. 40. The plasma column is formed by two identical conical plasma sources generating plasma flows along the 700 gauss magnetic field set up in the gap by the magnets (1). The plasma sources, consisting of duraluminum anodes (2), Li or Mg cathodes (3), and trigger electrodes (4), are powered through pulse-forming lines with square-wave, 350  $\mu\text{s}$ , 1.2 kA current pulses. The average degree of ionization, measured diametrically across the plasma channel along the negative ion beam axis, was 90% to 95%, as determined by the attenuation of 10 keV  $\text{H}^+$  and  $\text{H}^-$  ion beams. The electron temperature of the plasma, as measured with plasma probes, was determined to be 5 eV [86,138].

The relative ionization cross sections of  $\text{H}^0$  and  $\text{D}^0$  atoms ( $\sigma_{01}$ ) and the double-electron-detachment cross sections of  $\text{H}^-$  and  $\text{D}^-$  ( $\sigma_{-11}$ )

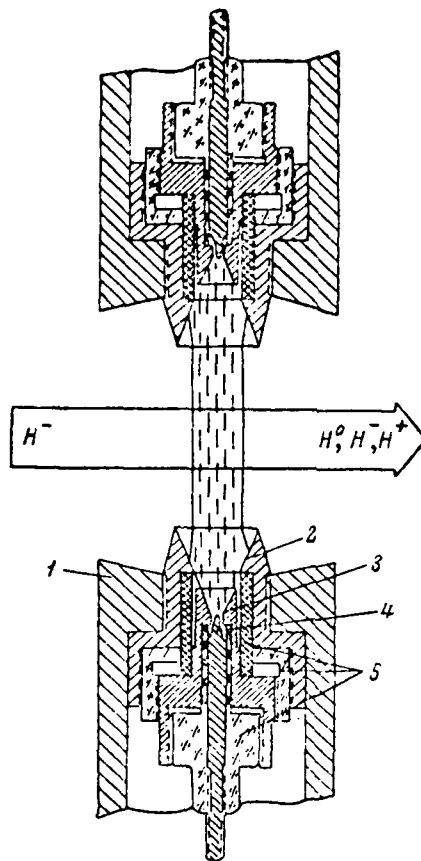


Fig. 40--Diagram of plasma target  
[86,138]

- 1--magnetic pole
- 2--anode
- 3--cathode
- 4--trigger electrode
- 5--insulators

in Li and Mg plasma targets were measured with the apparatus shown in Fig. 41. After being focused, the  $H^-$  ion beam was passed first through a  $CO_2$  target (1) to produce a mixed beam of  $H^0$ ,  $H^-$ , and  $H^+$  and then through a  $0.5 \times 8 \text{ mm}^2$  collimating slit (2) and magnet (3) with a zigzag field. The magnet separated the three components of the beam, allowing the  $H^+$  ion component to be removed and the other two components to be returned unperturbed to the beam axis and then passed through the plasma target (5), where they were measured and

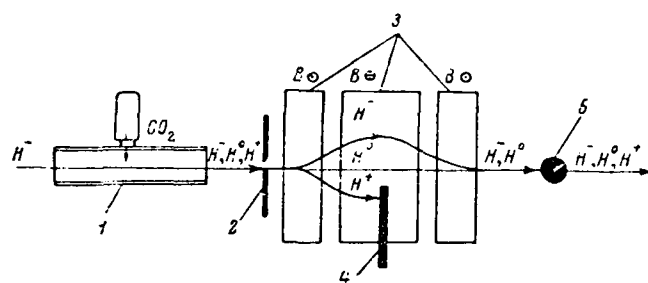


Fig. 41--Schematic of apparatus used to measure  $\sigma_{01}$  and  $\sigma_{-11}$  cross sections [138]

- 1--charge-exchange gas-target cylinder
- 2--collimating slit
- 3--analyzing magnet
- 4--movable beam stop
- 5--plasma target

analyzed in the same manner as in the experiments for determining conversion coefficients  $\eta^0$ , described above.

The electron detachment cross sections for  $H^-$  ions ( $\sigma_{-10}$ ) and  $H^0$  atoms ( $\sigma_{01}$ ) in a hydrogen plasma ( $H^+ + e^-$ ) are shown in Fig. 42; the  $\sigma_{-10}$  is considerably higher in plasma than in gases.

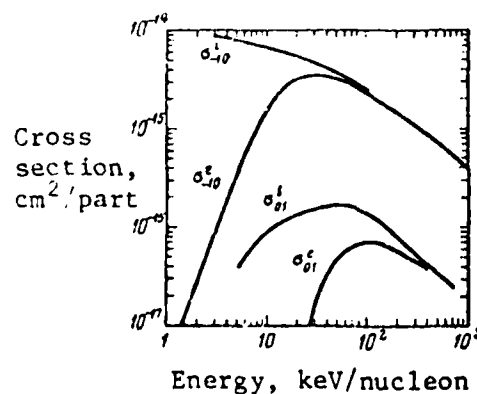


Fig. 42--Electron detachment cross sections for  $H^-$  ions ( $\sigma_{-10}$ ) and  $H^0$  atoms ( $\sigma_{01}$ ) in  $H^+ + e^-$  plasma (on ions  $\sigma^i$  and cold electrons  $\sigma^e$ ) [134]

## 2. NEUTRAL BEAM CONVERSION COEFFICIENTS

The maximum neutral yield from negative ions can be expressed as [138]:

$$\eta_{\max}^0 = \frac{\sigma_{-10}}{\sigma_{-10} + \sigma_{-11}} \left( \frac{\sigma_{01}}{\sigma_{-10} + \sigma_{-11}} \right)^{\frac{\sigma_{01}}{\sigma_{-10} - \sigma_{01} + \sigma_{-11}}},$$

and is obtained at the following optimum target thickness:

$$\delta_{\text{opt}} = n\ell_{\text{opt}} = \frac{1}{\sigma_{-10} + \sigma_{-11} - \sigma_{01}} \ln \frac{\sigma_{-10} + \sigma_{-11}}{\sigma_{01}}.$$

The double-electron-detachment cross section is much lower than the single-electron-detachment cross section:  $\sigma_{-11} \ll \sigma_{-10}$  [140]. For most gas targets,  $\sigma_{-11} \lesssim 4 \times 10^{-2} \sigma_{-10}$  and thus can be neglected in the above expressions, reducing  $\eta_{\max}^0$  to:

$$\eta_{\max}^0 \approx \left( \frac{\sigma_{01}}{\sigma_{-10}} \right)^{\frac{\sigma_{01}}{\sigma_{-10} - \sigma_{01}}},$$

where the conversion coefficient is basically determined by the ratio  $\sigma_{-10}/\sigma_{01}$ .

The relative beam outputs of  $H^0$ ,  $H^+$ , and  $H^-$ , as calculated in [138], are shown in Table 4 for various values of  $\sigma_{-10}/\sigma_{01}$  using optimum target thickness and neglecting  $\sigma_{-11}$ . For most gases used, the  $\sigma_{-10}/\sigma_{01}$  ratio lies between 2.5 and 3.5 for  $H^-$  energies in the hundred keV range;  $\eta^0$  therefore reaches 52% to 55% [52,137]. When alkali metal vapors replace the gases,  $\eta^0$  can reach 65% [73].

Researchers at NPI take credit for being the first--in 1969--to suggest the use of plasma targets for neutralizing negative ion beams [141]. For plasma targets,  $\sigma_{-11} < .06 \sigma_{-10}$  and the  $\sigma_{-10}/\sigma_{01}$  ratio was 22% in the 0.5 to 1 MeV energy range, providing an atomic yield

Table 4

CALCULATED RELATIVE BEAM OUTPUTS  
OF  $H^0$ ,  $H^-$ , AND  $H^+$  FOR VARIOUS  
VALUES OF  $\sigma_{-10}/\sigma_{01}$  [138]

$\frac{\sigma_{-10}}{\sigma_{01}}$	$\eta^0, \%$	$\eta^-, \%$	$\eta^+, \%$
1	36.8	36.8	24.6
2	50	25	25
3	57.7	19.3	23
4	63	15.7	21.3
5	66.9	13.4	19.7
10	77.4	7.8	14.8
15	82.4	5.5	12.1
20	85.4	4.3	10.3
22.5	86.5	3.9	9.6
25	87.5	3.5	9

of  $\eta^0 = 86.4\%$ , neglecting the  $\sigma_{-11}$  process. In the same energy range, NPI researchers in 1975-1976 used the apparatus described above to measure neutral beam production from the stripping of  $H^-$  and  $D^-$  ions in Li and Mg plasma targets; maximum neutral beam production reached 80% to 82% [86,138]. The conversion coefficients of  $H^-$  to  $H^0$  as a function of energy for gas and plasma targets, shown in Fig. 43, indicate the nondependence of neutral beam output on energy in this energy range. The efficiency of  $H^0$  beam production may be further increased by using photon targets, which convert 100% of the  $H^-$  to  $H^0$  [30,142,143].

The efficiency of transforming protons, molecular ions, and  $H^-$  ions into fast neutral atoms using optimized gas and plasma targets is summarized in Fig. 44. The inefficiency of  $H^0$  production from positive ions at energies greater than 100 keV, as seen in the figure, stems from the drop-off of the cross sections.

The presence of excited atoms in charge-exchange canals decreases the total neutral beam output. However, excited atoms have to be taken into account only at small target dimensions. The effects of excited atoms, as well as electron capture, can be neglected in the actual conversion of negative ions into atoms, because the axial dimensions of the target provide sufficient interaction distance to

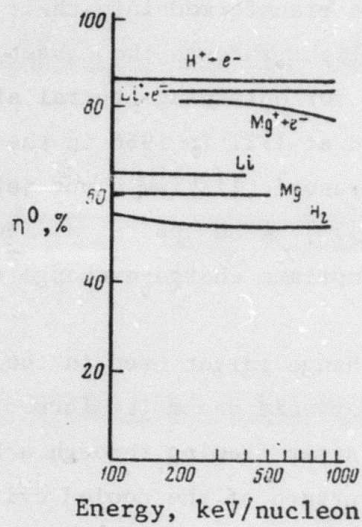


Fig. 43--Conversion coefficients of  $H^-$  ions into  $H^0$  in gas (Li, Mg,  $H_2$ ) and plasma ( $H^+ + e^-$ ,  $Li^+ + e^-$ ,  $Mg^+ + e^-$ ) targets [134]

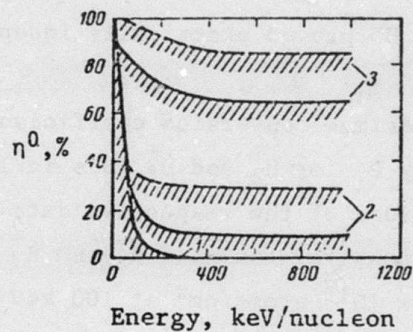


Fig. 44--Conversion coefficients for hydrogen ions into neutrals in gas targets (solid lines) and plasma targets (broken lines) for 1-- $H^+$ ; 2-- $H_2^+$  and  $H_3^+$ ; and 3-- $H^-$  [134]

allow the excited atoms to be transformed into their ground state in less than their time of flight through the target [138].

Conversion coefficients for obtaining neutral atoms from  $H^-$ ,  $H_2^+$ , and  $H_3^+$  ions were measured at IFTT in 1966 in the energy range of 100 to 400 keV, using an ultrasonic lithium vapor jet with a thickness of up to  $5 \times 10^{15}$  atoms/cm<sup>2</sup> [73]. The apparatus used to measure conversion coefficients and optimum charge-exchange cross sections was described in [73].

The Li vapor charge-exchange target used in the IFTT experiments (Fig. 45) consisted of a supersonic vapor jet formed by the evaporation of Li from the boiler (2). After flowing through a Laval nozzle (4), the vapor condensed on the surface of the cooled cylinder (7). The boiler and nozzle were heated by external heaters (3) and (5), respectively; thermocouples (6) and (8) monitored the temperature.

The neutrals were formed by either the dissociation of  $H_2^+$  and  $H_3^+$  ions or the electron stripping of  $H^-$  ions. The neutral output from the  $H_1^+$  in this energy range was negligible. The measurements (Fig. 46) showed a maximum neutral output from  $H_3^+$  of 90% at 100 keV and 60% at 400 keV; the neutral output from  $H_2^+$  at the same energies was only 41% and 23%, respectively. In the same energy range, the conversion coefficient for  $H^-$  proved practically independent of energy, reaching 65% in Li vapor.

Figure 46 shows the maximum conversion coefficient  $\eta_{\max}$  as a function of ion beam energy  $E_i$  for  $H_2^+$  and  $H_3^+$  ions in lithium; it also shows the analytic expressions of the respective data points. The optimum vapor target thickness for use with  $H_2^+$  and  $H_3^+$  ions was found to increase from  $\delta_{\text{opt}} \approx 3 \times 10^{15}$  atoms/cm<sup>2</sup> at 100 keV to  $\delta_{\text{opt}} \approx 5 \times 10^{15}$  atoms/cm<sup>2</sup> at 400 keV. For negative ions,  $\delta_{\text{opt}}$  changed correspondingly from 1.5 to  $5 \times 10^{15}$  atoms/cm<sup>2</sup>. For comparison,  $\eta_{\max}$  was also measured in Mg, Zn, and Hg vapor jets.

The maximum conversion coefficient was obtained by measuring the  $I_{\text{out}}/I_{\text{in}}$  ratio (where  $I_{\text{in}}$  is the ion beam current before the beam enters the vapor target and  $I_{\text{out}}$  is the current after the beam leaves the target) as a function of target thickness for  $H^-$  and  $H_3^+$  beams through Li and Mg. Figure 47 displays the measurements for



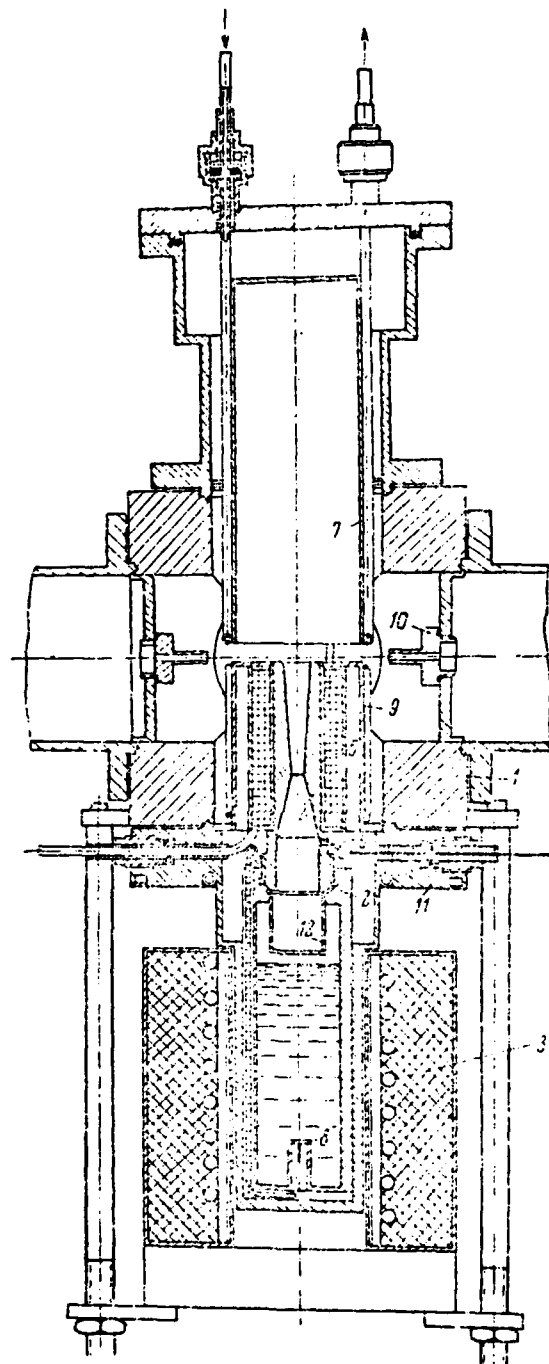


Fig. 45--Li vapor jet charge-exchange target [73]

- |                   |                             |
|-------------------|-----------------------------|
| 1--target housing | 6,8--thermocouples          |
| 2--boiler         | 7--cooled cylinder          |
| 3--boiler heater  | 9--heat shield              |
| 4--nozzle         | 10--collimating channel     |
| 5--nozzle heater  | 11--flange with feedthrough |
|                   | 12--reflector shield        |

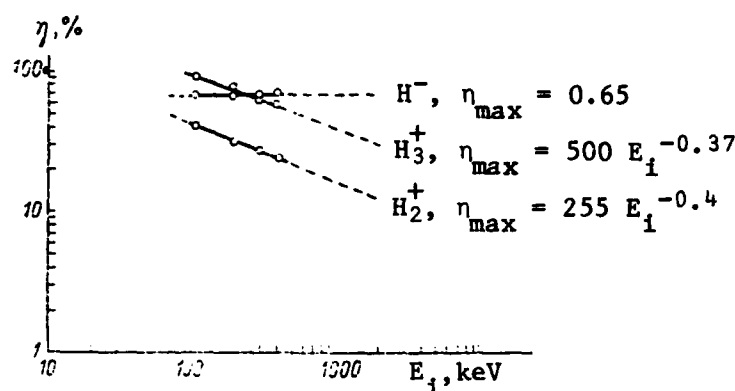


Fig. 46--Conversion coefficient as a function of ion energy for an Li vapor target [73]

an ion beam energy of 307 keV; the consumption of Li and Mg is shown along the abscissas as  $q$ , mg/s.

For the case of an  $H^-$  beam, the  $\eta_{\max}$  of 60% for Mg and 58% for Zn practically does not change with energy. For  $H_2^+$ , the  $\eta_{\max}$  was 42% for Mg (100 keV), 40% for Zn (200 keV), and 18% for Hg (400 keV) [73]. The experiments on Hg in [73] were performed on a target similar to that used by Ya. M. Fogel' in 1955 [144]. The neutral output using  $H_1^+$  and Li and Mg with a target thickness of  $3$  to  $5 \times 10^{15}$  atoms/cm<sup>2</sup> was insignificant, amounting to only several percent at 100 keV. The maximum yield for  $H_1^+$  at this energy, 14%, was obtained with Zn at  $\delta_{\text{opt}} = 10^{16}$  atoms/cm<sup>2</sup>.

Neutral output obtained by  $H_2^+$  dissociation in the 1 to 4.6 MeV range was investigated by Schmidt in 1964 [145]. The maximum conversion coefficient  $\eta_{\max}$  showed a weak energy dependence, with a value of about 12% for Ar and 17% for H<sub>2</sub>. The  $\eta_{\max}$  for the  $H^-$  beam in the range of 1 to 1.5 MeV in H<sub>2</sub>, N<sub>2</sub>, C<sub>2</sub>H<sub>2</sub>, C<sub>3</sub>H<sub>3</sub>, CO<sub>2</sub>, CF<sub>6</sub>, and CCl<sub>2</sub>F<sub>2</sub> gas targets, measured by the Fogel' group in 1955, showed weak dependence on both energy and type of target gas. The values ranged from 50% to 55% [146]. Neutral formation by passing an  $H^-$  beam through hydrogen and other gases at higher energy--4 to 18 MeV--was measured by R. Smythe et al. in 1965 [52]. At an  $H^-$  energy of 9.8 MeV, the  $\eta_{\max} \approx 58\%$  for hydrogen gas.

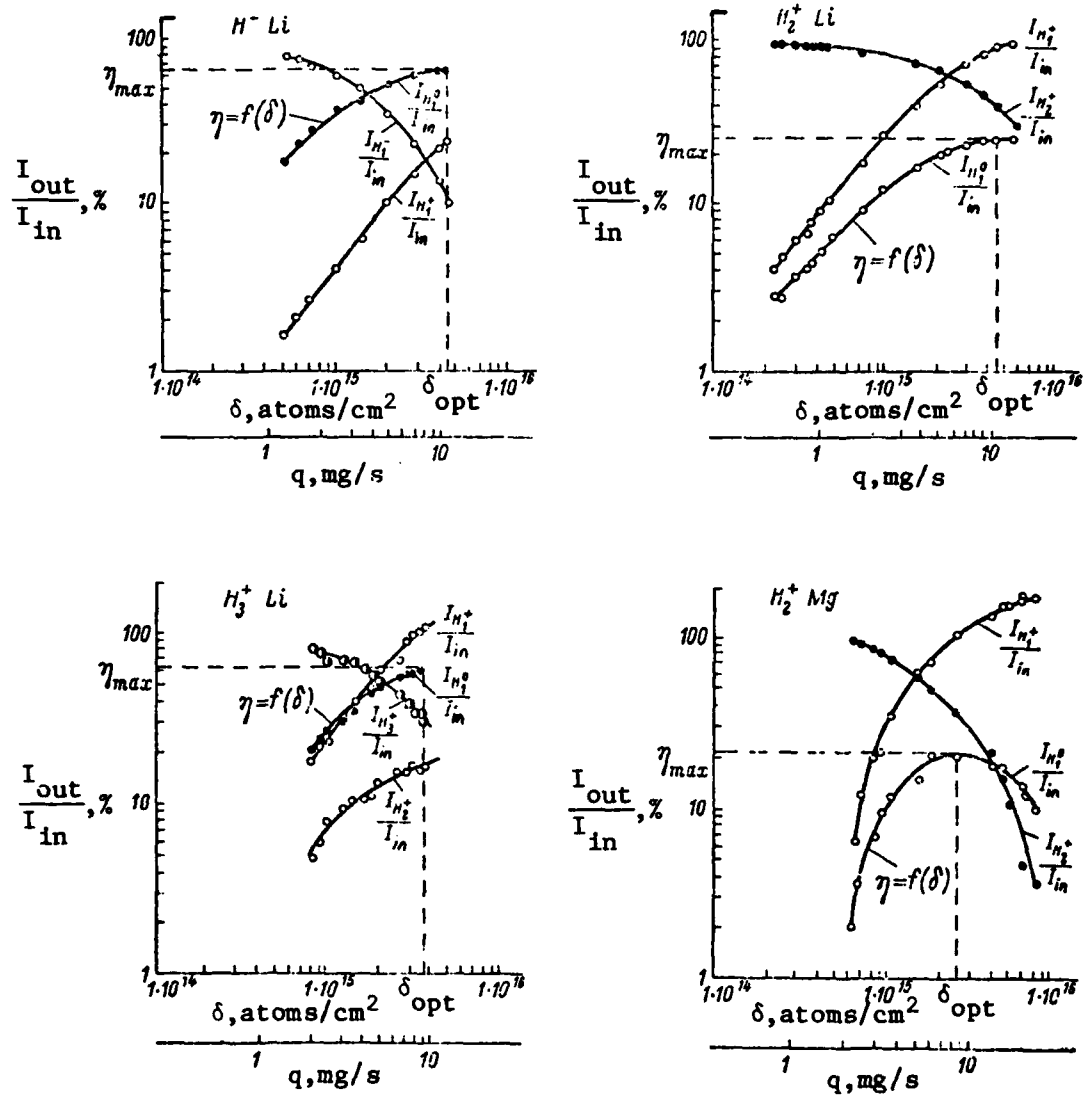


Fig. 47--Conversion coefficients for  $H^-$  and  $H_3^+$  ions through Li, and  $H_2^+$  through Li and Mg, as a function of target thickness, with  $E_1 = 307$  kV [73]

In 1974-1975, IFTT researchers measured the conversion of negative ions of  $C^-$ ,  $O^-$ ,  $F^-$ , and  $Cl^-$  into neutral beams in gases ( $H_2$ , He,  $CO_2$ , and air) and in metallic vapors (Li, Na, and Mg) [147]. The charge-exchange coefficient, measured as a function of energy in the range of 110 to 380 keV, typically varied from 40% to 60% in gases, 60% to 70% in metal vapors, and 35% to 45% in  $CO_2$  at 200 keV. These measurements are shown in Figs. 48 and 49.

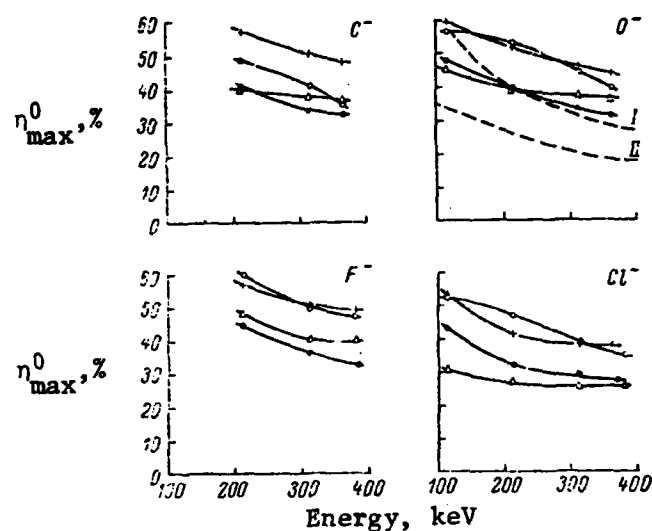


Fig. 48--Conversion coefficient  $\eta_{\max}^0$  as a function of negative ion beam energy in gas targets [147]

+--H      I-- $O^+ + H_2 \rightarrow O^0$   
 o--Ar      II-- $O^+ + He \rightarrow O^0$   
 Δ--He  
 ●--CO

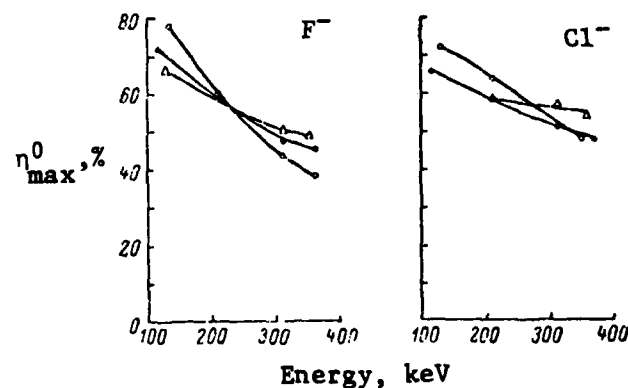


Fig. 49--Conversion coefficient  $\eta_{\max}^0$  as a function of negative ion beam energy in metallic vapor targets [147]

●--Li  
 o--Na  
 Δ--Mg

For comparison, data on  $\eta_{\max}$  for the process  $O^+ \rightarrow O^0$  in  $H_2$  and He gas targets, as given by T. Jorgensen et al. in [148], is shown by the dashed lines of the  $O^-$  ion plot in Fig. 48. As can be seen from the figure, the process  $O^+ \rightarrow O^0$  has a considerably lower conversion coefficient than the  $O^- \rightarrow O^0$  process in the same gases. Even at these relatively low energies at which positive ions can produce neutrals by charge exchange, negative ions still provide considerably higher neutral yields [147].

The experimental apparatus used to measure conversion coefficients (Fig. 50) consisted of an RF source (1) [149], 400 keV acceleration tube (3), magnetic lens (4), magnetic analyzer (5), and charge-exchange target (6). The metal vapor target operated with ultrasonic Li, Na, and Mg vapors injected into the vacuum from a Laval nozzle, as described in [136]; the  $H_2$ , He,  $CO_2$ , and Ar gas targets consisted of a tube 180 mm long with entrance and exit channels that served the same function as the collimating apertures of the metal vapor target.

### 3. NEUTRAL BEAM ANGULAR DISPERSION

In 1966-1967, IFTT investigated the angular dispersion  $\theta/2$  of a 100 keV neutral beam formed by charge exchange of  $H_1^+$ ,  $H_2^+$ ,  $H_3^+$ , and  $H^-$  beams in Li and Cd vapor jets [73]. The dispersion of 100 keV  $H^-$  and  $H_1^+$  in Li (at  $\delta = 10^{15}$  atoms/cm<sup>2</sup>) was very small (less than  $10^{-3}$  rad). The neutral beam formed by the dissociation of  $H_2^+$  (200 keV) and  $H_3^+$  (300 keV) in an Li jet had an angular dispersion of about  $10^{-2}$  rad. The order of magnitude increase in the dispersion of the neutrals formed by dissociation of the hydrogen ions over that of the neutrals formed by charge exchange is explained by the difference in the dispersion mechanisms. In the case of the dissociation of the  $H_2^+$  and  $H_3^+$  ions, the molecular binding energy is released, causing an energy spread of the formed particles, as well as an angular dispersion of the particle trajectories. The dispersion in the charge-exchange case is minimal because it is governed by single or multiple dispersion associated only with the loss or capture of the loosely bound electrons.

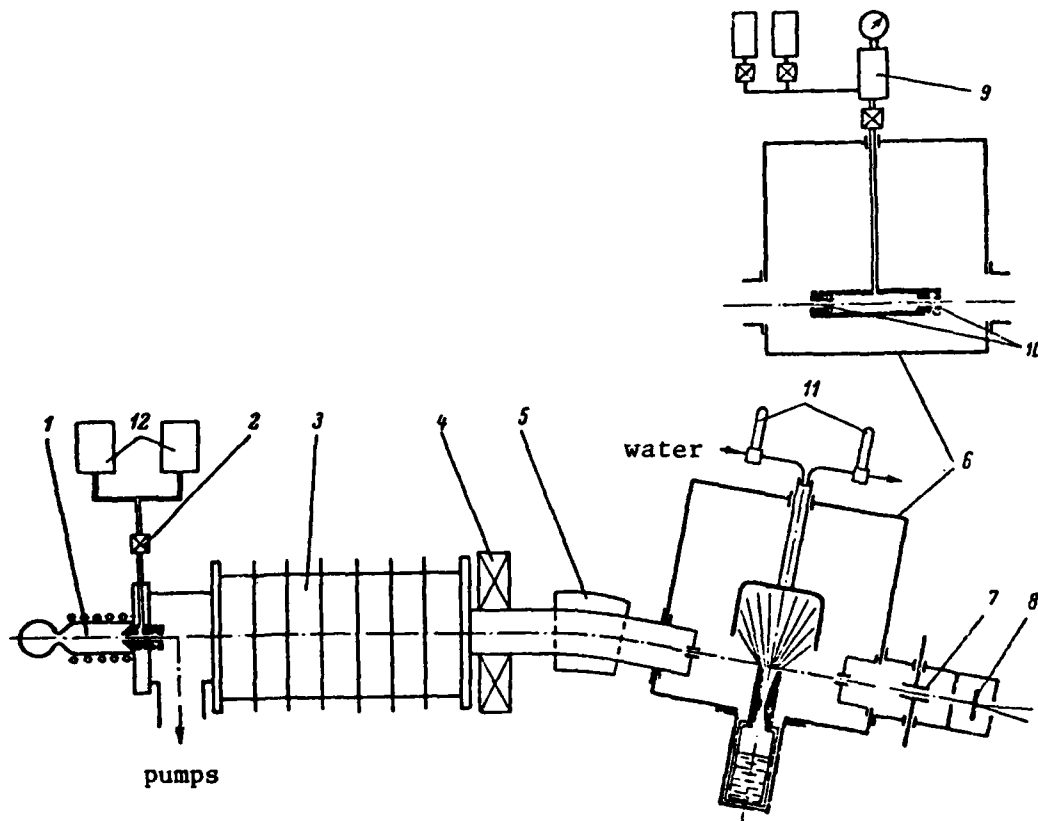


Fig. 50--Schematic of experimental apparatus for measuring conversion coefficients [147]

- 1--ion source
- 2--gas leak
- 3--acceleration tube
- 4--magnetic lens
- 5--magnetic analyzer
- 6--charge-exchange target chamber
- 7--electrostatic analyzer
- 8--detector
- 9--gas monitoring tank
- 10--collimating channels
- 11--thermometers
- 12--gas tanks

Current density distribution is shown as a function of beam radius in Fig. 51 for 100 keV neutral beams formed by charge exchange and by dissociation of hydrogen ions in Li and Cd targets, with target thickness  $\delta = 10^{15}$  atoms/cm<sup>2</sup>. The figure shows a well-collimated neutral beam formed from  $H^-$  or  $H_1^+$  ions and the added dispersion

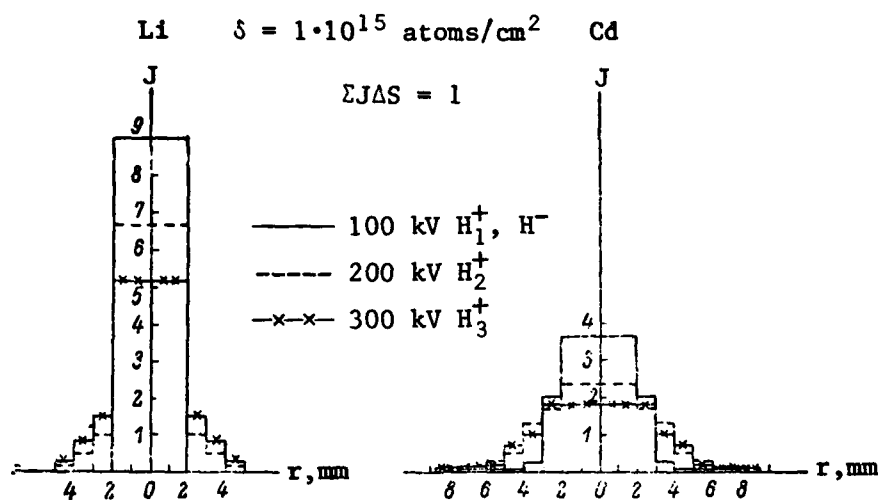


Fig. 51--Current density distribution of a 100 keV neutral beam formed by charge exchange and dissociation of hydrogen ions in Li and Cd gas targets as a function of beam radius [73]

obtained by using molecular ions. The ordinate, representing neutral beam current density, is normalized as  $\Sigma JAS = 1$  [73].

IFTT researchers concluded that the production of neutrals by electron stripping of negative ions offers considerably more advantages than production by the dissociation of  $H_2^+$  and  $H_3^+$  ions. When negative ions are used, the neutrals are produced with energies equal to the energy of the primary negative ion, and the value of the conversion coefficient  $\eta_{\max}$  is high and almost independent of  $H^-$  ion energy; when positive ions are used,  $\eta_{\max}$  decreases as  $H_2^+$  and  $H_3^+$  ion energy increases.

In 1974, IFFT made additional measurements on angular dispersion of neutral hydrogen formed by electron stripping of  $H^-$  ions [150], this time in  $H_2$ , He, and Li targets, with target thicknesses of  $5 \times 10^{14}$  to  $1 \times 10^{16}$  atoms/cm<sup>2</sup> at  $H^-$  beam energies of 50 to 150 keV. The dispersion angle of neutrals was found to be independent of target thickness in the normal thickness range. The angle was basically determined by the nonelastic electron stripping process and varied with increasing energy as  $E^{-1/2}$ . The data for  $H^- \rightarrow H^0$  in an  $H_2$

target in Fig. 52 show the dispersion angle as a function of energy. Neutrals formed by the charge exchange of protons demonstrated analogous dependence but larger dispersion angles.

The dispersion angle and charge-exchange coefficient are shown in Fig. 53 as functions of target thickness and energy for  $H_2$  and He. The values for the proton-to-neutral hydrogen conversion, shown by the dashed line, indicate inferior operation. As demonstrated in

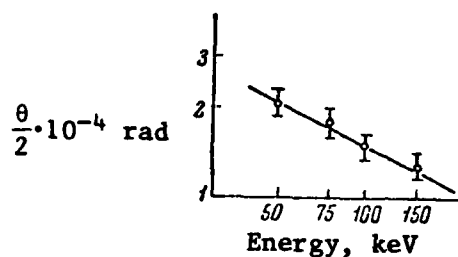


Fig. 52--Dispersion angle of neutrals as a function of  $H^-$  beam energy in an  $H_2$  target [150]

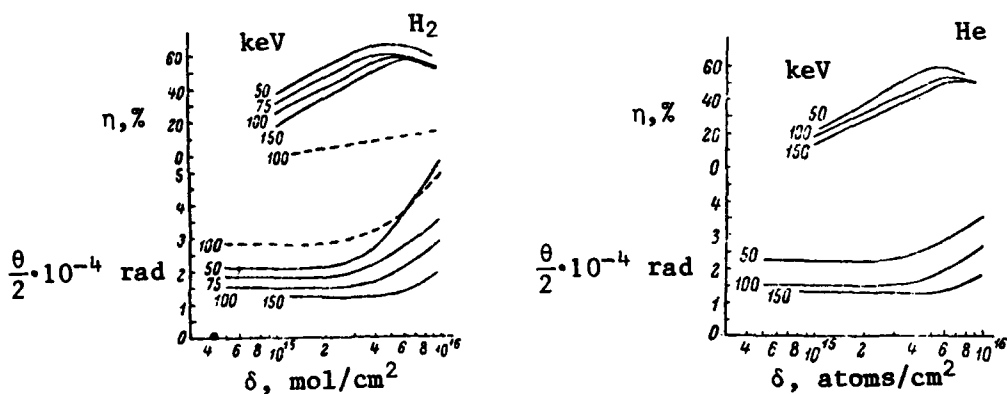


Fig. 53--Dispersion angle and charge-exchange coefficient as functions of target thickness [150]



Fig. 53, the dispersion angle of the neutrals obtained by stripping a 100 keV  $H^-$  beam is a factor of 2 smaller than that of the neutrals obtained by the charge exchange of a 100 keV  $H^+$  beam. Western research data [151] showed a slightly smaller dispersion angle of the neutrals formed by charge exchange of  $H^+$  ions.

The maximum dispersion angle of neutral beams formed by the charge exchange of the proton and the stripping of the  $H^-$  ion were compared, using classical considerations [150]. The momentum  $P$  of the fast ion and its change in momentum  $\Delta P$  in the formation of a neutral can be expressed as:

$$P = \sqrt{2ME} \quad ; \quad \Delta P = \sqrt{2ME_b}$$

where  $E$  = ion energy

$M$  = ion mass

$E_b$  = binding energy of the electron loss or capture.

In the case of charge exchange, the binding energy is:

$$E_b = V_1 = 13.59 \text{ eV}$$

where  $V_1$  = hydrogen atom ionization potential. In the case of electron detachment of the  $H^-$  ion:

$$E_b = S = 0.75 \text{ eV}$$

where  $S$  = hydrogen atom electron affinity. The maximum dispersion angle is then expressed as:

$$\theta_{\max} = \frac{\Delta P}{P} = \sqrt{E_b/E}$$

From here it can be seen that, because  $S < V_1$ , the dispersion angle of neutrals formed by the stripping of  $H^-$  ions must be smaller than that of neutrals formed by protons. The expression for  $\theta_{\max}$  provides a correct scaling behavior with  $E_b$  and  $E$  but does not give a good quantitative estimate of  $\theta$ .

These experiments led to the conclusion that the dispersion angle of the neutrals at small target thicknesses is basically determined by the inelastic collisions involved in the loss or capture of the electron. The less thick (flat ledge) region of the charge-exchange target corresponds to the region of single collision of beam particles with target atoms. Further IFTT measurements of the dispersion angle of a 100 keV neutral beam in an Ar gas target demonstrated a weak dependence of the dispersion angle on the atomic number  $Z$  of the target. With a change in  $Z$  of from 1 (H) to 18 (Ar), the dispersion half angle at 100 keV changed only from  $1.5 \times 10^{-4}$  to  $1.8 \times 10^{-4}$  rad [150].

REFERENCES

AE	<i>Atomnaya energiya</i>
FP	<i>Fizika plazmy</i>
PTE	<i>Pribory i tekhnika eksperimenta</i>
UFZh	<i>Ukrainskiy fizicheskiy zhurnal</i>
UFN	<i>Uspekhi fizicheskikh nauk</i>
ZhETF	<i>Zhurnal eksperimental'noy i teoreticheskoy fiziki</i>
ZhETF, Pis'ma	<i>Pis'ma v Zhurnal eksperimental'noy i teoreticheskoy fiziki</i>
ZhTF	<i>Zhurnal tekhnicheskoy fiziki</i>
ZhTF, Pis'ma	<i>Pis'ma v Zhurnal tekhnicheskoy fiziki</i>

1. Wells, Nikita, *The Development of High-Intensity Negative Ion Sources and Beams in the USSR*, The Rand Corporation, R-2816-ARPA, November 1981.
2. Alessi, J., A. Herscovitch, K. Prelec, and Th. Sluyters, "Development of Multiampere Negative Ion Sources," IEEE Transactions on Nuclear Science, NS-28, No. 3, June 1981, p. 2652.
3. Alessi, J., and Th. Sluyters, "Regular and Asymmetric Negative Ion Magnetron Sources with Grooved Cathodes," Proceedings of the Second International Symposium on the Production and Neutralization of Negative Hydrogen Ions and Beams, Brookhaven National Laboratory, BNL-51304, October 6-10, 1980, p. 153.
4. Prelec, K., "Progress in the Development of High Current, Steady State  $H^-/D^-$  Sources at BNL," in Proceedings ..., BNL-51304, 1980, p. 145.
5. Herscovitch, A., and K. Prelec, "Mark V Magnetron with Hollow Cathode Discharge Plasma Injection," in Proceedings ..., BNL-51304, 1980, p. 160.
6. Leung, K. N., and K. W. Ehlers, " $H^-$  Ion Formation from a Surface Conversion Type Ion Source," Journal of Applied Physics, Vol. 52, No. 6, June 1981, p. 3905.
7. Ehlers, K. W., and K. N. Leung, "Characteristics of a Large Self-extraction Negative Ion Source," Bulletin of the American Physical Society, Vol. 26, No. 7, September 1981, p. 1018.
8. Dagenhart, W. K., W. L. Stirling, H. H. Haselton, G. G. Kelley, J. Kim, C. C. Tsai, and J. H. Whealton, "Modified Colutron Negative Ion Source Operation and Future Plans," in Proceedings ..., BNL-51304, 1980, p. 217.

9. Staten, H. S., G. M. Haas, and F. E. Coffman, "U.S. Negative Ion Neutral Beam Development Program," in Proceedings ..., BNL-51304, 1980, p. 315.
10. Stewart, L. D., A. H. Boozer, H. P. Eubank, R. J. Goldston, D. L. Jassby, D. R. Mikkelsen, D. E. Post, B. Prichard, J. A. Schmidt, and C. F. Singer, "Merits of  $D^-$  Based Neutral Beam Injectors for Tokamaks," in Proceedings ..., BNL-51304, 1980, p. 321.
11. Pyle, R. V., "An Overview of the LBL/LLNL Negative-Ion-Based Neutral Beam Program," in Proceedings ..., BNL-51304, 1980, p. 194.
12. Alessi, J., V. K. Kovarik, and Th. Sluyters, "A 10 A, 200 kV Negative Ion D.C. Accelerator," Bulletin of the American Physical Society, Vol. 26, No. 2, February 1981, p. 128.
13. Hooper, E. B., Jr., P. Poulsen, and P. A. Pincosy, "High-Current  $D^-$  Production by Charge Exchange in Sodium," Journal of Applied Physics, Vol. 52, No. 12, December 1981, p. 7027.
14. Hooper, E. B., Jr., and P. Poulsen, "Prospects for Negative Ion Systems Based on Charge Exchange," in Proceedings ..., BNL-51304, 1980, p. 247.
15. Hooper, E. B., Jr., O. A. Anderson, T. J. Orzechowski, and P. Poulsen, "Sixty keV  $D^-$  Beams Using a Double Charge-Exchange System," Proceedings of the Symposium on the Production and Neutralization of Negative Ions and Beams, Brookhaven National Laboratory, BNL-50727, September 26-30, 1977, p. 163.
16. Tsai, C. C., R. R. Feezell, H. H. Haselton, P. M. Ryan, D. E. Schechter, W. L. Stirling, and J. H. Whealton, "Characteristics of a Modified Duopigatron Negative Ion Source," in Proceedings ..., BNL-51304, 1980, p. 225.
17. Whealton, J. H., C. C. Tsai, L. R. Grisham, and W. L. Stirling, "Production of Low Energy Positive Ions Suitable for Double Electron Capture Systems," in Proceedings ..., BNL-50727, 1977, p. 129.
18. Delaunay, M., J. L. Foucher, R. Geller, C. Jacquot, P. Ludwig, F. Mazhari, E. Ricard, J. C. Rocco, P. Sermet, and F. Zadworny, "Production of  $D^-$  Ions by Double Charge Exchange of  $D^+$  on Cesium," in Proceedings ..., BNL-51304, 1980, p. 255.
19. Bacal, M., J. M. Buzzi, H. J. Doucet, G. Labaune, H. Lamain, J. P. Stephan, M. Delaunay, C. Jacquot, P. Ludwig, and S. Verney, "Cesium Supersonic Jet for  $D^-$  Production by Double Electron Capture," in Proceedings ..., BNL-51304, 1980, p. 270.

20. McFarland, R. H., A. S. Schlachter, J. W. Stearns, and R. E. Olson, "D<sup>-</sup> Production by Charge Transfer of 0.3-3 keV D<sup>+</sup>, D<sup>0</sup>, and D<sup>-</sup> in Alkaline Earth Vapor Targets," Bulletin of the American Physical Society, Vol. 26, No. 7, September 1981, p. 1018.
21. Mayo, M., J. Stone, T. J. Morgan, I. Alvarez, and C. Cisneros, "H<sup>-</sup> Production in H<sup>+</sup> and H<sup>0</sup> Collisions with Alkaline-Earth Metal Vapors," in Proceedings ..., BNL-51304, 1980, p. 106.
22. Schlachter, A. S., "D<sup>-</sup> Production by Charge Transfer in Metal Vapors," in Proceedings ..., BNL-51304, 1980, p. 42.
23. -----, "D<sup>-</sup> Production by Multiple Charge-Transfer Collisions in Metal Vapor Targets," in Proceedings ..., BNL-50727, 1977, p. 11.
24. Anderson, L. W., C. J. Anderson, R. J. Girnius, and A. M. Howald, "The Stripping of 30-200 keV H<sup>-</sup> Ions," in Proceedings ..., BNL-51304, 1980, p. 285.
25. Fink, J., and K. Prelec, "A Simple, Efficient Neutralizer for D<sup>-</sup> Ions," in Proceedings ..., BNL-51304, 1980, p. 298.
26. Lam, C. K., "Neutralization of H<sup>-</sup> Beams with Gas Jets," in Proceedings ..., BNL-50727, 1977, p. 195.
27. Grisham, L. R., D. E. Post, B. M. Johnson, K. W. Jones, J. Barrette, T. H. Kruse, I. Tserruya, and Wang Da-Hai, "Efficiencies of Gas Neutralizers for Multi-MeV Beams of Light Negative Ions," Review of Scientific Instruments, Vol. 53, 1982, p. 281.
28. Berkner, K. H., R. V. Pyle, S. E. Savas, and K. R. Stalder, "Plasma Neutralizers for H<sup>-</sup> or D<sup>-</sup> Beams," in Proceedings ..., BNL-51304, 1980, p. 291.
29. Grossman, M. W., "Plasma Neutralizer for H<sup>-</sup> Beams," in Proceedings ..., BNL-50727, 1977, p. 189.
30. McGeoch, M. W., "Laser Neutralization of Negative Ion Beams for Fusion," in Proceedings ..., BNL-51304, 1980, p. 304.
31. Fink, J. H., and G. W. Hamilton, "Efficient Production of Neutral Beams by Photodetachment of Negative Ions," in Proceedings ..., BNL-50727, 1977, p. 185.
32. Hudgings, D. W., "Neutral Beam Injection for a Proton Storage Ring," IEEE Transactions on Nuclear Science, NS-26, No. 3, June 1979, p. 3556.
33. Jason, A. J., D. W. Hudgings, and O. B. VanDyck, "Neutralization of H<sup>-</sup> Beams by Magnetic Stripping," IEEE Transactions on Nuclear Science, NS-28, No. 3, June 1981, p. 2704.

34. Stinson, G. M., W. C. Olsen, W. J. McDonald, P. Ford, D. Axen, and E. W. Blackmore, "Electric Dissociation of  $H^-$  Ions by Magnetic Fields," *Nuclear Instruments and Methods*, Vol. 74, 1969, p. 33.
35. Webber, R. C., and C. Hojvat, "Measurement of the Electron Loss Cross Sections for Negative Hydrogen Ions on Carbon at 200 MeV," *IEEE Transactions on Nuclear Science*, NS-26, No. 3, June 1979, p. 4012.
36. Hojvat, C., M. Joy, and R. C. Webber, "Stripping Foils for Multiturn Charge Exchange Injection into the Fermilab Booster," *IEEE Transactions on Nuclear Science*, NS-26, No. 3, June 1979, p. 4009.
37. Barton, D. S., and R. L. Witkover, *Proceedings of the 1979 Linear Accelerator Conference*, Brookhaven National Laboratory, BNL-51134, 1979, p. 47.
38. Kramer, S. L., and D. R. Moffett, "Measuring Beam Emittance for High-Energy  $H^-$  Accelerators," *IEEE Transactions on Nuclear Science*, NS-28, No. 3, June 1981, p. 2174.
39. Moffett, D. R., and R. L. Barner, "An Intense  $H^-$  Source for the IPNS-I Rapid Cycling Synchrotron (RCS)," *Bulletin of the American Physical Society*, Vol. 26, No. 2, February 1981, p. 128.
40. Allison, P., H. V. Smith, Jr., and J. D. Sherman, " $H^-$  Ion Source Research at Los Alamos," in *Proceedings ...*, BNL-51304, 1980, p. 171.
41. Moffett, D. R., and R. L. Barner, "An Intense  $H^-$  Source for the IPNS-I Rapid Cycling Synchrotron," *IEEE Transactions on Nuclear Science*, NS-28, No. 3, June 1981, p. 2678.
42. Hamilton, G. W., private communication.
43. Anderson, O. A., "Large Aperture  $D^-$  Accelerators," in *Proceedings ...*, BNL-51304, 1980, p. 355.
44. Ehlers, K. W., and K. N. Leung, "A Multicusp Negative Ion Source," *Review of Scientific Instruments*, Vol. 50, 1979, p. 1353.
45. Prichard, B. A., Jr., R. Little, D. E. Post, and J. A. Schmidt, "Possible Neutral Beam Requirements for the TFTR Upgrades," in *Proceedings ...*, BNL-50727, 1977, p. 269.
46. Orthel, J. L., D. N. Birnbaum, A. Cole, T. K. Samec, and V. Vanek, "Neutral Beam Injection System for Current Drive in the Starfire Tokamak," *Bulletin of the American Physical Society*, Vol. 26, No. 7, September 1981, p. 1016. See also *A Design Analysis of Supplemental Heating Systems*, TRW Report, Contract DE-AC03-80 ER 52058, September 1981.

47. Hagena, O. F., W. Henkes, R. Klingelhöfer, B. Krevet, and H. O. Moser, "Negative Ion Production by Charge Exchange of Hydrogen Clusters with a Cesium Vapor Target--Status Report," in Proceedings ..., BNL-51304, 1980, p. 263.
48. Becker, E. W., H. D. Falter, O. F. Hagena, W. Henkes, R. Klingelhöfer, H. Moser, W. Obert, and I. Poth, "Negative Hydrogen Ions Produced from Clusters for Plasma Heating," in Proceedings ..., BNL-50727, 1977, p. 322.
49. Bel'chenko, Yu. I., and V. G. Dudinkov, "A Surface-Plasma Source of Negative Hydrogen Ions with an Extended Emitting Surface," Proceedings of the Fifteenth International Conference on Phenomena in Ionized Gases, Minsk, July 14-18, 1981, P-1504, p. 883.
50. Dimov, G. I., "Production of Intense Negative Hydrogen Ion Beams," Tenth European Conference on Controlled Fusion and Plasma Physics, Moscow, Vol. 2, September 1981.
51. Hooper, E. B., Jr., private communication.
52. Smythe, R., and I. W. Toevs, Physical Review, Vol. 139, No. 1A, 1965, p. A15.
53. Komarov, V. L., and A. P. Strokach, Yefremov Institute of Electrophysical Equipment, Preprint NIIEFA II-K-0488, Leningrad, 1980.
54. Kulygin, V. M., A. A. Panasenkov, N. N. Semashko, and I. A. Chukhin, "Ion Source Without an External Magnetic Field--IBM-5," ZhTF, Vol. 49, No. 1, 1979, p. 168.
55. Kulygin, V. M., A. A. Panasenkov, N. N. Semashko, and A. G. Boldasov, "Formation of an Intense Ion Beam with a Multiple-Slit Extractor," Proceedings of the Second Symposium on Ion Beams, Berkeley, CA., 1974.
56. Sluyters, Th., and K. Prelec, "High Energy Neutral Injectors Based Upon Negative Ion Plasma Sources," in Proceedings ..., BNL-50727, 1977, p. 280.
57. D'yachkov, B. A., A. I. Krylov, V. V. Kuznetsov, B. P. Maksimenko, and N. N. Semashko, "Generation of Negative Ions by Charge Exchange of a Hydrogen Beam in a Sodium Target," Kurchatov Institute Preprint, IAE-2523, Moscow, 1975.

58. D'yachkov, B. A., V. I. Zinenko, M. A. Pavliy, and V. Yu. Petrusha, "A Sodium Charge Exchange Target with a Large Aperture," PTE, No. 5, 1978, p. 37.
59. D'yachkov, B. A., A. I. Krylov, V. V. Kuznetsov, and N. N. Semashko, "Sodium Target for a Negative Ion Injector," AE, Vol. 49, No. 4, October 1980, p. 246.
60. Semashko, N. N., V. V. Kuznetsov, and A. I. Krylov, "Charge-Exchange Target of the Negative Ion Injector MIN," Proceedings of the Eighth Symposium on Engineering Problems of Fusion Research, IEEE, Vol. 2, No. 79CH1441-5, 1979, p. 853.
61. Semashko, N. N., et al., "Questions on Atomic Science and Technology," Thermonuclear Fusion Series, Vol. 3, No. 1, Moscow, 1979, p. 3.
62. Agafonov, Yu. A., B. A. D'yachkov, and M. A. Pavliy, "Choice of Target Material for an  $H^-$  and  $D^-$  Charge Exchange Ion Source, Determination of the Conversion Coefficient and Dispersion Angle of Ions in Cs and Na Targets," ZhTF, Vol. 50, No. 10, 1980, p. 2163.
63. D'yachkov, B. A., V. I. Zinenko, and A. V. Nasonov, "Apparatus for Measuring the Conversion Coefficient of Low Energy Positive Ions into Negative Ions," PTE, No. 5, 1975, p. 27.
64. D'yachkov, B. A., and V. I. Zinenko, "Use of the Vacuum Properties of Gas-Dynamic Alkali Metal Vapor Jets," ZhTF, Vol. 50, No. 11, 1980, p. 2369.
65. Agafonov, Yu. A., B. A. D'yachkov, and M. A. Pavliy, "Conversion of Protons of Energies 0.2 to 6.0 keV to Negative Ions in Cesium," ZhTF, Pis'ma, Vol. 2, No. 16, 1976, p. 757.
66. Vershinin, N. F., B. A. D'yachkov, and V. I. Zinenko, "Pumping and Vacuum Barrier Characteristics of a Sodium Vapor Target," ZhTF, Pis'ma, Vol. 5, No. 2, January 1979, p. 110.
67. D'yachkov, B. A., N. M. Zaryankin, V. I. Logunov, and A. V. Nasonov, "Low Energy RF Ion Source," PTE, No. 2, 1978, p. 191.
68. Krylov, A. I., and V. V. Kuznetsov, "A Supersonic Vapor Jet Acting as a Vacuum Barrier," Kurchatov Institute, Preprint IAE-3330/7, Moscow, 1980.
69. Gillespie, G. H., "A Survey of Negative Ion Neutralization Options," Physical Dynamics, Inc., Technical Memorandum PDL-82-229-TM, January 15, 1982.
70. Butusov, V. I., P. A. Mukhin, and V. S. Svishchev, "Neutralizer of Intense Ion Beams," ZhTF, Vol. 37, No. 10, 1967, p. 1818.



71. Artemenkov, L. I., N. I. Klochkov, V. V. Kuznetsov, V. M. Kulygin, N. P. Malakhov, P. A. Mukhin, D. A. Panov, V. S. Svishchev, and N. N. Semashko, "Energetic Hydrogen Atom Injector," Proceedings of the VII International Conference on Ionization Phenomena in Gases, Belgrade, 1965.
72. D'yachkov, B. A., S. M. Krivoruchko, and V. Yu. Petrusha, "Emission of Lithium from a Supersonic Vapor Stream," ZhTF, Vol. 39, No. 5, 1969, p. 918.
73. D'yachkov, B. A., "Production of High Energy Neutrals by Conversion of  $H_1^-$ ,  $H_2^+$ ,  $H_3^+$  Ions in a Supersonic Lithium Vapor Stream," ZhTF, Vol. 38, No. 8, 1968, p. 1259.
74. D'yachkov, B. A., V. M. Nesterenko, and V. Yu. Petrusha, "Lithium Ion Neutralizer," PTE, No. 2, 1974, p. 35.
75. D'yachkov, B. A., and V. I. Zinenko, "Development of an Intense  $He^-$  Ion Source," ZhTF, Vol. 41, No. 2, 1971, p. 404.
76. D'yachkov, B. A., V. I. Zinenko, and M. A. Pavliy, "Formation of  $H^-$  Ions by Charge Exchange of Protons of 1.5 to 10 keV Energy in Dense Li, Na, K, and Mg Vapor Streams," ZhTF, Vol. 41, No. 11, 1971, p. 2353.
77. Borisenko, A. G., M. Yu. Bredikhin, B. V. Glasov, O. S. Druy, A. M. Il'chenko, G. T. Nikolayev, Ye. I. Skibenko, and V. B. Yuferov, "Large Aperture Intense Neutral Atom Injector," Plasma Physics and Problems of Thermonuclear Fusion, AN UkSSR, No. 4, Kiev, 1973, p. 159.
78. Busol, F. I., Ye. I. Skibenko, and V. B. Yuferov, "Effect of the Nozzle Configuration Upon the Supersonic Gas Flow into Vacuum," ZhTF, Vol. 36, No. 12, 1966, p. 2154.
79. Busol, F. I., V. B. Yuferov, and Ye. I. Skibenko, "Upgrading the Vacuum in the Charge Exchange Chamber Near the Supersonic Gas Jets," ZhTF, Vol. 34, No. 12, 1964, p. 2156.
80. Borovik, Ye. S., F. I. Busol, V. B. Yuferov, and Ye. I. Skibenko, "Investigation of a Supersonic  $CO_2$  Gas Jet as a Target for Ion Charge Exchange," ZhTF, Vol. 33, No. 8, 1963, p. 973.
81. Bredikhin, M. Yu., V. B. Yuferov, ZhTF, Vol. 39, No. 11, 1969, p. 2092.
82. Ivanov, A. A., and G. V. Roslyakov, "Conversion of  $H^-$  Ions into Atoms in a Hydrogen Plasma Target," ZhTF, Vol. 50, No. 11, 1980, p. 2300.
83. Dimov, G. I., A. A. Ivanov, and G. V. Roslyakov, "Investigation of a Hydrogen Plasma Target," FP, Vol. 6, No. 4, 1980, p. 933.

84. Peart, B., D. S. Walton, and K. T. Dolder, *Journal de Physique*, No. 3, 1970, p. 1346.
85. -----, *Journal de Physique*, No. 4, 1971, p. 88.
86. Dimov, G. I., and G. V. Roslyakov, "Conversion of a Beam of Negative Hydrogen Ions to Atomic Hydrogen in a Plasma Target at Energies Between 0.5 and 1 MeV," *Nuclear Fusion*, No. 15, 1975, p. 551.
87. Dimov, G. I., A. A. Ivanov, and G. V. Roslyakov, Institute of Nuclear Physics, Siberian Department, Academy of Sciences USSR, IYAF SO AN SSSR, Preprint 79-22, Novosibirsk, 1979.
88. Dimov, G. I., G. V. Roslyakov, and V. Ya. Savkin, "Diagnostic Hydrogen Atom Injector," *PTE*, No. 4, 1977, p. 29.
89. Fedotov, A. P., V. V. P'yankov, V. V. Frolov, and V. B. Khvostov, "Beam Perturbation Diagnostics in Ion Linear Accelerators Using Secondary Particle Distributions," *PTE*, No. 3, 1980, p. 26.
90. Murin, B. P., and A. P. Fedotov, "Radiation Cleanliness and Efficiency Problems of Present Day Linear Accelerators of Protons and Negative Hydrogen Ions with Large Average Beam Currents," *AE*, Vol. 38, No. 3, March 1975, p. 146.
91. Murin, B. P., "The Linear Proton Accelerator--Meson Factory Project," *Proceedings of the Third All Union Conference on Charged Particle Accelerators*, Moscow, October 2-4, 1972, Nauka Publishers, 1973, Vol. 1, p. 234.
92. -----, "Development of the High Intensity Linear Accelerator of the Meson Factor," *Proceedings of the Fifth All Union Conference on Charged Particle Accelerators*, Dubna, October 5-7, 1976, Nauka Publishers, 1978, Vol. 1, p. 302.
93. Batskikh, G. I., A. A. Vasilyev, R. A. Meshcherov, and B. P. Murin, "Storage Rings for Grouping and Leveling in Time the Particle Beam Which Is Accelerated by an Intense Linear Accelerator (a Meson Factory)," *Proceedings of the Third All Union Conference on Charged Particle Accelerators*, Moscow, October 2-4, 1972, Nauka Publishers, 1973, Vol. 1, p. 249.
94. Kaminskiy, A. K., R. A. Meshcherov, and M. I. Popova, *Nuclear Instruments and Methods*, Vol. 137, 1976, p. 183.
95. Bulgakov, Yu. V., A. K. Kaminskiy, S. V. Lovstsov, and R. A. Meshcherov, *Proceedings of the Radiotechnical Institute, USSR Academy of Sciences*, Moscow, No. 30, 1977, p. 61.

96. Kaminskiy, A. K., Proceedings of the Sixth All Union Conference on Accelerators of Charged Particles, Dubna, Vol. 1, 1979, p. 91.
97. Kaminskiy, A. K., V. S. Nikolayev, M. P. Popova, A. A. Vasil'yev, and R. A. Meshcherov, "Target Calculations for Charge Exchange Injection into High Intensity Accelerators," Proceedings of the Fourth All Union Conference on Charged Particle Accelerators, Moscow, Nauka Publishers, 1975, Vol. 1, p. 262.
98. Kaminskiy, A. K., R. A. Meshcherov, M. I. Popova, and V. D. Sazhin, "Angular and Energy Distributions of Electrons Generated by Ion Accelerator Beams," Nuclear Instruments and Methods, Vol. 180, 1981, p. 231.
99. Kaminskiy, A. K., R. A. Meshcherov, V. S. Nikolayev, and M. I. Popova, Proceedings of the Radiotechnical Institute, USSR Academy of Sciences, Moscow, No. 16, 1973, p. 318.
100. Kaminskiy, A. K., R. A. Meshcherov, and V. S. Nikolayev, Proceedings of the Radiotechnical Institute, USSR Academy of Sciences, Moscow, No. 16, 1973, p. 330.
101. Fedotov, A. P., V. V. Kushin, and V. I. Rogachev, "Increase in Particle Capture with Short  $H^-$  Ion Bunch Formation at the Linear Accelerator Input," PTE, No. 6, 1974, p. 24.
102. Lukshin, S. A., V. P. Tkach, and A. P. Fedotov, "Formation of Short  $H^-$  Ion Bunches at the Input to a Linear Accelerator," PTE, No. 5, 1977, p. 40.
103. Kulygin, V. M., A. A. Panasenkov, A. G. Sveshnikov, and N. N. Semashko, "Intense Hydrogen Atom Injector," ZhTF, Vol. 40, No. 10, 1970, p. 2091.
104. Panasenkov, A. A., and N. N. Semashko, "Intense Hydrogen Atom Injector," ZhTF, Vol. 40, No. 12, 1970, p. 2525.
105. Oparin, V. A., R. N. Il'in, and Ye. S. Solov'yev, "Formation of Highly Excited Hydrogen Atoms by Charge Exchange of Protons in Metal Vapors," ZhETF, Vol. 52, No. 2, 1967, p. 369.
106. Il'in, R. N., V. A. Oparin, Ye. S. Solov'yev, and N. V. Fedorenko, "Charge Exchange of Protons in Alkali Metal Vapors with Formation of Highly Excited Hydrogen Atoms," ZhTF, Vol. 36, No. 7, 1966, p. 1241.
107. Kartashev, K. B., V. I. Pistunovich, V. V. Platonov, V. D. Ryutov, and Ye. A. Filimonova, "Ion Scattering of Dense Plasma Flow During Charge Exchange in Gas Targets," FP, Vol. 1, No. 5, 1975, p. 742.

108. -----, "Anomalous Energy Scattering of a Plasma Beam During Its Interaction with Gas Targets," ZhETF, Pis'ma, Vol. 19, No. 8, 1974, p. 493.
109. Pistunovich, V. I., V. V. Platonov, V. D. Ryutov, and Ye. A. Filimonova, "Investigation of Instabilities in Dense Ion Flow During Charge Exchange in Gas," FP, Vol. 2, No. 5, 1976, p. 750.
110. Kartashev, K. B., V. I. Pistunovich, V. V. Platonov, and Ye. A. Filimonova, "Investigation of Charge Exchange of a Dense Plasma Flow Through a Magnesium Target," ZhETF, Vol. 59, No. 3, 1970, p. 779.
111. Pistunovich, V. I., V. V. Platonov, V. D. Ryutov, and Ye. A. Filimonova, "Optical Investigations of the Turbulent Electrostatic Oscillations Formed During the Interaction of a Plasma Beam with a Partially Ionized Gas," ZhETF, Pis'ma, Vol. 23, No. 1, 1976, p. 30.
112. Semashko, N. N., V. V. Kuznetsov, and A. I. Krylov, "Production of Negative Hydrogen Ion Beams by Double Charge Exchange," in Proceedings ..., BNL-50727, 1977, p. 170.
113. Krylov, A. I., V. V. Kuznetsov, and N. N. Semashko, "An Injection System for Large Tokamaks and Open Traps," AE, Vol. 48, No. 3, March 1980, p. 186.
114. Zhil'tsov, V. A., and A. A. Skovoroda, "Electron Behavior in the OGRA-3B Open Trap with a Minimum Magnetic Field," FP, Vol. 8, No. 1, 1982, p. 12.
115. Sokolov, V. G., and I. Ya. Timoshin, "Pulsed Magnesium Vapor Charge Exchange Blocking Target for Intense Hydrogen Atom Injectors," ZhTF, Vol. 52, No. 2, 1982, p. 283.
116. Dimov, G. I., "State of Work on the AMBAL Experiment," IYaf SO AN SSSR Preprint for IAEA Technical Committee, Meeting on Open Confinement Systems, September 1981, translated by G. W. Hamilton, Lawrence Livermore Laboratory, UCID-19206, October 2, 1981.
117. -----, "Ambipolar Traps, UFN, Vol. 131, No. 4, 1980, p. 721.
118. Roslyakov, G. V., and V. Ya. Savkin, "Formation of a Modulated Hydrogen Atom Beam of 3 to 15 keV Energy," PTE, No. 1, 1978, p. 148.
119. Davydenko, V. I., I. I. Morozov, and G. V. Roslyakov, "A Hydrogen Atom Diagnostic Injector," FP, Vol. 7, No. 2, 1981, p. 464.
120. Dimov, G. I., and G. V. Roslyakov, "Pulsed Charge Exchange Source of Negative Hydrogen Ions," PTE, No. 1, 1974, p. 29.

121. Roslyakov, G. V., "Detector for Measuring Transverse Velocities of Ions of a Plasma Emitter," Institute of Nuclear Physics, Academy of Sciences USSR, IYaF SO AN SSSR, Preprint, Novosibirsk, 1979.
122. Davydenko, V. I., G. V. Roslyakov, and N. G. Khavin, "A Four Element, Multislit System for the Formation of Ion Beams," Institute of Nuclear Physics, Academy of Sciences USSR, IYaF SO AN SSSR, Preprint, No. 80-35, Novosibirsk, 1979.
123. Afrosimov, V. V., M. P. Petrov, and V. A. Sadovnikov, "Investigation of Fast Atomic Beams from Pulsed Plasma Injectors," ZhTF, Vol. 45, No. 5, 1975, p. 1091.
124. Berezovskiy, Ye. L., A. I. Kislyakov, S. Ya. Petrov, and G. V. Roslyakov, "Measurement of Ion Temperature in a Hot Plasma by the Scattering of Fast Atoms," FP, Vol. 6, No. 6, 1980, p. 1385.
125. Afrosimov, V. V., Ye. L. Berezovskiy, A. B. Izvozchikov, and M. P. Petrov, "Particle Diagnostics by Charge Exchange of Plasma Ions on a Target in a Tokamak-4 Installation," FP, Vol. 6, No. 2, 1980, p. 240.
126. Aleksandrov, Ye. V., V. V. Afrosimov, Ye. L. Berezovskiy, A. B. Izvozchikov, V. I. Marasev, A. I. Kislyakov, Ye. A. Mikhaylov, M. P. Petrov, and G. V. Roslyakov, "Measurements of the Local Ion Parameters in the Tokamak-4 Plasma," ZhETF, Pis'ma, Vol. 29, No. 1, 1979, p. 3.
127. Hiskes, J. R., private communication.
128. Fedorenko, N. V., "Electron Loss and Capture by Hydrogen Atoms, Protons, and Negative Ions in the Collision with Atoms and Molecules--Experimental Data on Cross Sections," ZhTF, Vol. 40, No. 12, 1970, p. 2481.
129. Tawara, H., and A. Russek, Review of Modern Physics, Vol. 45, No. 1, 1973, p. 178.
130. Allison, S. K., Review of Modern Physics, Vol. 30, 1958, p. 1137.
131. Risley, J. S., "A Review of Negative Ion Detachment Cross Sections," in N. Oda and K. Takayanagi (eds.), *Electronic and Atomic Collisions*, North Holland, Amsterdam, 1980, pp. 619-633.
132. Champion, R. L., "Collisional Detachment of Negative Ions," *Advances in Electronics and Electron Physics*, Vol. 58, 1982, pp. 143-189.

133. Schlachter, A. S., "Production and Destruction of  $D^-$  by Charge Transfer in Metal Vapors," U.S./Mexico Joint Seminar on the Atomic Physics of Negative Ions, April 1-4, 1981, Lawrence Livermore Laboratory, Preprint LBL-12995, June 1981.
134. Dimov, G. I., and V. G. Dudnikov, "Control of Particle Flow by Charge Exchange," FP, Vol. 4, No. 3, 1978, p. 692.
135. D'yachkov, B. A., "Measurements of Charge Exchange Cross Sections and Hydrogen Ion and Atom Ionization at Energies of 40 to 400 keV in Lithium," AE, Vol. 27, No. 3, September 1969, p. 220.
136. D'yachkov, B. A., and V. I. Zinenko, "Charge Exchange of 5 to 40 keV Protons in Dense Vapor Streams of Lithium, Sodium, Magnesium, and Zinc," AE, Vol. 24, No. 1, January 1968, p. 18.
137. Dimov, G. I., and V. G. Dudnikov, "Detachment Cross Sections of 1 MeV  $H^-$  Ions in Neutral Gases," ZhTF, Vol. 36, No. 7, 1966, p. 1239.
138. Dimov, G. I., A. A. Ivanov, and G. V. Roslyakov, "Electron Loss of Fast  $H^-$  Ions and H Atoms in a Plasma Target," ZhTF, Vol. 47, No. 9, 1977, p. 1881.
139. Dimov, G. I., and V. G. Roslyakov, "A 20 mA Negative Hydrogen Ion Beam Injector," PTE, No. 2, 1974, p. 33.
140. Buchel'nikova, N. S., UFN, Vol. 65, No. 3, 1958, p. 351.
141. Dimov, G. I., Preprint IYaF SO AN SSSR, No. 304, 1969.
142. Fink, I. E., W. L. Barr, and G. W. Hamilton, Lawrence Livermore Laboratory, UCRP-52173, 1976.
143. Van Zyl, B., N. G. Utterback, and R. C. Amme, Review of Scientific Instruments, No. 47, 1976, p. 814.
144. Fogel', Ya. M., L. I. Krupnik, and V. A. Ankudinov, "Formation of Negative Hydrogen Ions by Passing Positive Hydrogen Ions through an Ultrasonic Mercury Vapor Jet," ZhTF, Vol. 26, No. 6, 1956, p. 1208.
145. Schmidt, T. H., "Nuclear Instruments and Methods," Vol. 28, 1964, p. 52.
146. Fogel', Ya. M., G. A. Lisochkin, and G. I. Stepanova, "Mercury Vapor Jet as a Charge Exchange Target," ZhTF, Vol. 25, 1955, p. 1944.
147. D'yachkov, B. A., and V. I. Zinenko, "Production of Neutral Atoms C, O, F, Cl with Energy of 110-380 keV by Means of Electron Detachment from Negative Ions," ZhTF, Vol. 46, No. 2, 1976, p. 297.

148. Jorgensen, T., C. E. Kuyatt, W. W. Long, D. C. Lorents, and S. A. Sautter, Physical Review, Vol. 140, No. 5A, 1965, p. A1481.
149. Gornitsyn, G. A., B. A. D'yachkov, and V. I. Zinenko, "High Frequency Negative Ion Source," PTE, No. 5, 1969, p. 24.
150. D'yachkov, B. A., V. I. Zinenko, and G. V. Kazantsev, "Measurement of the Scattering Angle of Neutrals Obtained by the Stripping of Negative Hydrogen Ions," ZhTF, Vol. 47, No. 2, 1977, p. 416.
151. Wittkower, A. B., and H. B. Gilbody, Proceedings of the Physical Society, Vol. 90, 1967, p. 343.